RESPONSE AND FAILURE OF STRUCTURES UNDER STATIONARY RANDOM EXCITATION

Thesis by

Randolph Ademola Adu

In Partial Fulfillment of the Requirements

for the Degree of

Doctor of Philosophy

California Institute of Technology

Pasadena, California

1971

(Submitted May 21, 1971)

ACKNOWLEDGEMENTS

The author is very grateful to Professor G. W. Housner for his helpful guidance and assistance in the preparation of this thesis. The interest and cooperation of Professors D. E. Hudson, P. C. Jennings and T. K. Caughey is gratefully acknowledged.

Financial assistance from the California Institute of Technology and the African-American Institute through its African Graduate Fellowship Programme of American Universities is sincerely appreciated.

The author dedicates this thesis to his family.

ABSTRACT

The response of simple structural systems to stationary random excitation is considered under two criteria of failure. When failure is specified as the crossing of a maximum tolerable threshold by the response, the reliability of a structure is commonly measured by means of response spectra. These give the expected maximum value of the response parameter for a given excitation level. The statistical variations in these spectra are obtained here for viscously damped linear and elastoplastic single-degree of freedom systems by electronic analog simulation. The results obtained are compared with approximate statistical analyses; for example, the threshold crossing statistics of narrow-band oscillators. It is concluded that such methods give satisfactory, but conservative, estimates of the mean spectral values. It is significant that all the spectra obtained showed a very wide distribution about the mean. This was also true of the Fourier amplitude spectrum of the excitation.

For responses that are so large that structures actually collapse, the linear model was replaced by an elastoplastic system, and the effect of gravity on the collapse time was considered. Experimental simulation showed that the structural response in this case is essentially that of a linear oscillator with yielding occurring at intermittent intervals. Gravity acts to increasingly bias this yielding in one direction, eventually causing instability

in the system. Collapse of the system was sensitive to the distribution of peaks in the excitation and it was found that the wide dispersion in the collapse time can be reasonably represented by a Gamma distribution function.

An analytic method for estimating the mean collapse time was derived by considering the energy distribution of the excitation and its effect on the yielding of the structure. The response process was thus modelled by that of an equivalent linear oscillator whose base-line is biased by the yielding in the structure. It was concluded that this procedure gives a good estimate of the failure time for excitations strong enough to cause failure in less than 20 seconds.

A two-degree of freedom elastoplastic hysteretic system with gravity was also simulated. In a certain sense, the qualitative behavior is similar to that of the single-degree of freedom system. It was thus possible to estimate the failure time of the structure from that of a single-degree of freedom system once the transmission of vibration is accounted for by considering a linear two-degree of freedom system.

TABLE OF CONTENTS

Chapter I

INTRODUCTION

The ability of structures to withstand earthquake ground shaking is of great interest in seismic regions of the world. In the highly seismic regions it is customary to design structures so that they can withstand moderately strong ground shaking without significant damage but, for economic reasons, the design is such that in the event of very strong ground shaking the structure will be strained beyond the yield point. This means that a collapse process has been initiated and it is important to know how close to collapse the structure may come.

The design of structures to resist dynamic loads is often characterized by randomness in the rate of occurrence, magnitude and nature of the excitation and inherent uncertainties in the structural properties. Hence defining a criterion for the safety level of a structure becomes a complex problem most often tackled by the use of simplified models for the structures and either relevant known excitations or tractable stochastic models for them[1-8]. The particular simplifying assumptions made will depend on what is considered a satisfactory failure criterion. Such a criterion is generally either a maximum tolerable level of response or, more critically, the actual collapse of the structure.

The apparent statistical nature of many dynamic loads--earthquake ground accelerations, wind loads, machine vibrations, etc., the limitations in the number of available sample functions, and, in most instances, the versatility of stochastic models, have

led to increasing use of such models for predicting dynamic excitations[7-12, 14]. With respect to earthquake ground accelerations the existence of only a few sample excitations has led to the design of general models adaptable to many given records[10-12] or reflecting average properties of known records[9,14-17]. The properties most often considered are the spectral densities, correlation times, temporal modulation and response spectra of these excitations.

Since most records can be reasonably taken as having a stationary strong motion phase flanked by build-up and die-down phases with relatively weak motion, several investigators have assumed that most structural damage is done during the strong motion phase and therefore modelled the excitation by stationary random processes[14,36]. Natural extensions of these have included the addition of deterministic envelope functions and considerations of the joint effects of the three phases with each represented by an appropriate stationary random process[9-12]. Throughout this study the stationary random process model is used since one expects that the effect of the build-up and die-down phases will be negligible in both linear structures and those nonlinear structures where the degree of damage or permanent set is small. Its use in the study of the collapse time of structures is mainly for convenience in continuing the excitation up to the time of collapse. The effect of this assumption has been examined among others, by Amin, Ts'Ao and Ang[28] and will be noted whenever results indicate a need to adapt it.

The most common structural model is the linear one-degree of freedom oscillator. This is used not only because it is relatively easy to analyze but because it can serve as a basis for the analysis of more complicated structures. When the failure criterion used is the crossing of a tolerable level by the response, the structural effect of the excitation is typically characterized by the model's response spectra[15, 17], these being generally defined as the maximum response observed when the oscillator is subjected to the given excitation. In this way design criteria can be set up by using average response spectra to estimate the effect of the excitation's mean intensity and the properties of the structural model, i.e. its natural period and damping ratio. The availability of stochastic models for the excitations has led to several analytic and experimental determinations of these spectra[23-26,29,16-18].

More recently, observations of permanent set in buildings subjected to strong excitation, and the fact that some buildings have survived excitations stronger than their design loads with minor damage while low magnitude excitations have caused unexpectedly large damage, have motivated the use of nonlinear structural models [36,50-52], the inclusion of the effect of gravity on structures undergoing large deformations[46-48], and pointed out the need for studies of the statistical variation in response of linear and nonlinear building models even when the mean excitation level is known. Two recent examples of structural damage are shown in figures 1.1a,b. These occurred at the Olive View Hospital in Los Angeles during the San Fernando earthquake of Feb. 9, 1971. Figure 1.1a shows appreci-

(a)

(b)

Fig. 1.1 Structural Damage at
Olive View Hospital; Feb. 9, 1971

able yielding in the lower columns of the 5-story structure while the upper columns only suffered minor cracks. The form of deformation resembles the bending of a single-story building under lateral force. The two-story building in figure 1.1b appears to have vibrated in a similar fashion although it resulted in complete collapse of the lower story as its columns moved over about 5 feet.

While it has been possible to obtain approximate analytical solutions for the maximum response of linear systems subjected to stationary random excitation[29,30], the analytical problem becomes increasingly difficult with the introduction of nonlinearity in the model's restoring force and inclusion of the destabilizing effect of gravity. No analytic solutions have been found in such cases. Investigators have therefore tended to obtain mean response spectra and failure times by generating a few sample excitation functions. The distribution of the response spectra of linear oscillators excited by white noise base excitations was investigated by Brady[18] in an experimental test of the approximate analytical solutions of Rosenblueth and Bustamante.

The present study examines the response of structural models under both criteria of failure. In chapter II the electronic analog computer is used to simulate a stationary random process designed to have mean response spectra similar to those of some past earthquakes[14]. With this excitation the response spectra of linear and elastoplastic oscillations are obtained by analog simulation, the Monte Carlo method being used to estimate their means and density

functions. These are compared with approximate analytical estimates whenever possible and the use of equivalent linear oscillators in predicting the elastoplastic oscillator's spectral properties is examined. Finally, the frequency characteristics of the excitation are examined through its Fourier amplitude spectrum.

The last three chapters consider the collapse of nonlinear structures with gravity. Emphasis is placed on the time to failure, its mean value and density function. Chapter III is concerned with an electronic analog simulation of a single-degree of freedom structural model having an elastoplastic restoring force that is either hysteretic or non-hysteretic and subjected to the influence of gravity. The effect of the latter on the yielding characteristics of the model are observed and the effect of the excitation on failure times is considered both from the point of view of its average magnitude and the scatter in its temporal energy distribution. The wide scatter observed in the failure times of structures subjected to the same mean relative excitation level is attributed in part to this energy distribution.

Observations of the responses in chapter III are used in chapter IV as a basis for developing an analytical method for estimating the mean failure time of the one-degree of freedom hysteretic system with gravity. The given filtered white noise process is relaxed to a shot noise process whose temporal energy distribution can be accounted for by considerations of clumping in the arrival of the impulses. Structural response to such impulses is considered as a stationary random process with a biased mean level reflecting

yielding and gravity effects. The use of the shot noise model limits the application of the method to relatively strong excitations that cause failure in less than about 20 seconds; though the results indicate that it gives fairly reliable estimates within that range.

The investigation is extended to a two-story structural model in chapter V. Electronic analog simulation of this model showed that basic response properties like the yielding characteristic and distribution of failure times are unchanged. Therefore an attempt was made to estimate the failure time of this model by using the response of a linear two-degree of freedom system to account for dynamic floor interactions and the results of the earlier single-degree of freedom system to correlate the expected failure time with the mean stationary response.

CHAPTER II

GENERATION OF A RANDOM EXCITATION PROCESS AND RESPONSE OF SOME STABLE OSCILLATORS

A. Analog Simulation of the Random Excitation

Studies of structural response to random excitation have been both deterministic--using actual accelerograms--and probabilistic. Apart from the fact that it gives little or no information on the statistics of structural response to the complete excitation process, the deterministic approach is limited by the number of accelerograms available. This limitation also affects the reliability of any stochastic model that may be used to simulate the complete excitation process--assuming the recorded functions can be reasonably taken to be sample functions of some stochastic process. However, such models have the advantage that they can be formulated to reflect average properties of the known accelerograms and, in certain cases, can be adapted as more recordings are made. Furthermore, the response of a wide class of structures to such models can be established, in a probabilistic sense, either by direct mathematical analysis or by an experimental procedure such as the Monte Carlo method.

In this chapter the Monte Carlo method is used to experimentally obtain the distribution of the response of linear and elastoplastic, single degree of freedom oscillators to a stationary process. The results obtained are compared with current analytical

theories[25,29,30] where these exist. Previous work in this vein has considered the digital response of different types of non-linear oscillators to stationary[36] and nonstationary[26] random processes; the distribution of analog response of linear oscillators to white noise[17,18]; and the analog response of linear and elastoplastic oscillators to different types of stationary processes[16]. While these studies have confirmed that the excitations thus generated have the desired response spectra, it is felt that in no case have enough sample functions of non-white noise been used to demonstrate the statistical distribution of the response processes.

The particular excitation process used here was designed such that its expected velocity response spectrum is equal to the average of those obtained for a set of past earthquakes[14,15]. The velocity response spectrum is defined by

$$S_v(\omega,n) = \max_t \left[\dot{x}^2(t) + (\omega_o x(t))^2\right]^{\frac{1}{2}} \doteq \max_t \left|\omega_o x(t)\right| \tag{2.1}$$

where $\dot{x}$, x, ω_o, n are the velocity, displacement, resonant frequency and damping factor of an oscillator respectively. The last approximation is the pseudo-velocity and serves as a good approximation to the true spectrum when the response process is truly narrow band. This requires that the duration of excitation be much longer than the oscillator's period and that the period be neither so short that the response is principally a rigid body motion nor so long that the frequency approaches zero. These requirements

are met by the systems examined here. Caughey and Gray[30] have shown that the velocity spectrum of an undamped oscillator excited by white noise is related to the power spectral density of the white noise, $S_o(\omega)$, by

$$\langle S_v(\omega,0)\rangle = 1.174\sqrt{\pi S_o(\omega)s} \qquad (2.2)$$

where s is the duration of each excitation sample. Since the response of an undamped oscillator to a random excitation is a narrow band process--under the conditions specified above--equation (2.2) may be assumed to apply for a more general non-white spectral density which is sufficiently smooth[6,22]. Hence the excitation spectral density is known once a suitable expression is obtained for the average undamped velocity spectrum of known records.

Many authors have considered the simulation of random processes having a given spectral density. The methods used include application of linear filters[8-10,14,36], or a cascade of linear filters[25] to white noise or shot noise processes and summation of random functions with known density distribution[12]. Aside from its distinct advantages of low cost, speed and flexibility mentioned earlier, the analog computer is particularly suitable for simulation by linear filtering: In the first place, the use of an indefinitely long, continuous sample function makes it unnecessary to generate random initial conditions. Secondly, the filters may be obtained directly from the given spectral density without obtaining the associated differential equations. Let $x(t)$ be the given input function with spectral density

$S_o(\omega)$ and let $y(t)$ be the desired output with spectral density $G(\omega)$. The overall transfer functions of the filters is simply

$$H(s) = Y(s)/X(s) \tag{2.3}$$

where $Y(s)$ and $X(s)$ are the Laplace transforms of $y(t)$ and $x(t)$. For a stable, linear filter $H(s)$ has the general form

$$H(s) = \sum_{j=0}^{n-1} a_j s^j \Big/ \sum_{j=0}^{n} b_j s^j . \tag{2.4}$$

If the coefficients in equation (2.4) are constant, then, since one may assume zero initial conditions, the equation can be rewritten formally as (37)

$$H(s) = \mathfrak{L}\left[\sum_{j=0}^{n-1} a_j p^j \Big/ \sum_{j=0}^{n} b_j p^j \right] \tag{2.5}$$

where $\mathfrak{L}[\cdot]$ and p are the Laplace and differential operators respectively. On substituting (2.5) in (2.3) one finds that the inverse transform is

$$\sum_{j=0}^{n} b_j p^j y = \sum_{j=0}^{n} a_j p^j x$$

i.e.

$$py = \sum_{j=0}^{n-1} p^{j-n+1}(a_j x - b_j y) . \tag{2.6}$$

Since the operator p^{-1} represents an integrator, it is seen that equation (2.6) requires only a set of integrators and summers to generate the required output. Amplitude and time scaling are conveniently done on the computer diagram.

Using (2.2) it has been shown that a reasonable random pro-

cess representing past earthquakes has the spectral density[14,15, 38,39]

$$G(\omega) = \frac{\rho^2}{3\pi} \cdot \frac{c^4 + 4b^2c^2\omega^2}{(c^2-\omega^2)^2 + 4b^2c^2\omega^2} \tag{2.7}$$

where $b^2 = 0.410$; $c^2 = 242$ and ρ is a scale factor. The stationary random process (2.7) was generated on an analog computer using a single linear filter with a white noise input. The white noise, generated by a Hewlett-Packard model 3722A Noise Generator, is Gaussian, with zero mean, fixed r.m.s. level of 3.16 volts, fixed power output of 10 volts and a bandwidth from d.c. to a variable cutoff frequency. The noise may be either truly random or any one of several repeatable pseudo-random sample functions. Appendix I gives further details of the noise generator; and the actual experimental setup.

It is of interest in the studies following to examine some properties of the simulated process. To do this two of the repeatable sample functions were digitized for processing on the digital computer. Figures 2.1 and 2.2 show these sample functions, their rate of approach to a stable standard deviation and their auto-correlation functions. These are compared to the corresponding analytical values given by

$$\phi(\tau) = \int_0^{\omega_f} G(\omega) \cos \omega\tau \, d\omega \tag{2.8}$$

$$\sigma_y = [\phi(0)]^{\frac{1}{2}} = 2.21 \tag{2.9}$$

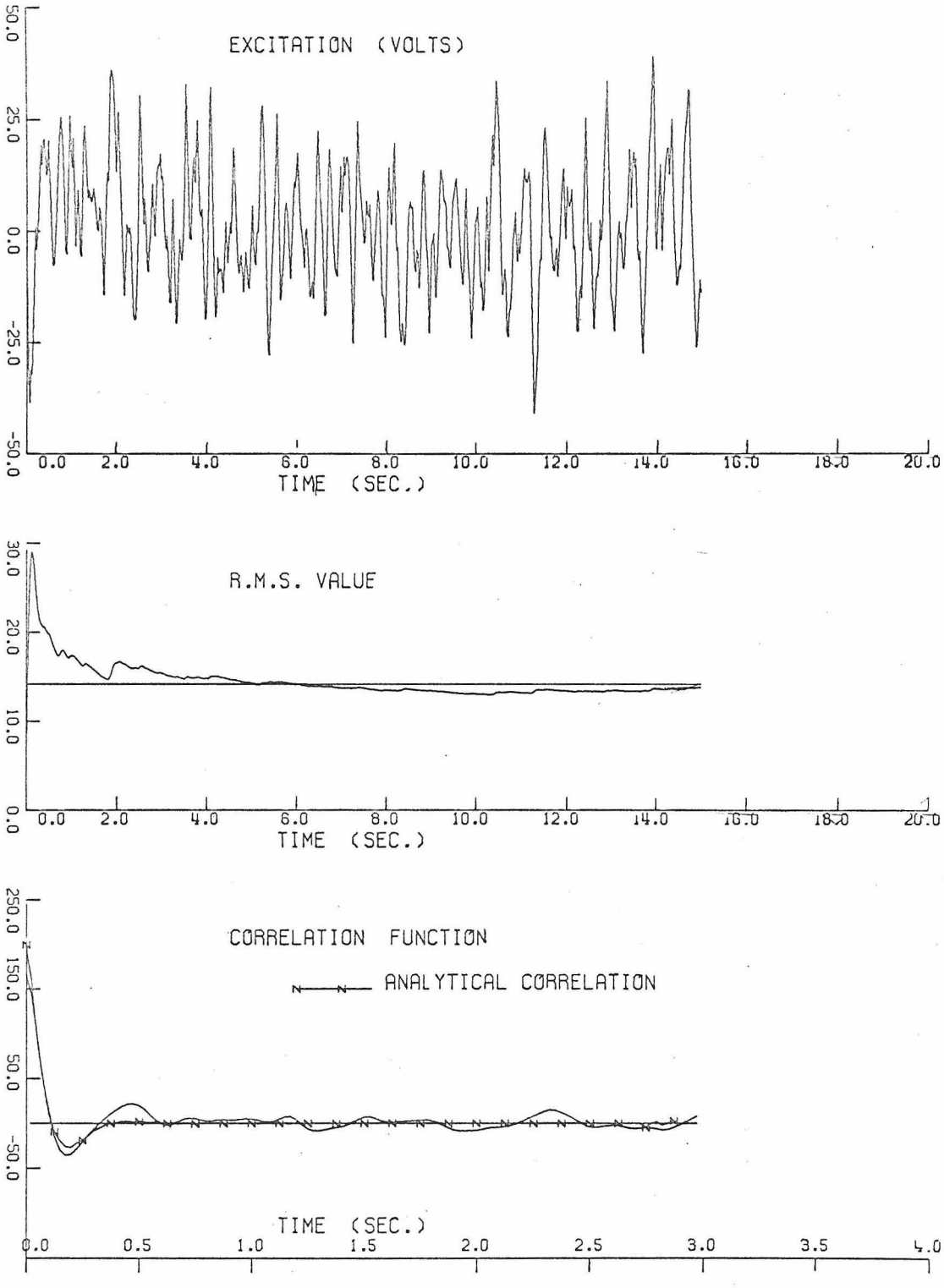

Fig. 2.1 PROPERTIES OF PSEUDO-RANDOM FUNCTION (N=8191)

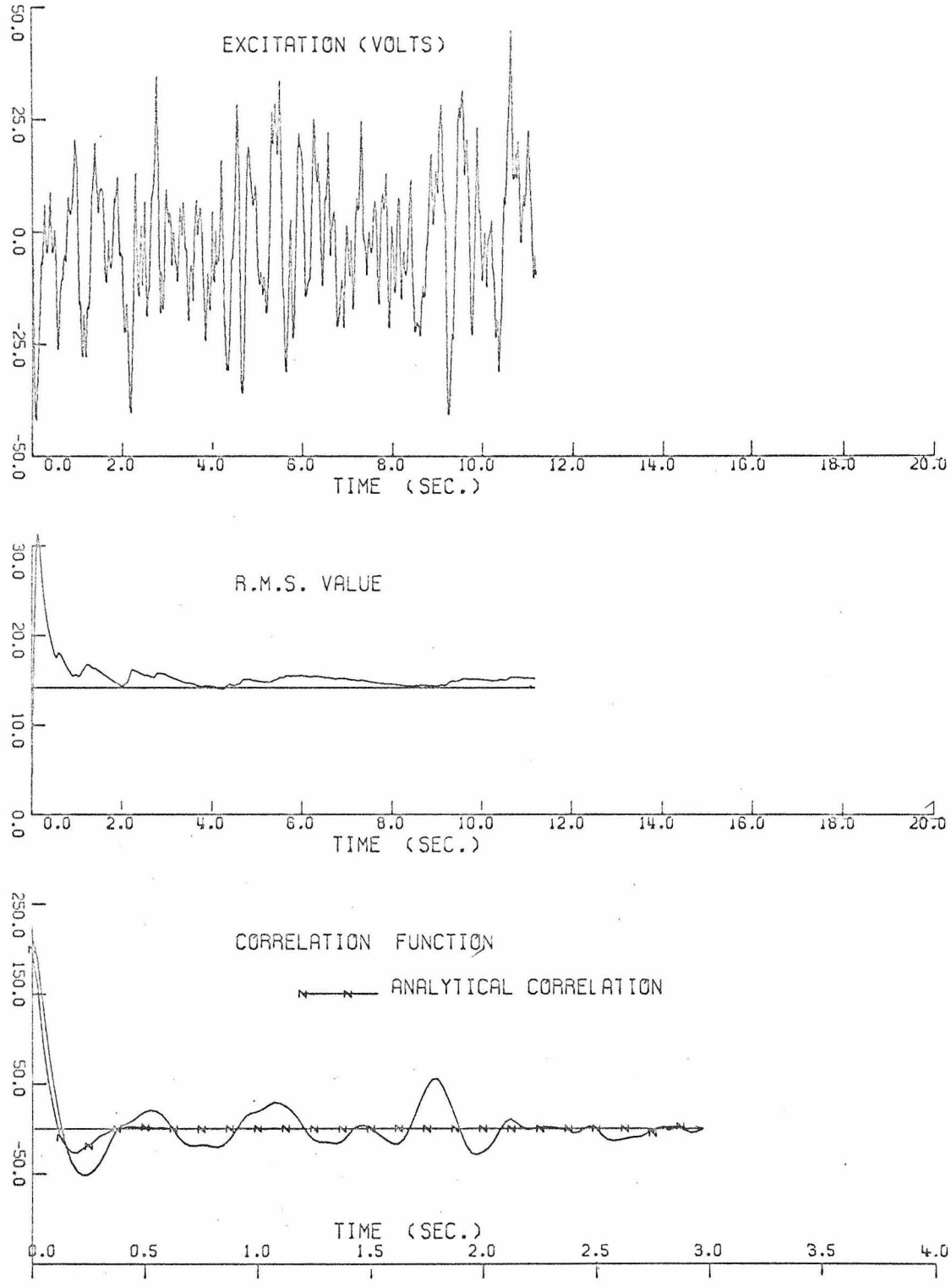

Fig. 2,2 PROPERTIES OF PSEUDO-RANDOM FUNCTION (N=16383)

where ω_f is the cutoff frequency of the white noise input, set at 15 Hz, and its spectral density is $10/\omega_f$. For sample excitations digitized at equal intervals, the correlation function becomes

$$\phi(k\Delta t) = \frac{1}{N}\sum_{j=2}^{N-k}\left\{y_{j-1}y_{j+k-1} + \frac{1}{2}(s_j y_{j+k-1} + s_{j+k}y_{j-1})\Delta t + \frac{1}{3}s_j s_{j+k}\Delta t^2\right\} \tag{2.8a}$$

where $N\Delta t$ is the duration of the record and

$$s_j = (z_j - z_{j-1})/\Delta t \ .$$

It is seen that the standard deviation settles down remarkably rapidly, being within 10% of its mean value in less than 1 second. Furthermore, it does not fluctuate beyond this narrow range after that time. The accuracy of the simulation procedure is indicated by the closeness of the observed mean values to the predicted value of 14.16 volts. This error of less than 10% was verified by several spot-checks using a random-noise voltmeter with an averaging time of 100 seconds.

The correlation functions show significant correlation over only about a half second, though they fluctuate higher than the analytical correlation for longer times. However, such fluctuations are to be expected in any individual sample functions. Quite similar correlation functions have been observed for several strong earthquakes (25,36).

Comparing this correlation time with the observed rate of zero-crossings of approximately 9 per second, one may conclude that the process can be adequately represented by uncorrelated

random pulses with an arrival rate equal to the rate of zero crossings. The applicability of such a model will also depend, of course, on the characteristics of the system being excited. As an example, Ward[16] has shown that while the response spectrum of an undamped oscillator is radically different for white noise and filtered white noise excitations, those of viscously damped oscillators seem insensitive to the difference in excitation; provided their spectral densities are nearly equal in the neighborhood of the oscillators' resonant frequency.

It can also be concluded that relatively short samples of the process, longer than 4 sec., say, may be adequately characterized by the average properties of the whole process. Equation (2.2) shows that the spectral properties of the process may be demonstrated by its undamped velocity spectrum. This is considered in the following section, as well as the Fourier amplitude spectrum.

B. Response of Linear and Elastoplastic Single Degree of Freedom Systems

Investigations of structural response to random excitation have been primarily focused on the response of single degree of freedom systems. Apart from the relative analytical simplicity of such models, the results obtained from them give insight into the response of more complicated structures and may be used to compute the response of multi-story structures[42,43]. Since the object of these studies was not the collapse of the structures, the effect of gravity was usually neglected and emphasis was placed on the maximum value of the response; in particular, the velocity and pseudo-velocity

spectra defined earlier. In such a case, the equation of motion for a viscously damped, one degree of freedom oscillator takes the form

$$m\ddot{x} + c\dot{x} + kf(x,\dot{x}) = - mg(t)$$

where x is the displacement of the mass m relative to its base, $g(t)$ is the base acceleration, c is the amount of viscous damping, k the spring restoring force and $f(x,\dot{x})$ is the general, non-linear form of the spring force. Defining the natural frequency, ω_o and per cent of critical damping n by

$$\omega_o \equiv \sqrt{k/m} \quad , \quad n \equiv c/2\sqrt{km}$$

gives

$$\ddot{x} + 2n\omega_o\dot{x} + \omega_o^2 f(x,\dot{x}) = - g(t) \ . \qquad (2.9)$$

Equation (2.9) was simulated on an analog computer for both a linear and an elastoplastic system. The elastoplastic system has a unit yield level and was simulated by an integrator with its output voltage limited. The simulation is described in the appendix. The random acceleration input's spectral density is given by equation (2.7). The experimental procedure used was to generate a continuous function for $g(t)$ and then apply this to the analog model of the oscillator for a fixed interval of time during which the maximum response is measured. This procedure makes it unnecessary to set random initial conditions on the linear filter used to generate $g(t)$. The effect of the offset voltages of the circuits used to measure the

maximum amplitude was obtained by plotting several of the responses of a Brush Recorder and comparing their maximum values with the meter values. These consistently showed a difference of between -0.7 and -0.9 volts, hence the net offset voltage was taken as -0.8 volts. No frequency dependence was observed in the offset. This procedure also confirmed the design criterion that the meter should react fast enough to record sharp peaks in the response. The expected error in the meter readings of about 0.1 volts compares with actual readings ranging from 2 volts to 11 volts. A negative damping factor--between 0.1 and 0.15%--was found to be necessary in the case of undamped oscillators. This error was thought insignificant for the 2% damped oscillators.

Linear Oscillators

For a linear oscillator, equation (2.9) becomes

$$\ddot{x} + 2n\omega_o\dot{x} + \omega_o^2 x = - g(t). \qquad (2.9a)$$

Its power spectral density is simply

$$S(\omega) = G(\omega) \cdot |H_x(\omega)|$$

$$= G(\omega) / \left\{ (\omega_o^2 - \omega^2)^2 + 4n^2\omega_o^2\omega^2 \right\} . \qquad (2.10)$$

The pseudo-velocity response of this oscillator was obtained as outlined above for periods ranging from 0.3 seconds to 2.5 seconds and for damping factors of 0.0 and 0.02. This period range covers the observed range of periods of the fundamental modes of most

structures. The damping factors were chosen to reflect the qualitative difference, if any, in the distribution of response of undamped and viscously damped oscillators. It was expected that the former would be more sensitive to the distribution of peaks in the excitation. Higher values of damping were not used since past studies suggest that these will give qualitatively the same response as the 0.02 damping. Enough samples were obtained for each value of period and damping to assure that the response mean and variance had stabilized. It is noteworthy that this required at least 300 samples in each case. The stability of these values, and the repeatability of the whole experiment was checked and confirmed by repeating the readings for some cases. These deviated by less than 2% for the means and 5% for the variance.

The results of these studies are presented in figures 2.3 and 2.4 and Tables 2.1 and 2.2. The points on the distribution functions represent the midpoints of the tops of the steps of the histograms computed at one-eighth of the mean value. This assures that an average histogram step has about 20 sample points. To account for small experimental variations, a weak smoothing was performed on the histograms. This was of the form

$$f_j = 0.5 f_j + 0.25 (f_{j+1} + f_{j-1}) \qquad (2.11)$$

where f_j is the value of the j^{th} step of the histogram. The figures also include the projected variation of maximum response with period; plotted at varying fractions of the mean maximum response. Approxi-

mate extensions of the plots to low periods were made on the basis of the fact that the maximum response approaches zero as the period approaches zero.

One may examine certain analytical solutions for comparison with these observations. The probability that the maximum value of some response property, $r(x,\dot{x})$, is R may be obtained by considering the distribution function

$$F_r(R) = p(r \leq R \,|\, 0 \leq t < s) ,$$

i.e. the probability that r does not exceed a barrier at R for the duration of excitation, s. The solution to this problem may be obtained either by solving the barrier problem for the transition probability of equation (2.9a)[30] or by using approximate expressions for either the rate of threshold crossings of the peak distribution of the response r[25,40,41]. A solution has been obtained by Rosenblueth and Bustamante[29] for the quantity

$$r^2 = (\omega_o x)^2 + \dot{x}^2 .$$

It was shown that if the excitation is a white noise of intensity k, then the distribution function for an undamped oscillator is

$$F_r(R) = 2 \sum_m \exp\left\{ - ks\lambda_m^2 / R^2 \right\} / \lambda_m J_1(\lambda_m) , \qquad (2.12)$$

where J_o and J_1 are Bessel functions of the first kind and the λ_m are zeros of J_o. Using (2.12), the density function and mean become

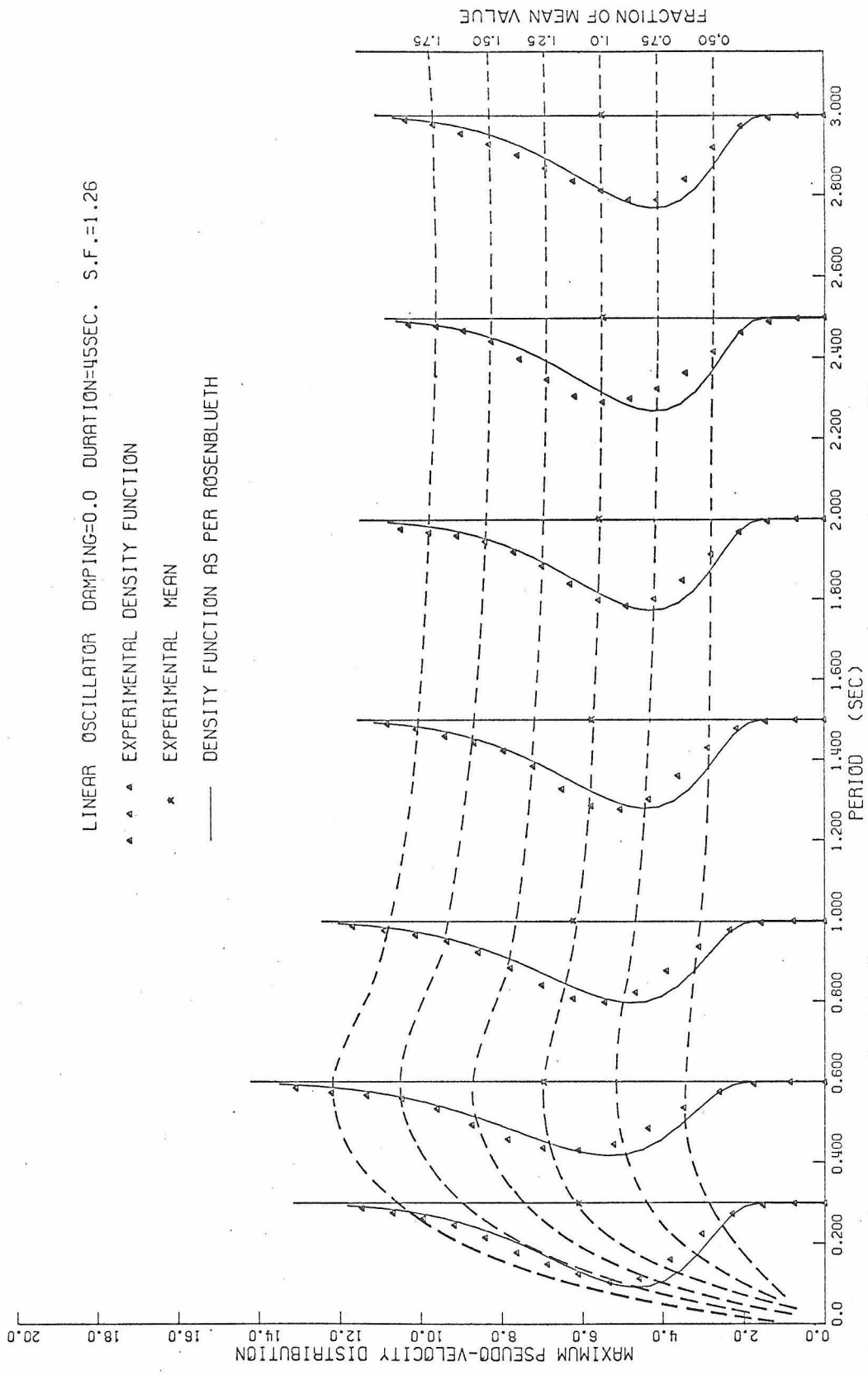

Fig. 2.3 Distribution of Pseudo-velocity of Undamped Linear Oscillator

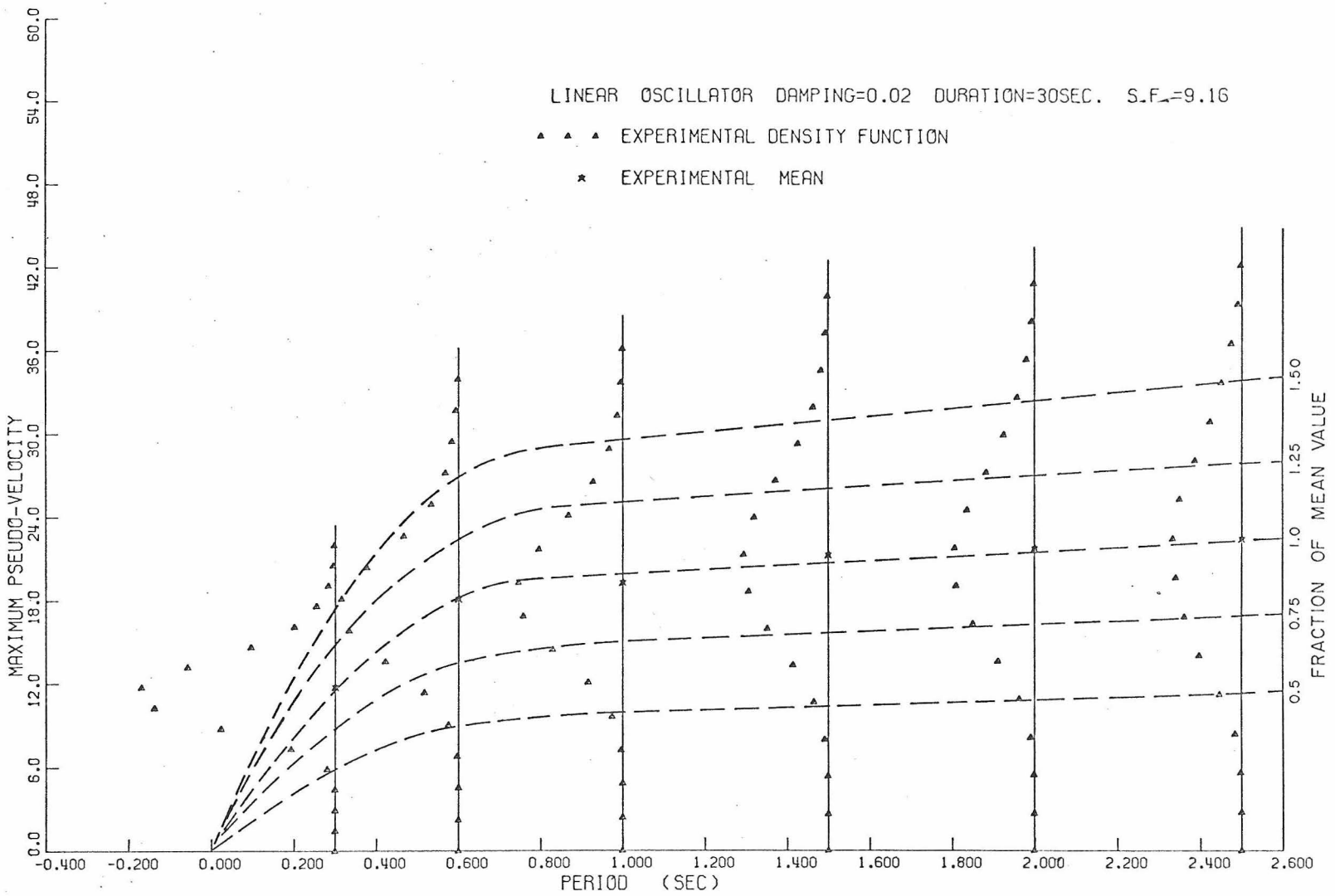

Fig. 2.4 Distribution of Pseudo-velocity of Damped Linear Oscillator

$$f(R) = (4ks/R^3) \cdot \sum_m \lambda_m \exp\left\{- ks\lambda_m^2/R^2\right\} /J_1(\lambda_m) \qquad (2.13)$$

and

$$\langle R\rangle = 2.348\sqrt{ks} \ . \qquad (2.14)$$

In the study by Caughey and Gray[30], it was concluded that this solution may be applied to an input with a more general spectral density provided it is slowly varying in the neighborhood of the resonant frequency ω_o, and the duration s is much greater than the oscillator's period. Then the intensity function becomes

$$k = G(\omega_o) \ . \qquad (2.15)$$

Furthermore, the results in equations (2.12) - (2.14) will apply to the pseudo-velocity response of the process given by equation (2.7) whenever the assumption on long duration is satisfied; since it has been observed that the maximum response of an undamped oscillator usually occurs well after the start of the excitation. These results are compared with the experimental results in table 2.1 and figure 2.3. It was observed that the summation in equation (2.13) need only be carried to a small finite number (≤ 20) as the convergence is rapid whenever $f(R)$ is significantly different from zero. In figure 2.3 the mean of the theoretical curve has been adjusted to that of the experimental curve in order to facilitate comparison of the density functions.

TABLE 2.1

Pseudo-velocity of Undamped Linear Oscillator $\rho = 1.26$

Period	$\langle S_v \rangle$	σ_{S_v}	$\langle R \rangle$	$\sigma/\langle S_v \rangle$
0.3	6.11	1.97	6.76	0.322
0.6	6.97	2.24	8.36	0.321
1.0	6.22	1.91	7.40	0.322
1.5	5.75	1.78	6.91	0.309
2.0	5.58	1.91	6.72	0.342
2.5	5.48	1.78	6.63	0.325
3.0	5.52	1.77	6.58	0.321

It is seen that the variation with period of the mean values of both the experimental and theoretical spectra agree very closely with the average spectrum from which the excitation was derived[44] i.e. there is a sharp rise up to about 0.5 seconds, then an almost exponential decay to a constant value after 2.0 seconds. However, the actual magnitudes of these means differ by 10 to 20%, though the difference is less than 1 standard deviation in all cases. A better agreement is observed between the predicted and experimental density functions.

While it has thus been shown that the analysis by Rosenblueth and Bustamante[29] predicts the response of an undamped oscillator within acceptable limits, the functional forms of the results are fairly complicated and become even more so for the damped oscillator. It is therefore of interest to consider simpler, approximate solutions using comparable assumptions. A general threshold crossing problem is considered in chapter 3 but it will suffice to

consider the well known results for a constant barrier here.

Whenever the necessary derivative exists, it can be shown[40, 41] that the expected rate at which a weakly stationary process crosses a threshold at a constant level R is

$$\nu(R) = \int_{-\infty}^{\infty} |\dot{x}| p_{X\dot{X}}(R,\dot{x})\, d\dot{x} \ .$$

In particular, if $x(t)$ is a stationary Gaussian process with zero mean, the above joint density function becomes

$$p_{X\dot{X}}(R,\dot{x}) = \frac{1}{2\pi\sigma\sigma_1} \exp\left\{-\frac{R^2}{2\sigma^2} - \frac{\dot{x}^2}{2\sigma_1^2}\right\}$$

giving

$$\nu(R) = \frac{\sigma_1}{\pi\sigma} \exp\left(-R^2/2\sigma^2\right) \qquad (2.16)$$

where σ^2 and σ_1^2 are the displacement and velocity variances defined by

$$\sigma^2 = \int_0^{\omega_f} S(\omega)\, d\omega \doteq \int_0^{\infty} S(\omega)\, d\omega$$

$$\sigma_1^2 = \int_0^{\omega_f} \omega^2 S(\omega)\, d\omega \doteq \int_0^{\infty} \omega^2 S(\omega)\, d\omega \ .$$

If it is now assumed that the threshold crossings are independent[19, 20], they become a Poisson process with stationary increment $\nu(R)$. The expected time to one crossing is then[6]

$$E[T] = 1/\nu(R) \ , \qquad (2.17)$$

A straightforward scheme for obtaining bounds on R is to choose R such that

$$E[T] \leq s < 2E[T], \tag{2.18}$$

i.e. the expected 'waiting times' to one and two crossings respectively[33]--equation (3.14). Substitution of equations (2.16) and (2.17) in (2.18) leads to the bounds

$$\sqrt{2 \ln [s\nu(0)/2]} \quad < \quad R/\sigma \leq \sqrt{2 \ln [s\nu(0)]} \, . \tag{2.19}$$

The same bounds have been obtained recently by Yamada and Takemiya[25] from considerations of the response peaks; using the heuristic approach of Huston and Skopinski[45] for lightly damped systems. Although the assumption that the threshold crossings of a narrow band process are independent is questionable in general[20], the demand of equation (2.18) that there be at most two crossings in the time interval s--s >> P--forces R to be so high that considerations of envelope crossings, peak crossings and clumps in threshold crossings should give comparable results. In particular, the approximate analysis of Yamada and Takemiya applies exactly to the case of envelope crossings when the response process is Gaussian[22].

Table 2.2 shows that the bounds in equation (2.19) are very close although both bounds are higher than the observed values. These bounds may serve as conservative estimates of the expected mean maximum response. The disadvantage in the approach used to derive them is that nothing can be said about the distribution of this peak

response since no solution exists for the probability distribution of the time to threshold crossings.

TABLE 2.2

Pseudo-velocity of 2% Damped Oscillator, $\rho = 9.16$

Period	$\langle S_v \rangle$	σ_{S_v}	R_{min}	R_{max}	$\sigma/\langle S_v \rangle$
0.3	11.74	2.13	13.03	14.00	0.182
0.6	18.12	3.58	20.76	22.52	0.198
1.0	19.26	4.00	22.26	24.38	0.208
1.5	21.28	4.96	23.90	26.52	0.233
2.0	21.77	5.32	25.53	28.61	0.244
2.5	22.48	6.17	26.98	30.53	0.274

Elastoplastic Oscillator

The investigation of the elastoplastic oscillator was made principally to examine the feasibility of using equivalent, linear oscillators. Earlier work on this problem has considered the stationary response of the oscillators using the method of equivalent linearization[35,50-52] and equivalent, viscously damped linear oscillators[34,36]. Here, the elastoplastic response will be compared to the predicted response of viscously damped linear oscillators using the results obtained earlier.

The maximum absolute displacement of the elastoplastic oscillator was measured for 300 sample excitations lasting 30 seconds each; and for natural periods from 0.5 to 2.5 seconds. The excitation level was selected to give yield ratios between roughly 2 and 10.

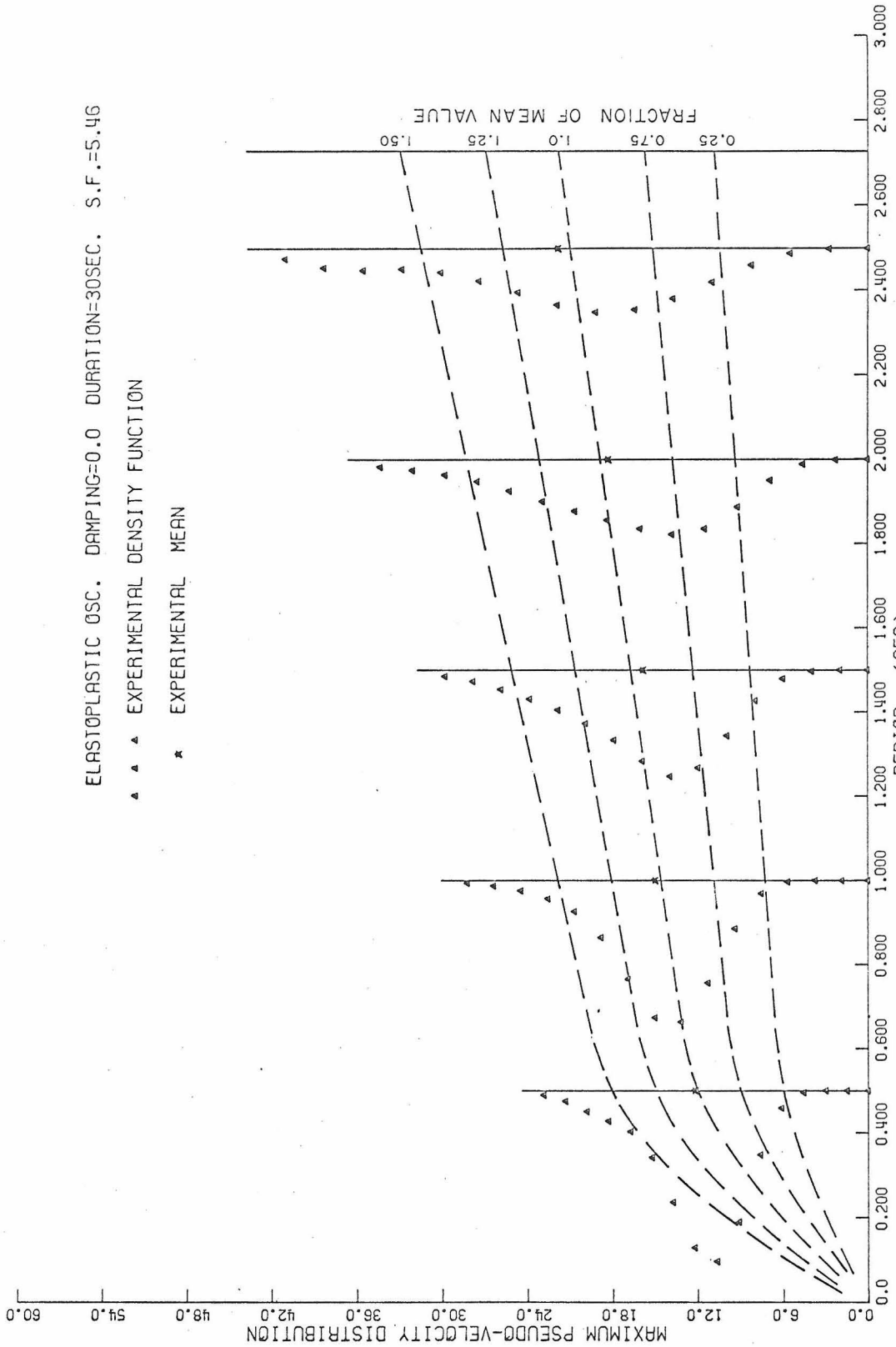

Fig. 2.5 Distribution of Pseudo-velocity of Elastoplastic Oscillator

Table 2.3 shows the observed mean maximum absolute displacement, the standard deviation and values for linear oscillators as given by the lower bound in equation (3.19). The distribution of pseudo-velocity is shown in figure 2.5 to facilitate comparison with linear responses.

TABLE 2.3

Comparison of Displacements of Undamped Elastoplastic Hysteretic Oscillators with Predicted Displacements of Viscous Damped Linear Oscillators

Period	$\langle x_m \rangle$	σ_{x_m}	Predicted x_{min} n=0.015	Predicted x_{min} n=0.02	$\sigma_x/\langle x_m \rangle$
0.5	0.971	0.237	1.08	0.94	0.244
1.0	2.39	0.58	2.44	2.10	0.243
1.5	3.78	1.17	3.93	3.40	0.309
2.0	5.81	2.45	5.59	4.84	0.422
2.5	8.67	3.20	7.39	6.39	0.370

The significant observations from these results are: (1) the elastoplastic oscillator's mean response may be adequately represented by that of a linear oscillator with about 1.5 or 2% damping; (2) this equivalence seems to be slightly dependent on the natural period, especially with regard to the dispersion in the response. Hudson[34] has aptly noted that such low damping values should be expected for random excitations since the oscillator yields, and energy energy is dissipated, only a small fraction of the excitation's

duration.

One should note in applying these conclusions that the displacements of both oscillators depend on their natural period and the duration of excitation. It has been shown[36] that, for long periods and excitations, the dependence on duration is approximately linear in both cases.

Fourier Amplitude Spectrum

Although pertinent information may be obtained from the undamped response spectrum, the frequency distribution's average energy is most directly measured by its Fourier amplitude spectrum. The square of this amplitude may be viewed as the power spectral density of the excitation[53]. Hence extensive use has been made of Fourier Spectra. However, since very few sample functions were used to derive these spectra they tend to show very wide fluctuations[18]. It is of interest, therefore, to investigate the existence of a mean spectrum, and its density function; and to compare these with the undamped pseudo-velocity spectrum.

If each sample lasts for a finite time s, and it can be assumed that the excitation process is ergodic, then its Fourier transform is

$$F_g(\omega) = \int_0^s g(\tau) e^{i\omega\tau}\, d\tau. \qquad (2.20)$$

The magnitude of this transform may be obtained from the response of an undamped oscillator which, from equation (2.9a) is given by the convolution integral [6,22]

$$x(t) = \int_0^t g(\tau)h(t-\tau)\, d\tau \qquad (2.21)$$

where $h(t)$, the impulse response of the oscillator, is

$$h(t) = -\frac{i}{\omega_o} e^{i\omega_o t} \qquad t > 0 \ .$$

In particular, for $t \geq s$, the response becomes

$$x(t) = -\frac{i}{\omega_o} \int_0^s e^{i\omega_o(t-\tau)} g(\tau)\, d\tau$$

$$= -\frac{i}{\omega_o} e^{i\omega_o t} F_g(\omega_o) \qquad t \geq s$$

hence the magnitude of the response is

$$|x(t)| = \frac{1}{\omega_o} |F_g(\omega_o)| \qquad t \geq s . \qquad (2.22)$$

Thus the free vibration of an undamped oscillator, measured after the cessation of excitation, gives the latter's Fourier amplitude coefficient, at the oscillator's natural period.

The experimental procedure is therefore identical to that of the undamped oscillator except for the use of a different switching arrangement. This permits the analog model to oscillate freely for at least five cycles after the excitation has been removed. The maximum pseudo-velocity of this free oscillation is measured as usual. A block diagram of the system is given in the appendix. It was found that at least 600 samples had to be used at each frequency

to obtain a satisfactorily stable mean. Since quite low voltages were recorded, one should recall that the measuring process is accurate only to within 0.1 volt, though the effect of this error should be negligible.

TABLE 2.4

Fourier Amplitude Spectrum

P	$\langle F_g(P) \rangle$	σ_F	$\sigma_F / \langle F \rangle$	$\langle S_v \rangle$
0.3	5.70	2.98	0.52	9.31
0.6	5.92	3.06	0.52	10.61
1.0	5.71	2.79	0.49	9.48
1.5	5.42	2.71	0.50	8.76
2.0	5.36	2.82	0.53	8.50
2.5	5.26	2.61	0.50	8.35
3.0	5.05	2.66	0.53	8.40

In general, table 2.4 shows that the mean Fourier amplitude spectrum has essentially the same shape as the undamped pseudo-velocity spectrum, although, unlike the latter, it shows no sign of peaking at any period. For the range of periods considered, the spectra are related approximately as

$$\langle S_v(P,0) \rangle \doteq 1.65 \langle F_g(P) \rangle . \qquad (2.23)$$

This compares with equation (2.2). However a most radical differ-

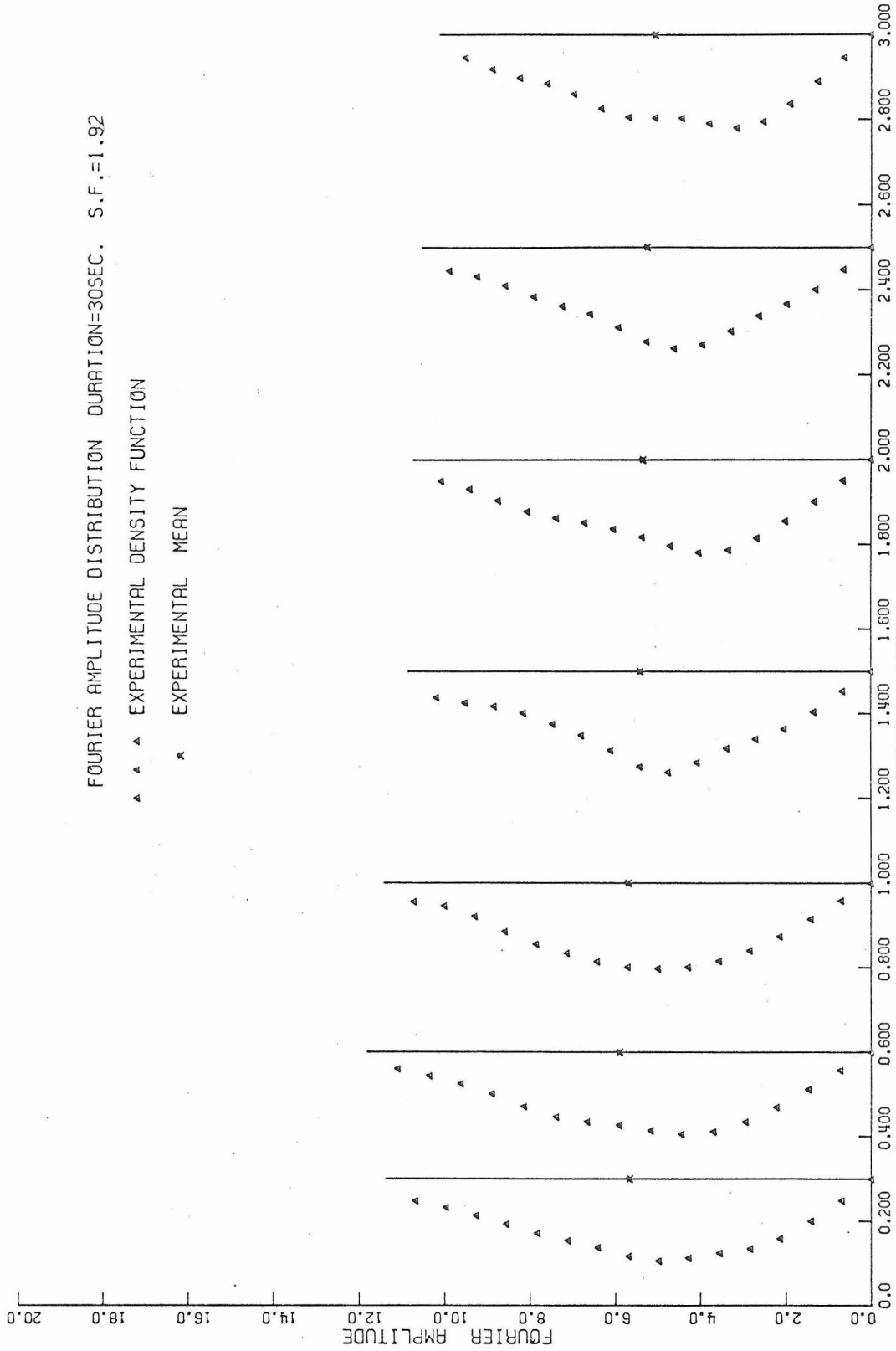

Fig. 2.6 Distribution of Fourier Amplitude Spectrum of Excitation

ence is observed in their density functions--figures 2.6 and 2.3. While the ratio of standard deviation to mean value of the Fourier spectrum is only about half, it can be seen that values one standard deviation removed from the mean have a relatively high probability of occurrence. This explains the wide fluctuations observed in measurements of Fourier spectra from few sample excitations and makes the use of approximate relations like (2.23) appealing.

C. Summary and Conclusions

The problem of using an electronic analog computer to generate a random process whose spectral density is known was considered. It was shown that analog linear filters can be designed directly from this spectral density. In lieu of necessary measuring equipment, the properties of the process can be obtained by digitizing a few sample functions and analyzing them on the digital computer. This hybrid method permits checks on the accuracy of subsequent analog simulations. In this way it was found that a process designed to represent average properties of some past earthquakes has a rate of zero crossings of about 9 per second, a correlation time of about a half second, and can be adequately represented by sample functions of more than four second duration. Such information determines restrictions on the use of the process.

The structural properties of this type of excitation were next investigated using the method of response spectra and considering analog models for linear and elastoplastic single-degree of freedom oscillators. It was found that at least 300 sample functions were

needed to establish a stable mean value for the response spectra. The means of the linear oscillators agree in general outline with the mean spectra from which the excitation process was derived. Additionally, it was possible to exhibit the probability density functions of the spectra. The damped linear oscillator and the elastoplastic oscillator showed fairly symmetric, near-normal distributions while the undamped density functions were skewed to the right. Ratios of standard deviation to mean of between 0.2 and 0.5 were observed.

The wide spread observed in these distributions is very significant in evaluating the reliability of structural studies which use only a single earthquake accelerogram or a few sample excitations. The weight assigned the results of such deterministic studies have to consider the number of samples and the degree of randomness in their choice. In particular, one expects an ensemble of real earthquakes to give even wider dispersions in response than those obtained here for a well-defined process.

An attempt to compare these results with analytical solutions showed that the solution given by Rosenblueth and Bustamante for white noise excitations and extended by Caughey and Gray to more general spectral densities gives a good fit to the density functions of the undamped oscillator but a conservative estimate of their mean values. A method of estimating the mean maximum response of damped oscillators was derived by considering the mean rate of threshold crossings of the response. The conditions of derivation

imply that similar results should be obtained by using either the peak distribution or the envelope crossing statistics of the response. Although it supposedly gave upper and lower bounds to the maximum response, both bounds turned out to be close but conservative estimates. Advantage was taken of this analysis to consider equivalent linear models for the elastoplastic oscillator. This confirmed earlier observations that a very low value of equivalent viscous damping was necessary but illuminated the highly approximate nature of such an equivalence.

The distribution of the Fourier amplitude spectrum of the excitation was also considered. Since this and the undamped pseudo-velocity spectrum can be related to the excitation's spectral density an attempt was made to find the relationship between them. An approximate linear relationship between the mean values was found though it must be noted that it is limited to a period range of between 0.3 and 3.0 seconds and that the density functions are radically different. Since values of Fourier spectra usually fluctuate more, one concludes that a better estimate for their mean value can be found by using the pseudo-velocity spectra in situations where few sample excitations are available.

Finally, although as many as 300 samples were used to calculate the mean maximum responses, it was noted that these values can be estimated to within 15% for as few as 75 samples. However, these estimates deteriorate rapidly as the number of samples is reduced.

CHAPTER III

FAILURE OF NON-LINEAR SINGLE DEGREE OF FREEDOM SYSTEMS WITH GRAVITY

A. Introduction and Definition of Problem

When interest is focused on exciting forces strong enough to cause the collapse of structures, simple linear structural models become inadequate. Furthermore, the instability of such structures reflects the biasing effect of gravity forces. Therefore, the failure of bilinear systems with gravity--both hysteretic and non-hysteretic--is considered in this and the following chapters. The aim is to examine the statistical distribution of the failure time of such structures and their underlying behavior as they approach failure.

Several investigators have considered the effect of gravity on structural response[46-48]. While it has been observed that small increases in the yield slope result in a much stiffer structure[46], the mechanism of collapse is unchanged. Consequently the present study, being interested principally in the overturning effect of gravity, considers bilinear systems with a flat yield level only. The single-degree of freedom model is shown in figure 3.1a. The girder, of mass m, and the massless columns, length ℓ, are considered rigid. Torsion springs couple the columns to the girder and the base. These springs have a net non-linear restoring moment of $KF(\phi, \dot{\phi})$ which is shown in figure 3.1b for the non-hysteretic case. The viscous damper is linearly related to the angular velocity $\dot{\phi}$.

The model is highly simplified in order to achieve relative

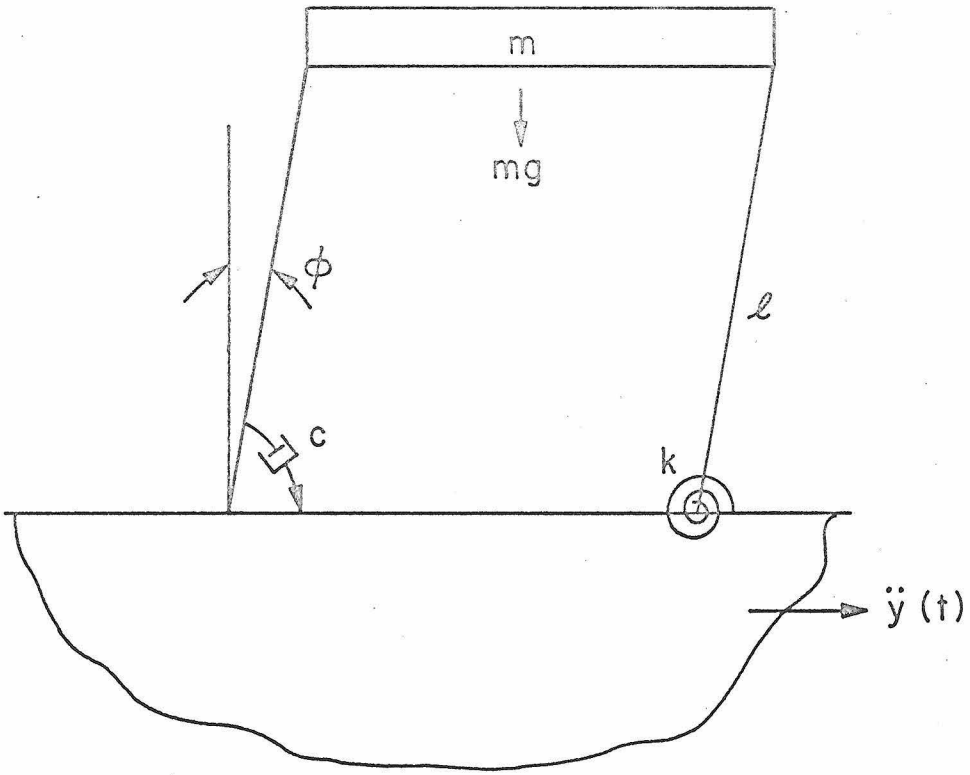

One Degree of Freedom Structure

Fig. 3.1a

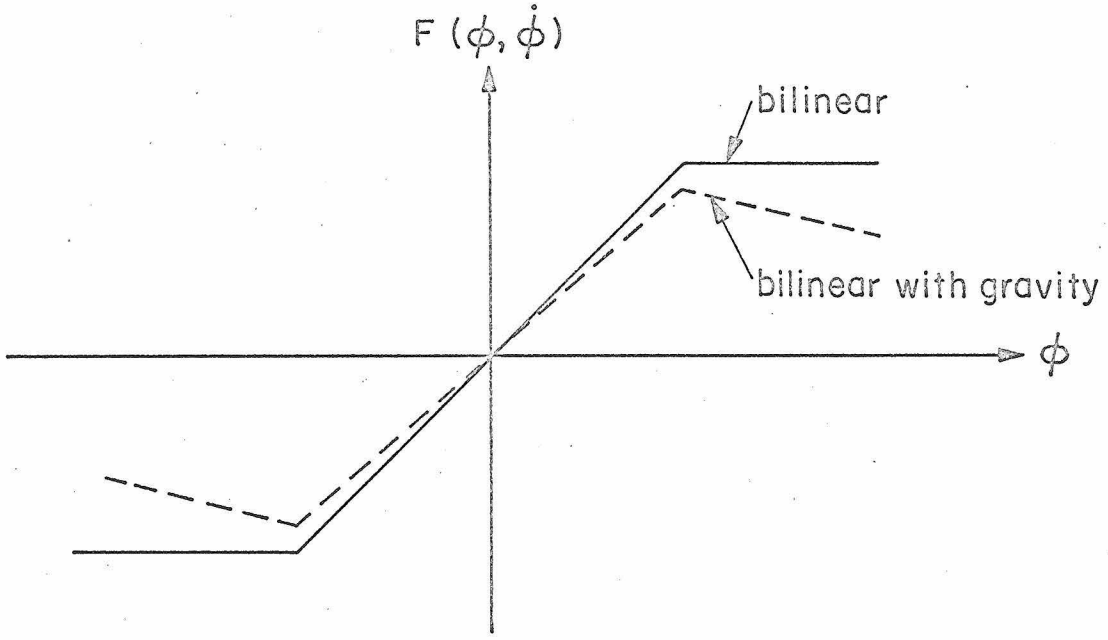

Restoring moment - Displacement relation

Fig. 3.1b

mathematical simplicity and to concentrate attention on the effect of yielding on the structure's failure. It neglects the effect of all but bending deformation of the columns, assumes that the structural motion is planar and that, even with gravity, girder rotation is negligible and girder buckling is not of immediate concern. The motion of the model is thus completely specified by its angle of rotation ϕ. One notes that no analytic solution has been derived for the response of even this simplified model to a stationary random excitation. The results of analog simulation studies are presented here and an approximate scheme for obtaining the mean failure time of the hysteretic model is presented in the next chapter.

The equation of motion of the model may be obtained from the Lagrangian equation

$$\frac{d}{dt}\left(\frac{\partial L}{\partial \dot{\phi}}\right) - \frac{\partial L}{\partial \phi} = Q_{\phi} , \tag{3.1}$$

where Q_{ϕ} is a generalized force including the non-conservative spring, dashpot and D'Alembert forces, and L is the Lagrangian. From figure 3.1a one obtains

$$L = \tfrac{1}{2}m(\ell\dot{\phi})^2 - mg\ell\cos\phi$$

$$Q_{\phi} = -KF(\phi,\dot{\phi}) - c\dot{\phi} - m\ddot{y}\ell\cos\phi \ .$$

Substitution in equation (3.1) gives

$$\frac{d}{dt}(m\ell^2\dot{\phi}) - mg\ell\cos\phi = -KF(\phi,\dot{\phi}) - c\dot{\phi} - m\ddot{y}\ell\cos\phi. \tag{3.2}$$

Define

$$\omega_o^2 \equiv \frac{K}{m\ell^2} - \frac{g}{\ell}; \quad n \equiv \frac{c}{2\omega_o m\ell^2}; \quad z \equiv \frac{\phi}{\phi_y} \tag{3.3}$$

where ϕ_y is the yield level of the springs. Then

$$\ddot{z} + 2n\omega_o\dot{z} + (\omega_o^2 + \frac{g}{\ell})f(z,\dot{z}) - \frac{g}{\ell\phi_y}\sin\phi = -\ddot{y}\cos\phi/\ell\phi_y \tag{3.4}$$

where $f(z,\dot{z})$ has a unit yield level and ω_o can be recognized as the natural frequency of small amplitude vibrations of the system. It is convenient to put this equation in non-dimensional form by defining the ratio of a measure of the excitation's magnitude to a measure of the structure's strength. Since the excitation process is defined by its power spectral density, equation (2.7); its magnitude is best measured by its r.m.s. value. Although direct integration gives an r.m.s. value of 2.21 for $\rho = 1$, a value of 0.697 is chosen to facilitate comparison with currently available sample functions[14, 46]. The base acceleration is thus specified by a factor γ such that

$$\ddot{y}(t) = \gamma x(t) \tag{3.5}$$

where $x(t)$ has a spectral density given by equation (2.7) and r.m.s. value of 0.697.

Similarly the structure's strength is measured by the level of acceleration torque necessary to initiate yielding in the springs. Examination of figure 3.1 gives this as

$$m\ell\ddot{u} = K\phi_y - mg\ell\phi_y,$$

i.e.

$$\ddot{u} = \ell \omega_o^2 \phi_y .$$

It is now possible to define a non-dimensional form of the excitation's relative intensity as

$$\theta \equiv \gamma g / \ddot{u} = \gamma g / \ell \omega_o^2 \phi_y . \tag{3.7}$$

Finally, one notes that failure of the model by collapse is equivalent to the crossing of a given level by the response, $z(t)$, without return. When the level is sufficiently high, this problem of an absorbing barrier may be replaced by the more tractable one of threshold crossing for, in such a case, the instability of the response will ensure that a negative crossing is highly improbable. As a practical matter, only the latter criterion can be simulated readily in an experiment; and, although the argument is heuristic, its validity is easily tested in an experiment.

Alternatively, one may define failure of the structure by the behavior of the r.m.s. value of the response. This has the dual advantage that it can be related to the energy of the structure and that it is often easier to consider in analytical work. However, the displacement is easier to measure in a simulation process and, furthermore, one does not expect the different measures to give qualitatively different results in the case of an unstable system.

The collapse level chosen is the angular displacement at which the model collapses statically. From figures (3.1a,b) this gives

$$z_c = K/mg\ell = 1 + \ell\omega_o^2/g \tag{3.8}$$

and is the point at which the restoring moment of the springs becomes zero. It was assumed in deriving equation (3.8) that ϕ is small enough enough such that $\sin\phi \doteq \phi$ even up to collapse. The validity of this and the choice of failure level has been confirmed by the studies of Husid[46]. In summary, then, the equation of motion becomes

$$\ddot{z} + 2n\omega_o\dot{z} + (\omega_o^2 + \frac{g}{\ell})f(z,\dot{z}) - \frac{g}{\ell}z = -\frac{\theta\omega_o^2}{g}x(t). \tag{3.9}$$

Hence the motion is completely specified by the damping factor, n, length ℓ, period P and intensity factor θ.

B. Response of Analog Models

To design an electronic analog model for equation (3.9) it is necessary to scale it such that the yield and collapse levels are high enough to minimize inherent errors in measurement and amplifier drift while being sufficiently low to prevent saturation of any equipment. This can be conveniently done by redefining z such that

$$z = \delta\phi/\phi_s \tag{3.10}$$

where ϕ_s is the collapse angle. The model now collapses at the fixed voltage, δ, in all cases while the yield level varies with length and period as

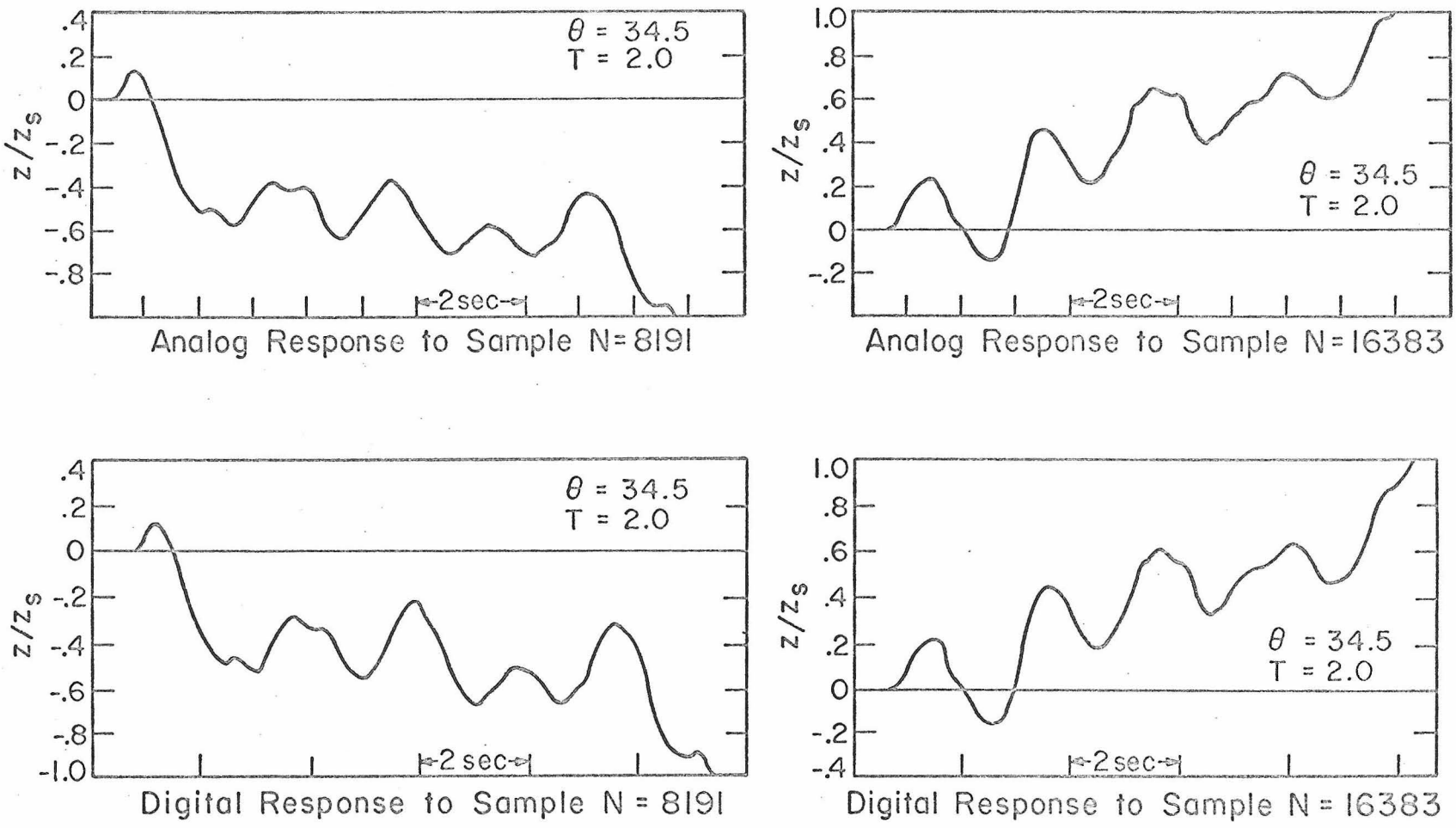

Fig. 3.2 Comparison of Digital and Analog Response of Elastoplastic System with Gravity

$$b = \delta\phi_y/\phi_s = \delta/\{1 + \ell\,\omega_o^2/g\}. \qquad (3.11)$$

If one now considers that the elastoplastic function generator yields at a level e_z, the scaled equation of motion becomes

$$\ddot{z} + 2n\omega_u \dot{z} + (\omega_o^2 + \frac{g}{\ell})\frac{b}{e_z} f\left[\frac{e_z}{b} y, \frac{e_z}{b} \dot{y}\right] - \frac{g}{\ell} z = -\frac{b\omega_o^2\theta}{g} x(t). \qquad (3.12)$$

The solutions of equation (3.12) are actually run at 0.1 real time by a straightforward time scaling of all integrators. Since amplifier drifts can be adjusted to less than 0.02 volts per second, and the solution time is less than 15 seconds in all cases, the scale factor, δ, depends only on the saturation voltage of the amplifiers. This is just over 50 volts so δ was chosen as 40 or 30 volts as convenient. A switching and timing system made it possible to accurately detect collapse of the model, reset and restart it and measure the time to collapse. Details of the circuitry are given in the appendix, which also examines the accuracy of the analog set-up with respect to the coefficients of equation (3.12). The values set for these are usually within a 5% error limit.

As a test of the effect of errors in the experiment--in particular that of the elastoplastic function generator--a comparison of the analog response with digital computer response was made using the two repeatable pseudo-random functions already digitized. Two sets of the results are shown in figure 3.2. Noting that the digitizing procedure is not error-free[18], the agreement between these responses was considered satisfactory.

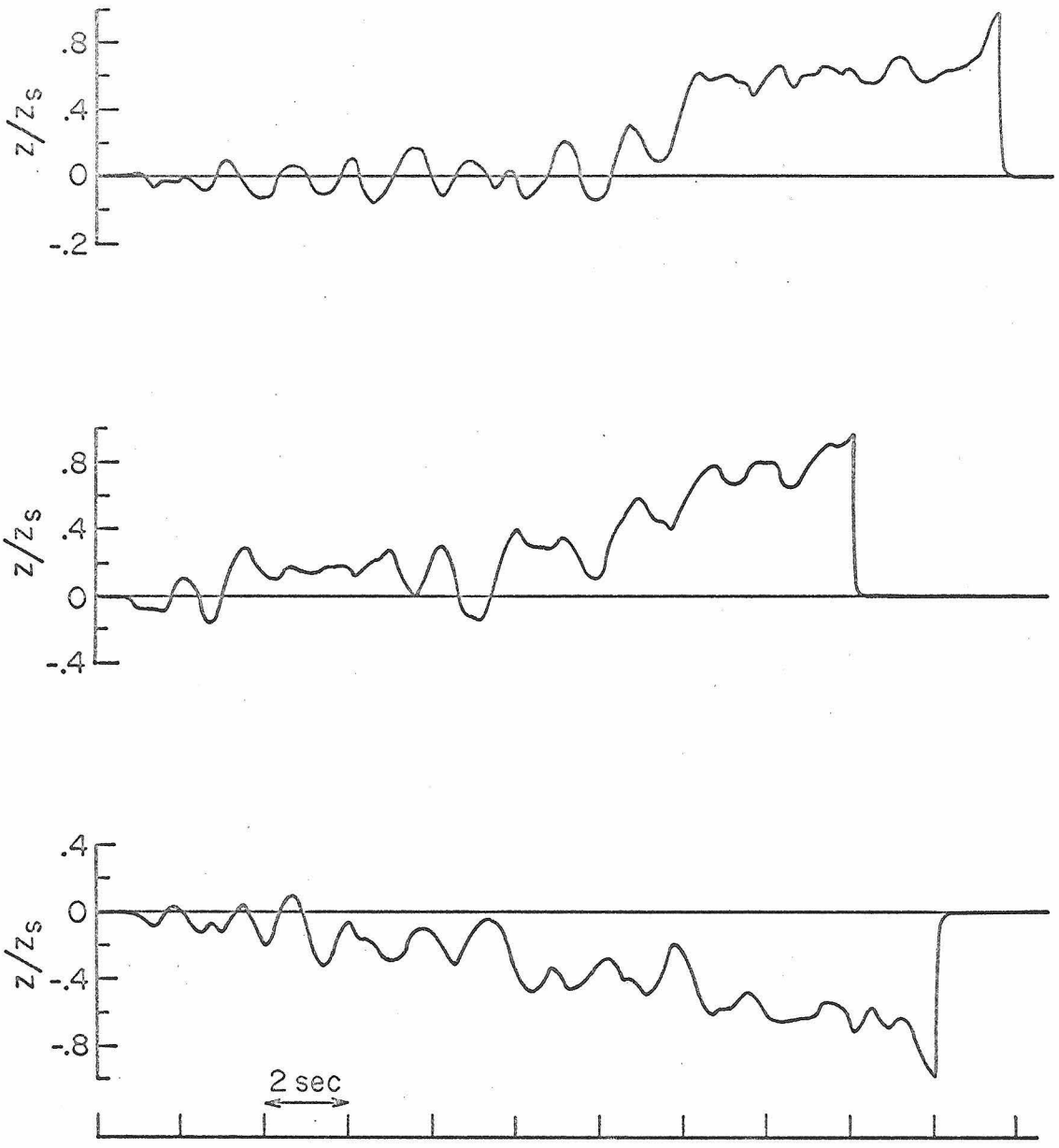

Response Samples: $N = \infty$, $\theta = 34.5$, $T = 2.0$

Fig. 3.3 Hysteretic Structure

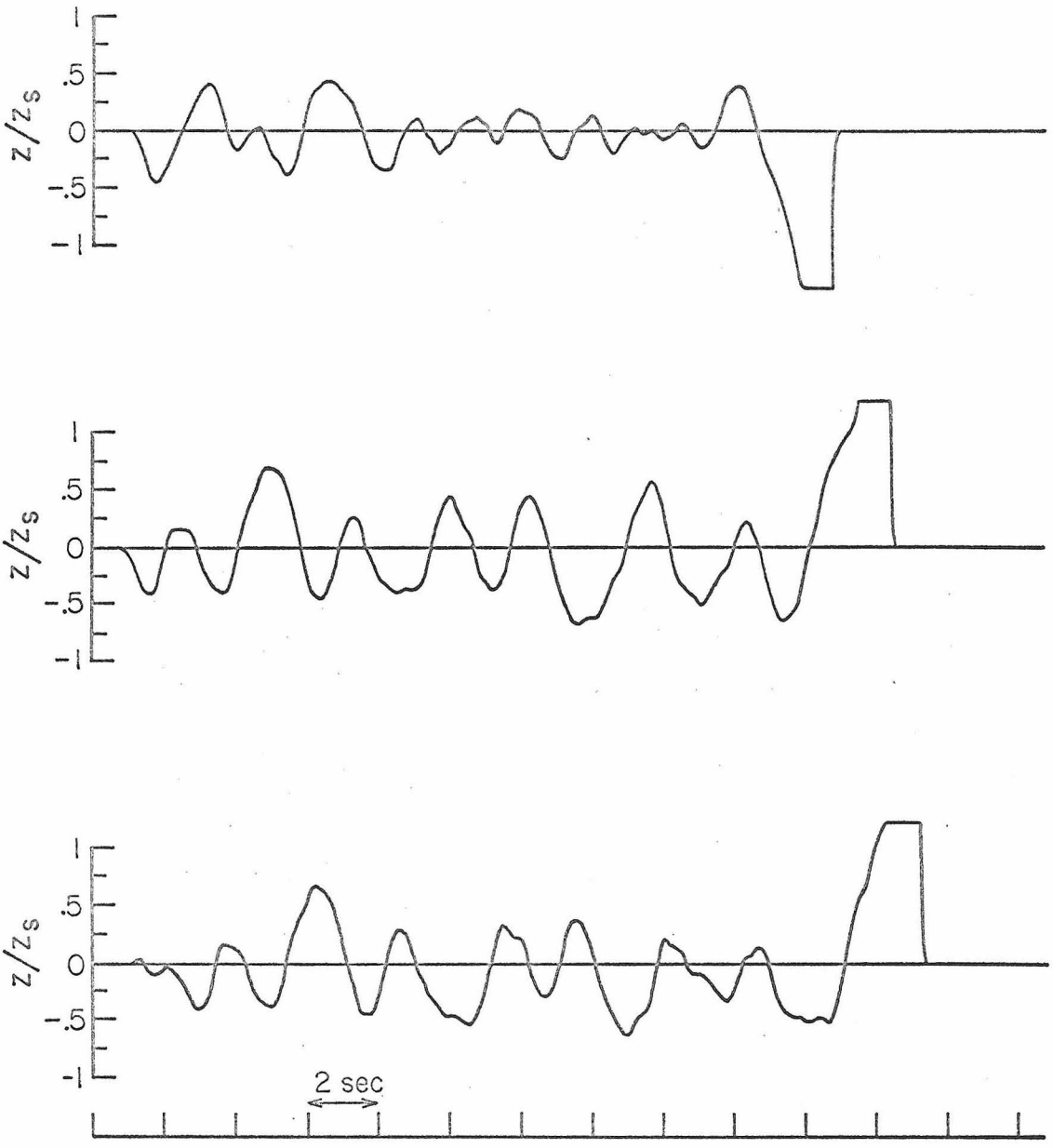

Response Samples: $N = \infty$, $\theta = 46.$, $T = 1.5$

Fig. 3.4 Non-hysteretic Structure

To limit the number of parameters, only the period and θ were varied. Because of interest in the collapse of buildings, representative values for the model's length and damping factor were chosen as 10 feet and 0.02 respectively[46,49]. Similarly, because of interest in the behavior of multi-story buildings, the period was varied between 1.5 and 2.5 seconds; the lower limit being imposed by the yield level of the elastoplastic function generator--6.15 volts, the saturation limit of the integrators--50 volts, and the ratio of the yield to collapse level--equation (3.8). Values of the parameter θ were chosen such that the mean collapse time of most of the structures studied was of the order of 30 seconds. Most earthquakes recorded so far show strong motion for less than this interval.

It was observed that 300 samples were enough to obtain a stable mean and standard deviation of the failure time; stability being in the sense that fluctuations about the mean were less than 5% with no appreciable decrease with increasing sample size. However, 600 samples were used in order to produce smoother density functions. A weak smoothing of these functions was performed as given in equation (2.11). Tables 3.1 and 3.2 show the means and standard deviations obtained while some response samples are given in figures 3.3 and 3.4.

TABLE 3.1

Failure Times for 1 Degree of Freedom Hysteretic System

θ	P	$\langle t_f \rangle$	σ_{t_f}	$\sigma/\langle t_f \rangle$	m	ν	t_c
23.0	1.5	35.43	14.30	0.40	6.14	0.17	35.54
23.0	2.0	39.55	16.84	0.43	5.52	0.14	41.06
23.0	2.5	47.47	20.57	0.43	5.33	0.11	45.92
34.5	1.5	16.34	7.44	0.45	4.80	0.29	16.88
34.5	2.0	18.35	8.85	0.47	4.30	0.23	19.50
34.5	2.5	20.91	10.21	0.49	4.16	0.20	21.81
46.0	1.5	10.46	5.35	0.51	3.82	0.36	9.96
46.0	2.0	11.08	5.91	0.53	3.51	0.32	11.50
46.0	2.5	12.04	6.56	0.54	3.36	0.28	12.86
69.0	1.5	5.69	3.42	0.60	2.77	0.49	4.73
69.0	2.0	6.15	3.50	0.57	3.09	0.50	5.46
69.0	2.5	6.70	4.06	0.61	2.72	0.41	6.11

$\langle t_f \rangle$ = experimental mean failure time

t_c = regression analysis estimate

TABLE 3.2

Failure Times for 1 Degree of Freedom Non-Hysteretic System

θ	P	$\langle t_f \rangle$	σ_{t_f}	$\sigma/\langle t_f \rangle$	m	ν	t_c
34.5	1.5	25.39	22.07	0.87	1.32	0.05	26.19
34.5	2.0	26.37	22.70	0.86	1.35	0.05	21.88
34.5	2.5	24.77	19.20	0.78	1.66	0.07	19.03
46.0	1.5	13.72	11.83	0.86	1.34	0.10	17.93
46.0	2.0	13.28	10.65	0.80	1.56	0.12	14.98
46.0	2.5	13.00	10.29	0.79	1.60	0.12	13.03
69.0	1.5	7.09	7.01	0.99	1.02	0.14	10.51
69.0	2.0	6.68	5.33	0.80	1.57	0.24	8.78
69.0	2.5	7.09	5.17	0.73	1.08	0.27	7.64

C. Observations and Conclusions

It is seen that both the hysteretic and non-hysteretic systems show a measurable variation of collapse time with period, though for a period difference of one second such variation is less than half the scatter in the collapse time as measured by the standard deviation.

Normalizing the standard deviation to a unit mean shows that its dependence on period is, at most, slight. Such subjective inferences can be tested by standard statistical techniques of correlation and regression[55,56]. A non-linear regression equation of the the form

$$t_f = a_1 P^{a_2} \theta^{a_3} \tag{3.13}$$

was investigated using a direct method combining the Gauss-Newton and gradient methods as described by Marquardt[56]. Apart from using the least squares estimates of the parameters to predict mean failure time t_c (tables 3.1 and 3.2), correlation between the parameters and their standard errors were obtained. Both the values of these parameters and their ratios to their respective standard errors show that all parameters are significant. However, on noting the large variance of the failure times one may conclude that the effect of period may be neglected relative to that of the excitation strength for the period range considered here. It should be noted that this does not imply a complete independence of period in the results since the definition of θ already reflects the model's periods.

TABLE 3.3

Regression Analysis of Hysteretic Structure

	Parameter	Std. Error	Parameter Correlation a_1	a_2	a_3
a_1	0.917×10^4	0.10×10^4	1.00		
a_2	0.50	0.04	-0.26	1.00	
a_3	-1.84	0.03	-0.97	0.02	1.00

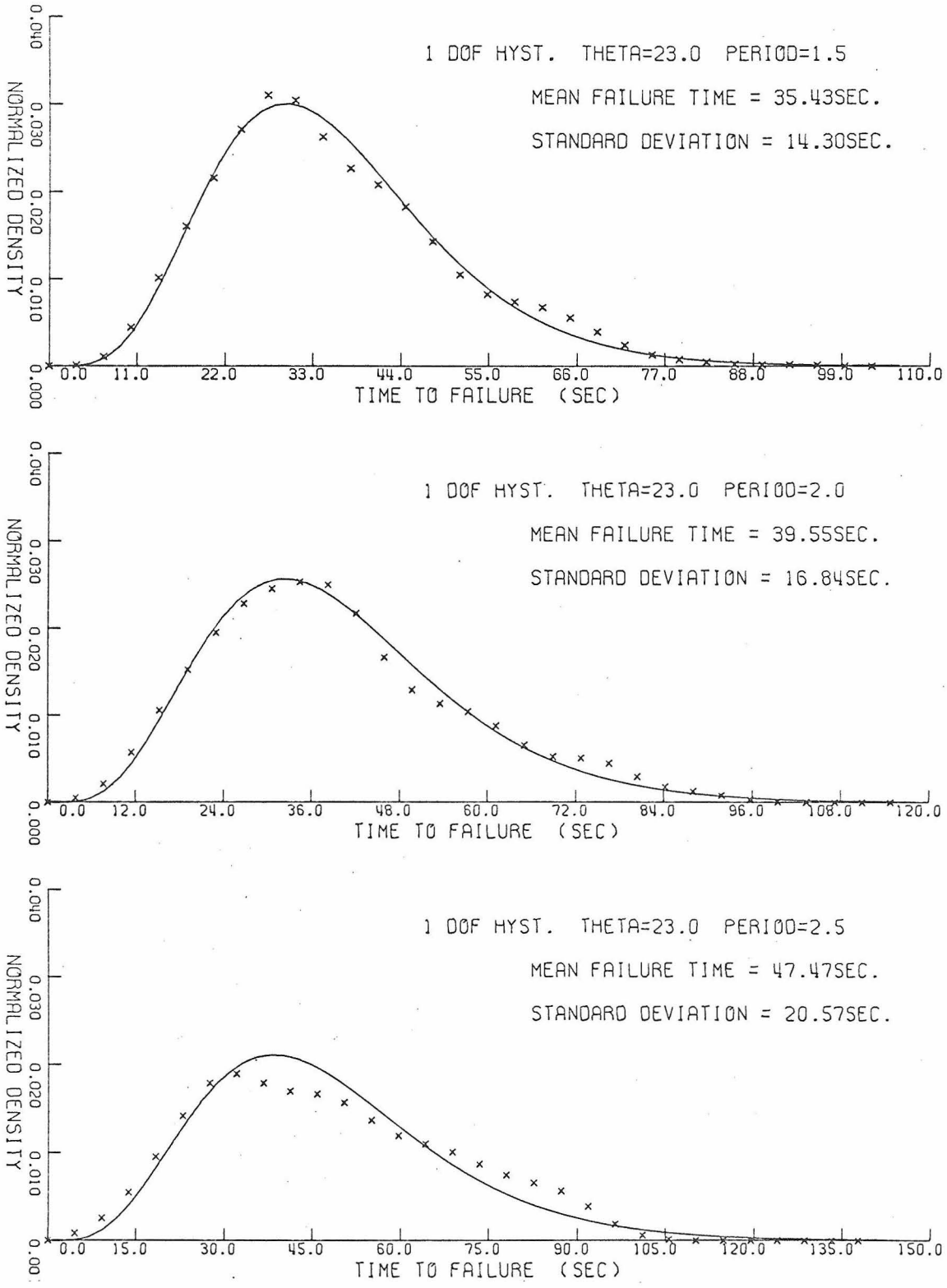

Fig. 3.5 Distribution of Failure Times of Hysteretic System

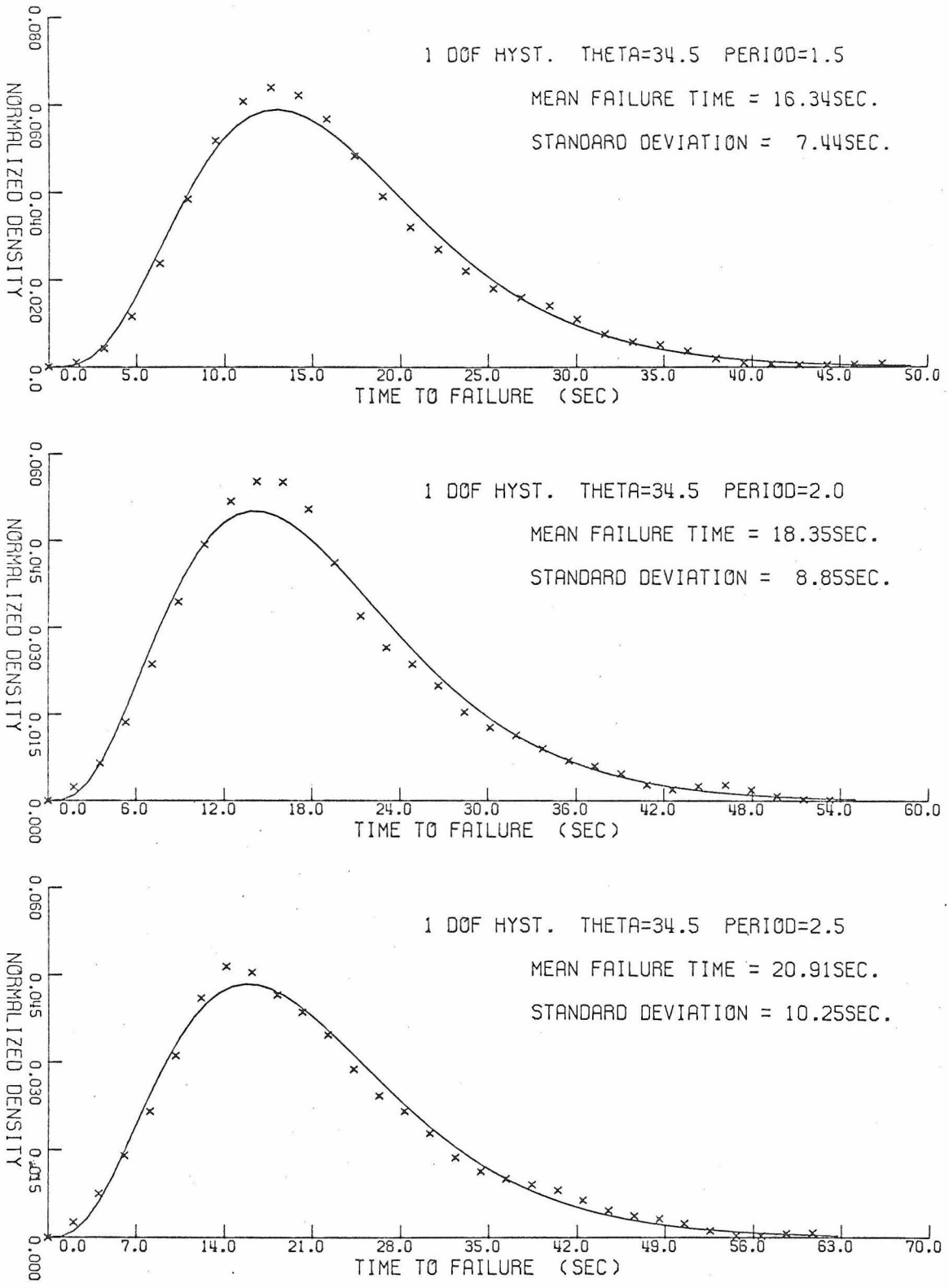

Fig. 3.6 Distribution of Failure Times of Hysteretic System

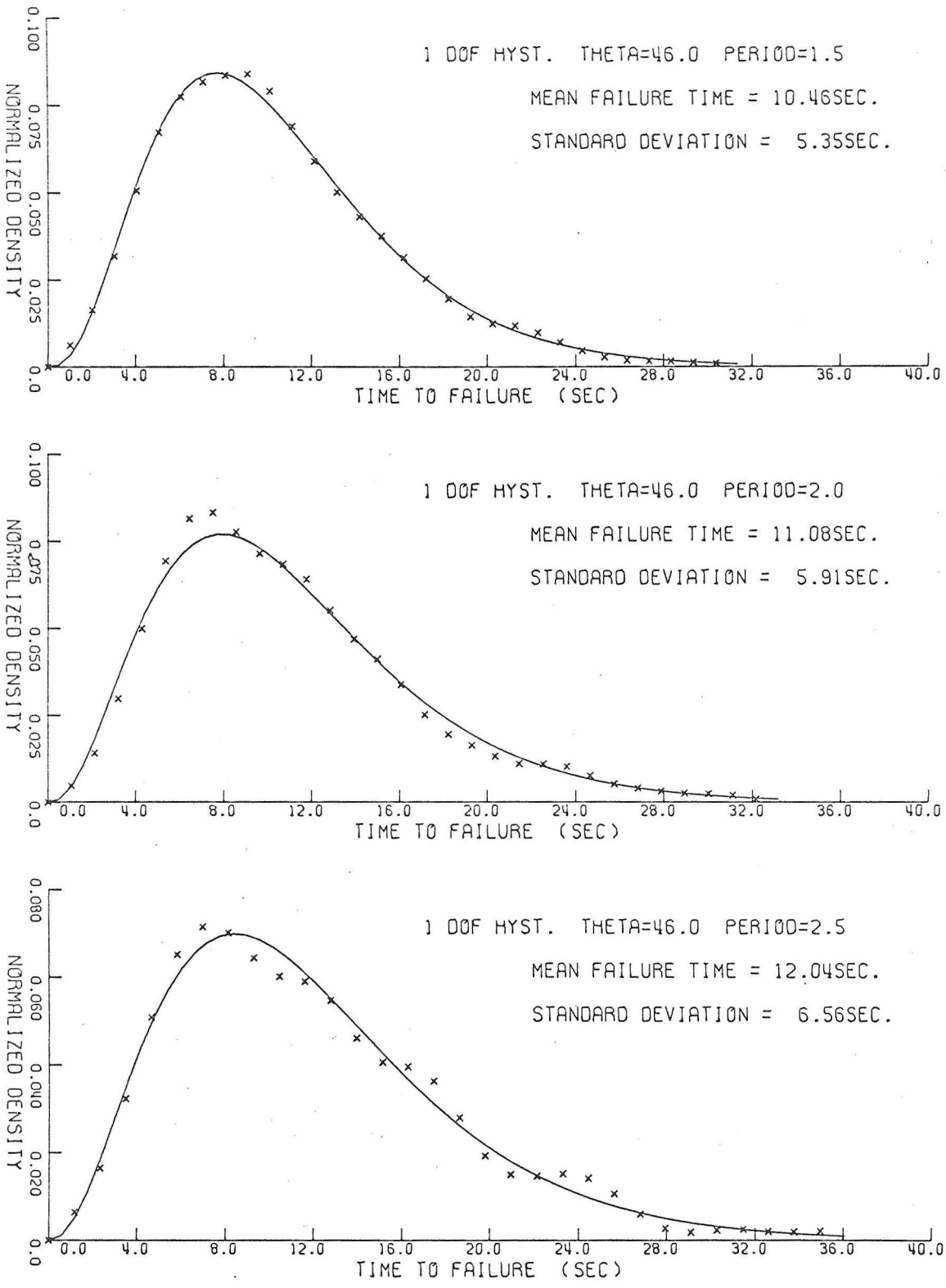

Fig. 3.7 Distribution of Failure Times of Hysteretic System

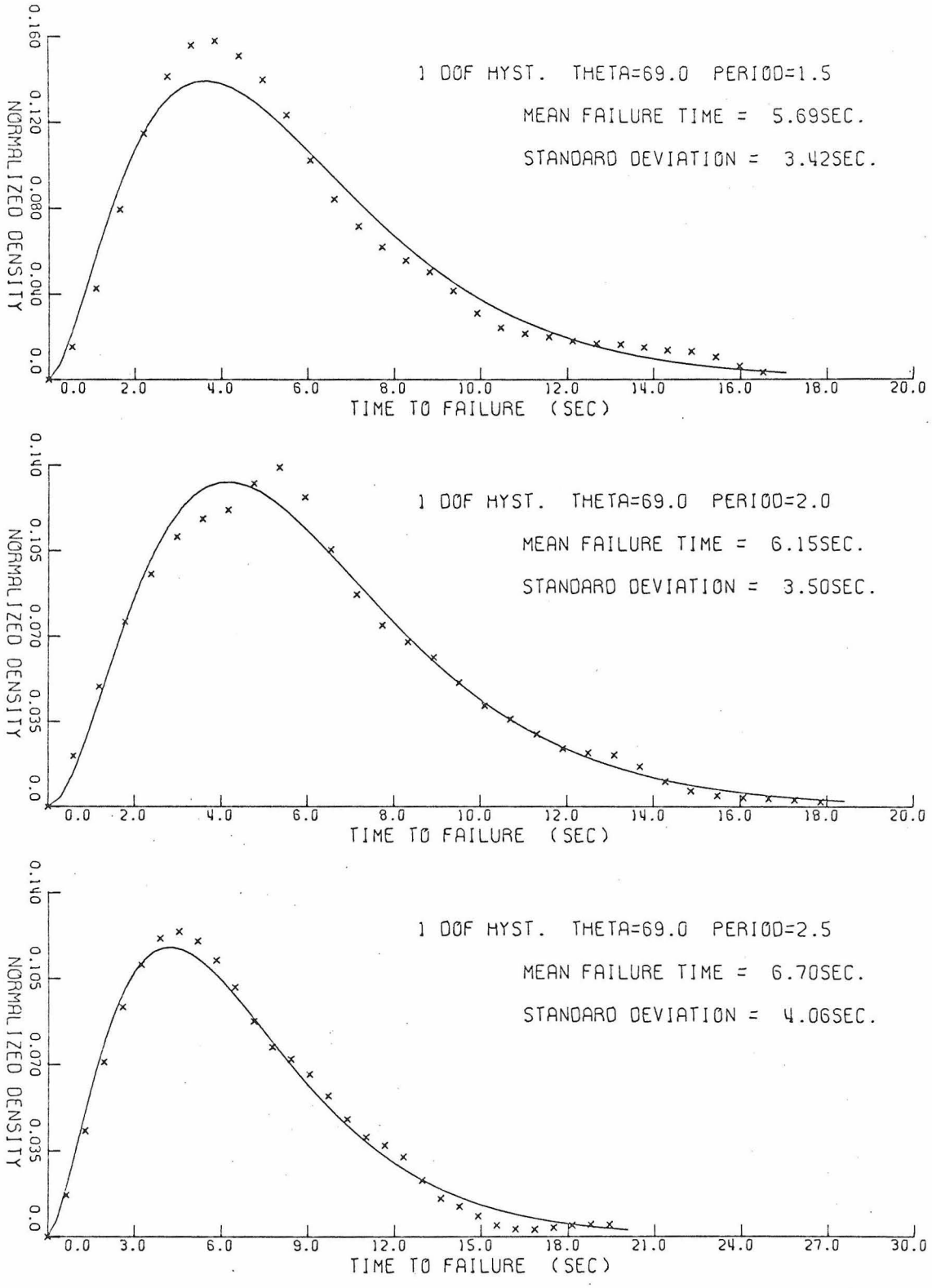

Fig. 3.8 Distributions of Failure Times of Hysteretic System

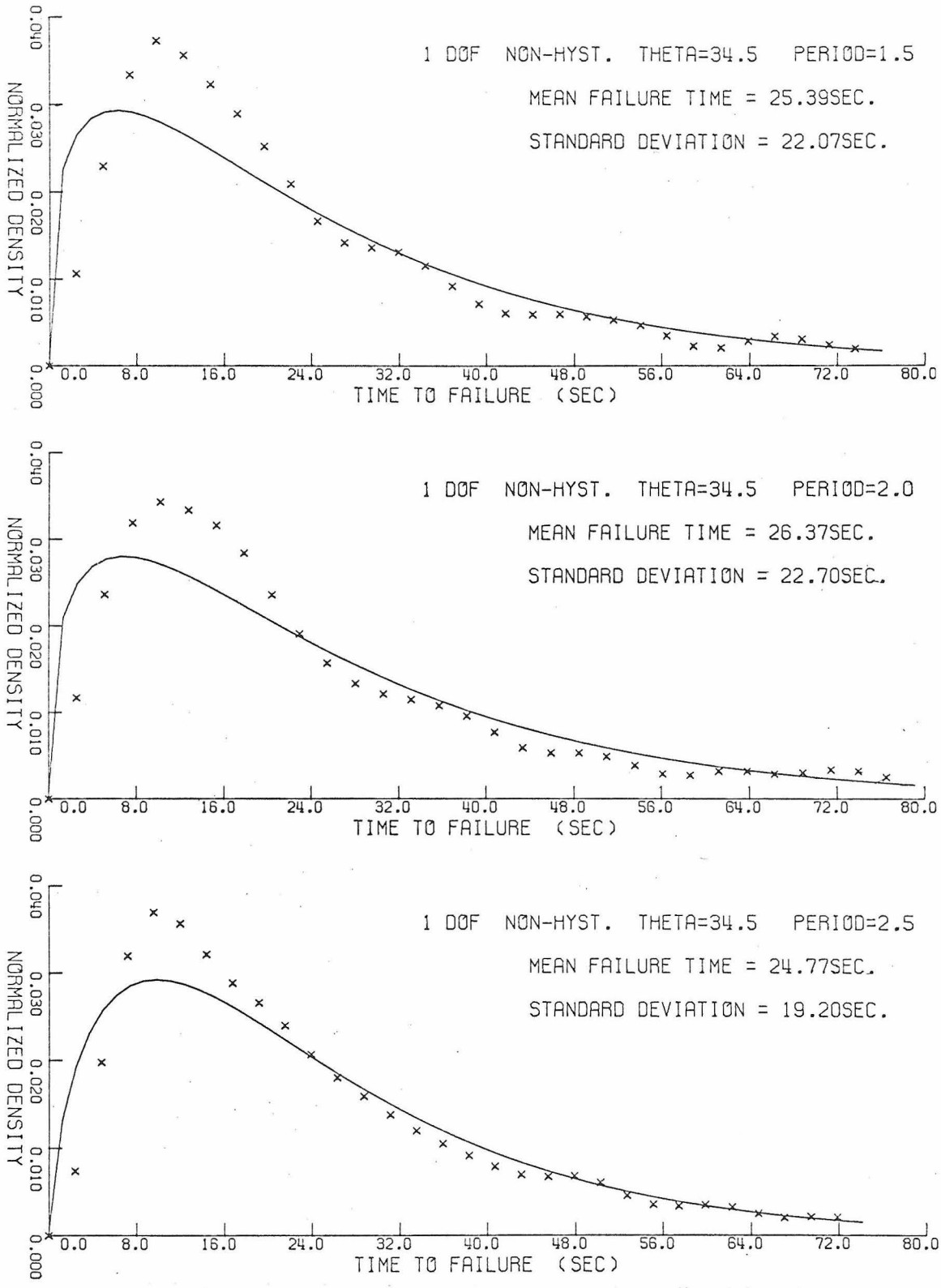

Fig. 3.9 Distribution of Failure Times of Non-hysteretic System

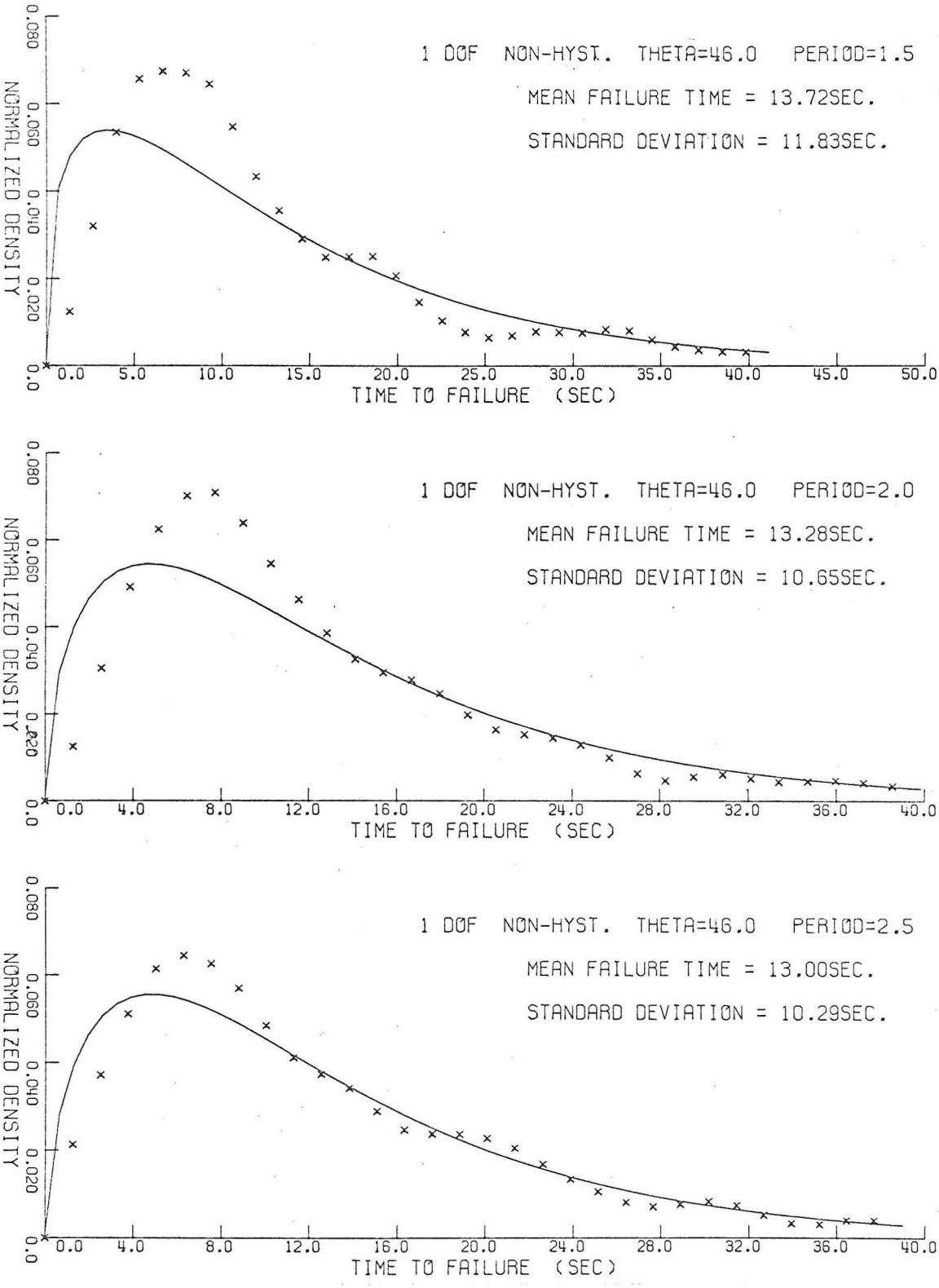

Fig. 3.10 Distributions of Failure Times of Non-hysteretic System

TABLE 3.4

Regression Analysis of Non-Hysteretic Structure

	Parameter	Std. Error	Parameter Correlation a_1	a_2	a_3
a_1	3.57×10^3	0.94×10^3	1.0		
a_2	-0.62	0.08	-0.06	1.0	
a_3	-1.32	0.07	-0.98	-0.11	1.0

As was the case with the linear oscillators, the significant implication of the large variance observed is in the weight to be assigned to deterministic studies using only a few sample excitations. It is noteworthy that because of the skewness of the distribution small samples will probably underestimate the mean collapse time.

Observation of several responses--as in figures 3.3 and 3.4--shows that structural collapse is sensitive to the high peaks in the excitation, the hysteretic system collapsing from an accumulation of permanent set due to such peaks. To pursue this, consider that the arrival of peaks above a given level is a homogeneous Poisson process[16] with mean arrival rate ν i.e. a threshold crossing problem where the probability of m crossings in time t is

$$P_{N(t)}(m) = (\nu t)^m \exp(-\nu t)/m! \qquad (3.14)$$

where $N(t)$ counts the random number of crossings up to time t. If one defines W_n as the time to m crossings and $F_{W_m}(t)$, $f_{W_m}(t)$ its distribution and density functions respectively, then[33]

$$1 - F_{W_m}(t) = P(W_m > t)$$

$$= \sum_{k=0}^{m-1} P_{N(t)}(k)$$

$$f_{W_m}(t) = \frac{d}{dt} E_{W_m}(t)$$

$$= \frac{d}{dt}\left\{ 1 - \sum_{k=0}^{m-1} (\nu t)^k e^{-\nu t}/k! \right\}$$

$$= \nu e^{-\nu t}(\nu t)^{m-1}/(m-1)!$$

$$= \nu^m t^{m-1} e^{-\nu t}/\Gamma(m) \qquad m \text{ an integer}$$

(3.15)

where $\Gamma(\cdot)$ is the Gamma function. For any rational m and m $\nu > 0$, equation (3.15) is the standard Gamma distribution with mean m/ν and m/ν^2. An attempt was made to fit this distribution to the experimental data. The results appear in tables 3.1 and 3.2 and as solid lines in figures 3.5-3.10. The Gamma distribution had been independently observed to give the best fit to the hysteretic system's data of all the standard two-parameter continuous distributions.

While examination of the records confirms the expectation that the effect of gravity is to bias the plastic drifts of the hysteretic system, these records and the close fit of the Gamma distribution suggest that basically such a drift is not a relatively smooth process but occurs as jumps in the response. Furthermore, the time between such jumps decreases progressively implying, in effect, a relative weakening of the structure. Therefore, estimation of the duration of excitations strong enough to cause collapse should take account of

both their die-down and strong-motion phases. The weight accorded the former will depend on the latter's duration and relative magnitude. For example, a die-down phase estimated at $\theta = 23$ and lasting 5 seconds will have a significant influence on the expectation of collapse if it follows a strong-motion phase of $\theta = 46$ that lasted 10 seconds. This points out the need for a scheme for approximating the extent of progressive damage in the hysteretic structure.

The influence of gravity may also be viewed as causing progressive asymmetry in the force-deflection properties of the hysteretic system by lowering the yield force in one direction while increasing it in the other. This suggests that the above investigation of response to a zero mean random excitation can be applied to excitations like random wind loads which possess a non-zero mean component[13] and hence unsymmetric yield levels to start with. The sole difference will be that the direction of initial yield is predetermined in the latter case.

Gravity appears to affect the non-hysteretic system only by causing instability when excessive yielding occurs. This observation is supported by the results of the Gamma distribution fit which shows between one and two threshold crossings to failure. The poor fit of the density functions may be partially ascribed to the inefficiency of the moment method in estimating the parameters of the distribution[54] but there is no real advantage, here, in improving the estimates.

The observed failure times lead one to conclude that the choice of yielding model is important only for low intensity, long duration

excitations. Observation of several responses--as in figure 3.3--leads to the conclusion that, between the jumps in response, the motion of the structure is essentially a narrow band response.

Finally, as a numerical example, consider that a building is designed to yield under a lateral force $F = m \times 0.15$ g. If it is subjected to an earthquake whose strong motion phase is 15 seconds long and has an rms level of about 4 ft/sec^2--corresponding to a peak acceleration of 0.5 g, say--then the relative excitation intensity is

$$\theta = \frac{4.00}{0.697 \times 0.15} = 50. \qquad (3.16)$$

Hence using equation (3.13) and table 3.3 one estimates the mean failure time to be 9.5 seconds. However, it is well to note that there is a very wide dispersion of the failure time such that the probability that it will fail in 5 seconds is 17%, in 10 seconds 60% and in 15 seconds 87%. Thus, one sees that working backwards to estimate the ground motion on the basis of having seen a building collapse is very unreliable.

CHAPTER IV

ANALYTICAL MODELS FOR THE EXCITATION AND MEAN RESPONSE PROCESSES

A. Introduction

In this chapter an analysis of the single story elastoplastic hysteretic structure with gravity is developed by modelling the excitation and response processes separately. The models are based on two of the conclusions of the last chapter that a) the response process is essentially the narrow band response associated with a lightly damped linear structure; but with a bias of the mean level reflecting elastoplastic yielding and the center repulsion of gravity; b) the probability density function of the failure time is strongly influenced by the scatter in the peak distribution of the excitation.

The first observation leads one to examine a response model of form

$$y(t) = x(t) + f(t) \tag{4.1}$$

where

$x(t) \equiv$ stationary narrow band response of a linear oscillator

$f(t) \equiv$ a deterministic bias function

The second observation merely states that the inception of instability is strongly influenced by the local character of the excitation. Hence an approximate model for the excitation may appropriately be taken to be a filtered sequence of independent and independently

arriving random impulses (i.e. filtered shot noise[5]). For a narrow band process the intensity function of the shot noise may be related to the spectral density of the given excitation at the structure's resonant frequency. Further, by noting that the rate of zero crossings of the excitation is much higher than that associated with any of the structures considered, the model is relaxed to a sequence of shot noise impulses.

This model has the desired effect of distributing the excitation's average energy randomly in time while local energy considerations may be obtained by considering the clumping in the arrival of these impulses. The effects of such clumps of impulses are used to approximate the mean behavior of the bias function f(t). Statistics of the collapse time of the structure are then obtained by defining collapse as the first crossing of a given barrier by y(t). The method used is a slight extension of that by Middleton[41] and Lin[5].

B. Shot Noise Model for Excitation

As defined earlier, the excitation, g(t) is a stationary Gaussian random process with zero mean and power spectral density

$$G(\omega) = \frac{\rho^2}{3\pi}(1 + 4b^2\omega^2/c^2)/\{(1 - \omega^2/c^2)^2 + 4b^2\omega^2/c^2\} \qquad (2.7)$$

where $c^2 = 242$; $b^2 = 0.410$. Its rate of zero crossings is thus given by[5]

$$\nu_o = 2\int_0^\infty \dot{g}\, p_{G\dot{G}}(0,\dot{g})\, d\dot{g}$$

$$= \frac{1}{\pi}\sigma_{\dot{g}}/\sigma_g$$

$$= \frac{1}{\pi}\left[\frac{\int_o^{\omega_f}\omega^2 G(\omega)\, d\omega}{\int_o^{\omega_f} G(\omega)\, d\omega}\right]^{1/2} = 8.9044 \qquad (4.2)$$

where $P_{G\dot{G}}(g,\dot{g})$ is the joint density function of the excitation and its first derivative, and ω_f is their band limit. Since the integrands have no singularities, the integrals were evaluated numerically by Simpson's rule. (Note that, as defined, ν_o is infinite for an infinite pass-band process.) By comparison, the rate of zero crossings of the response of the structures considered may be approximated closely by the narrow band response of lightly damped oscillators to random excitation[5,22]

$$\nu_s = \frac{1}{\pi}\left[\frac{\int_o^{\omega_f}\omega^2 |H_T(i\omega)|^2 d\omega}{\int_o^{\omega_f} |H_T(i\omega)|^2 d\omega}\right]^{1/2} = \frac{\sigma_1}{\pi\sigma} \qquad (4.3)$$

where

$$|H_T(i\omega)| = G(\omega)/\{(\omega_o^2 - \omega^2)^2 + 4n^2\omega_o^2\omega^2\} \qquad (4.4)$$

$n;\omega_o \equiv$ damping factor and natural period of oscillator

$\sigma, \sigma_1 \equiv$ std. deviations of oscillator's displacement and velocity.

For a wide pass band little error is involved in extending the upper limits of integration to infinity in equation (4.3) and evaluating the integral either by contour integration or from tables[27]. For $n = 0.02$ and 1.5 second one obtains

$$\nu_s = 1.337. \tag{4.5}$$

Thus, comparing with (4.2) we see that a model of the excitation by a sequence of shot noise impulses having a mean arrival rate ν_o and zero mean will be reasonable provided the excitation is strong enough that impulse clumps of size four or less cause appreciable permanent set. Such a process may be written as

$$S(t) = \sum_{k=1}^{N(t)} Y_k \delta(t - t_k) \tag{4.6}$$

where

$N(t) \equiv$ number of impulses in $(0,t)$

$Y_k \equiv$ identically distributed, independent random variables

$\delta(t - t_k) \equiv$ unit impulse at random time t_k.

The counting process $N(t)$ is a Poisson process with a stationary arrival rate ν_o. The mean and covariance functions of (4.6) become

$$\mu(t) = 0$$

$$K_{ss}(t_1, t_2) = I\delta(t_1 - t_2) \tag{4.7}$$

$$= \nu_o E[Y^2]\,\delta(t_1 - t_2)$$

where I is the constant intensity function related to the power spectral density by

$$\phi_{ss}(\omega) = I/\pi . \tag{4.8}$$

Invoking the narrow-bandedness of the response, one may make the approximation

$$\phi_{ss}(\omega) \doteq G(\omega_o) \tag{4.9}$$

where ω_o is the natural frequency of the structure under small amplitude displacements and it is assumed that $G(\omega)$ is slowly varying around ω_o. From (4.7) through (4.9) one obtains

$$E[Y^2] = \pi G(\omega_o)/\nu_o . \tag{4.10}$$

We now define a clump of impulses[21,57] as the consecutive arrival of similarly oriented impulses; an n-clump being a train of n such impulses. If p is the probability that an impulse is positive (p = 0.5) then the following relations hold for the variables as defined[57]

prob. an impulse begins an n-clump $\equiv p_n = p^n(1 - p)^2$

expected number of positive n-clumps per unit tune (4.11)

$$\equiv C_n = \nu_o p^n (1 - p)^2 .$$

From any given moment, the probability that an n-clump starts after the m^{th} impulse is

$$p(n,m) = p_n \prod^{m-1} (1 - p_n) = p_n(1 - p_n)^{m-1}$$

where the independent arrival of the impulses has been invoked. The expected number of impulses before an n-clump is then

$$N_n = \sum_{m=1}^{\infty} mp(n,m) = p_n \sum_{m=1}^{\infty} m(1 - p_n)^{m-1} \qquad (4.12)$$

$$= 1/p_n \qquad \text{for} \qquad 0 < p_n < 1.$$

The expected time to an n-clump is seen to be

$$\tau_n = N_n/\nu_o = (\nu_o p_n)^{-1} = 1/C_n. \qquad (4.13)$$

It should be noted that since the process (4.4) is stationary, the mean properties defined in equations (4.11) through (4.13) hold for any period of observation. This is important when considering the response of a yielding structure to the impulses.

One can now consider the effect of an n-clump on the model of an elastoplastic, hysteretic structure with gravity given in equation (4.1). The linear oscillator's amplitude may be represented by

$$x(t) = A(t) \sin \omega_o t \qquad (4.14)$$

where $A(t)$ is a 'slowly varying' amplitude[40] assumed constant during any given cycle of oscillation. Each acceleration impulse imparted by the excitation, Y_k, at time t_k, causes an instantaneous velocity change v_k whose effect depends on the position of the oscillator $x(t_k)$ and its current mean level $x_o = f(t_k)$. The problem is then to find the average residual displacement due to a clump of impulses and thereby

obtain a scheme for evaluating the bias function.

If there is a net displacement of Δx at any position $x(t)$ such that yielding occurs and if $A(t) < x_y$ then conservation of energy gives

$$\frac{1}{2} m(\dot{x} \pm n\bar{v})^2 - \frac{1}{2} m\dot{x}^2 \pm mg\ell y\Delta x = Kx_y(x+\Delta x) - \frac{1}{2}K(x_y^2 + x^2) \qquad (4.15)$$

where x_y is the yield level of the spring, and $\pm \bar{v}$ is the average velocity change per impulse. $\bar{v}$ is related to the intensity function of the excitation through

$$\bar{v}^2 = E[Y^2]. \qquad (4.16)$$

The positive gravity effect applies if the impulses are 'positive' i.e. in the direction of x_o, and the negative sign applies otherwise. Equation (4.15) is now averaged over a whole cycle, noting that each position is equally probable as the start of the clump.

$$\frac{\omega_o}{2\pi}\int_0^{2\pi/\omega_o}\left\{\frac{1}{2} mn^2\bar{v}^2 \pm mg\ell\Delta x(x_o+x)\right\} d\xi + \frac{m\omega_o}{4\pi}\int_{\pi/2\omega_o}^{\pi/2\omega_o} 2n\dot{x}\bar{v}\, d\xi$$

$$- \frac{m\omega_o}{4\pi}\int_{\pi/2\omega_o}^{3\pi/2\omega_o} 2n\dot{x}\bar{v}\, d\xi = \frac{K\omega_o}{2\pi}\int_0^{2\pi/\omega_o}\left\{x_y(x+\Delta x) - \frac{1}{2}(x_y^2+x^2)\right\} d\xi$$

where ξ is measured from the start of the cycle. Evaluation gives

$$\Delta x = \left\{\left(\frac{n\bar{v}}{\ell\omega}\right)^2 + x_y^2 + \frac{1}{2}A^2 + 4A\omega_o n\bar{v}/\ell^2\omega^2\pi\right\} / \left\{x_y \mp gx_o/\ell\omega^2\right\} \qquad (4.17)$$

where

$$\omega^2 = K/m\ell^2 = \omega_o^2 + g/\ell \ .$$

The minus sign applies to 'positive' clumps. In the spirit of the approximation in equation (4.14), the mean amplitude A is evaluated from the envelope response of x(t)[22]. For a Gaussian excitation this procedure gives

$$A = E[A(t)] = \int_0^\infty \frac{a^2}{\sigma^2} \exp\left\{- a^2/2\sigma^2\right\} da$$

$$= \sigma\sqrt{\pi/2} \qquad (4.18)$$

where σ is the standard deviation defined in equation (4.4) i.e.

$$\sigma^2 = \int_0^{\omega_f} |H_T(i\omega)|^2 \, d\omega \doteq \int_0^\infty |H_T(i\omega)|^2 \, d\omega \ . \qquad (4.19)$$

At high levels of excitation, the stationary response x(t) involves yielding of the structure. A similar analysis to the one above may be made, however, by using the concept of an equivalent linear system with viscous damping[34]. Equivalence in this case is taken to mean that the two systems have the same mean maximum amplitude in stationary response to the excitation. Such an equivalence was investigated and reported earlier. It showed that the increase in viscous damping for the equivalent linear system was about 0.02.

Using this equivalent linear system, the mean response amplitude of x(t) will be given by equation (4.18). Its mean rate of energy dissipation becomes

$$\frac{dE}{dt} = 4Kx_y(A - x_y)/P \ .$$

From its definition, an n-clump corresponds to a local n-fold increase in mean rate of energy input; hence conservation of energy gives the following expression for the permanent set due to an n-clump:

$$\Delta P.E. = \Delta x(Kx_y - mg\ x_o) = \frac{n}{\lambda} \cdot n \cdot 4Kx_y(A - x_o)/P$$

$$\Delta x = \frac{4n^2 x_y}{\lambda P}(A - x_y) \cdot \frac{1}{x_y - \frac{gx_o}{\ell \omega^2}} \cdot \qquad (4.17a)$$

On the average, therefore, some residual displacement is incurred whenever a clump of size n occurs such that Δx is greater than x_y. It is important to note that the averaging done above is particularly sensitive to the requirement imposed earlier that the size of clumps be smaller than the ratio of zero crossings of the excitation and response processes. One sees then that the whole development applies only for relatively strong excitations.

Turning now to the excitation, one redistributes the arrival of impulse clumps so that a given size, say a positive n-clump, arrives evenly in time at rate τ_n. One is thus assured that the average rate of impulses is maintained while being able to consider the effect of each clump size sequentially. A problem becomes apparent here if the effect of the simultaneous arrival of one positive and one negative n-clump is considered. The result is a partial erasure of the influence of the excitation's intensity leaving gravity as the principal cause of displacement. The following schedule will therefore be observed:

$$\Delta x_n(x_o) = \Delta x_n^+(x_o) - \Delta x_n^-(x_o + \Delta x_n^+(x_o)) \qquad (4.20)$$

where the various quantities are residual displacements at the indicated mean levels. This fictitious ordering is necessary only to get the yielding started. For appreciable mean displacements one expects Δx_n^- to be less than x_y when the minimum clump size to cause positive yielding is chosen. What is being said, in effect, is that yielding is initiated by a large clump in a given direction.

Finally, the bias function is the summation of the permanent set accruing from the impulse clumps. It is thus of the form

$$f(t) = \sum_k d_k \, \delta(t - t_k) \qquad (4.21)$$

where a clump occurs at time t_k, causing a residual displacement of d_k as evaluated from equation (4.20).

C. First Excursion Failure of a Biased Linear Oscillator

By relaxing the failure criterion for equation (4.1) to that of a first excursion failure it is possible to obtain the distribution of its time to failure, T. The analysis follows the standard one used for lightly damped linear oscillators[15,19,22]. In particular, one retains Coleman's[19] suggestion that failures arrive independently at a rate $\lambda(t)$ equal to the expected rate at which the system will cross the assumed failure level; if the structure is considered capable of immediate recovery from such a failure. Here, however, $\lambda(t)$ is no longer a constant in time so that the counting process for the

number of failures is a non-homogeneous Poisson process.

Consider the non-stationary, random process

$$y(t) = x(t) + \xi(t) \tag{4.22}$$

where $x(t)$ is a continuously valued, stationary random process as in equation (4.1) and $\xi(t)$ is any bounded, deterministic function that is monotonically non-decreasing and has a finite number of discontinuities. If $N'(U,t_1,t_2)$ is the number of times $y(t)$ crosses a threshold at $\pm U$ in the interval (t_1,t_2) then[40]

$$N'(U,t_1,t_2) = \int_{t_1^+}^{t_2^+} |\dot{y}(t)|\, \delta(y - U)\, dt$$

$$\equiv \int_{t_1^+}^{t_2^+} N(U,t)\, dt \,.$$

$N(U,t)$ can be identified as the rate of threshold crossings per unit time. Its expectation is thus

$$E[\, N(U,t)] = \int_{-\infty}^{\infty} |\dot{y}|\, P_{Y\dot{Y}}(U,\dot{y},t)\, d\dot{y} \,.$$

Using equation (4.22) and the fact that $\xi(t)$ is a deterministic function gives

$$P_{Y\dot{Y}}(y,\dot{y},t) = P_{X\dot{X}}(y - \xi(t), \dot{y} - \dot{\xi}(t)) \,.$$

Hence

$$E[\,N(U,t)] = \int_{-\infty}^{\infty} |\dot{x} + \dot{\xi}|\, P_{X\dot{X}}(U - \xi, \dot{x})\, d\dot{x} \,. \tag{4.23}$$

We now use the fact that $x(t)$ is a stationary Gaussian process with zero mean to obtain

$$P_{X\dot{X}}(U - \xi, \dot{x}, t) = A(t) \exp(-\dot{x}^2/b^2)$$

where

$$A(t) = \frac{1}{\pi bc} \exp\left[-\frac{1}{c^2}(U - \xi(t))^2\right]$$

$$b^2 = 2\sigma_1^2 \quad , \qquad c^2 = 2\sigma^2 \,.$$

$$\therefore \quad E[\,N(U,t)] = A(t) \int_{-\infty}^{\infty} |\dot{x} + \dot{\xi}| \exp(-\dot{x}^2/b^2)\, d\dot{x} \tag{4.24}$$

$$= -A \int_{-\infty}^{-\dot{\xi}} (\dot{x} + \dot{\xi}) \exp(-\dot{x}^2/b^2)\, d\dot{x}$$

$$+ A \int_{-\dot{\xi}}^{\infty} (\dot{x} + \dot{\xi}) \exp(-\dot{x}^2/b^2)\, d\dot{x} \,.$$

Let $\omega = -\dot{x}$ in the first integral and $\omega = \dot{x}$ in the second, then

$$E[N(U,t)] = A \int_{\dot{\xi}}^{\infty} (\omega - \dot{\xi}) e^{-\omega^2/b^2}\, d\omega + A \int_{-\dot{\xi}}^{\infty} (\omega + \dot{\xi}) e^{-\omega^2/b^2}\, d\omega$$

$$= 2A \int_{\dot{\xi}}^{\infty} \omega e^{-\omega^2/b^2}\, d\omega + 2A\dot{\xi} \int_{0}^{\dot{\xi}} e^{-\omega^2/b^2}\, d\omega$$

$$= Ab^2 e^{-\dot{\xi}^2/b^2} + Ab\dot{\xi}\sqrt{\pi}\, \mathrm{erf}\,(\dot{\xi}/b) \tag{4.25}$$

where the error function is defined by $\mathrm{erf}\,(x) \equiv (2/\sqrt{\pi}) \int_0^x e^{-u^2}\, du$. One notes that though equation (4.25), as derived, is not defined at

the discontinuities in $\xi(t)$, the requirements of finiteness on ξ permit the evaluation of (4.24) at all other points. In particular, if ξ is a staircase function as in equation (4.21) then equation (4.25) becomes simply

$$E[N(U,t)] = A(t)b^2 \tag{4.26}$$

except at the discontinuities. If the m^{th} stair is defined as the interval (t_{m-1}, t_m) i.e. the time between the $(m-1)^{th}$ and the m^{th} jump, then one has

$$\xi(t) = \sum_{k=1}^{m-1} d_k = \text{constant} \qquad t_{m-1} < t < t_m \tag{4.27}$$

and, by equation (4.26), the mean rate of threshold crossings is a constant. Hence it, too, is a staircase function with discontinuities at t_k.

A. Ya Khinchin[32] has studied sequences of chance events with discontinuous arrival rates similar to equation (4.27). He showed that if the occurrence of such events are independent and if the probability of occurrence of n events at any given moment in t_i is Poisson distributed i.e. has the form

$$\exp(-\alpha_i)\alpha_i^n/n!$$

then the probability that n events occur in the interval (t_1, t_2) must necessarily be of the form

$$p_n(t_1,t_2) = \left(\int_{t_1}^{t_2} \lambda(t)\, dt \right)^n \exp\left\{ - \int_{t_1}^{t_2} \lambda(t)\, dt \right\} / n! \tag{4.29}$$

where $\lambda(t)$ is the non-stationary arrival rate of the process. $\lambda(t)$ need not be continuous but must be non-decreasing.

Obviously the failure process being considered, with a rate of arrival given by

$$\lambda(t) = E[\, N(U,t)] \tag{4.30}$$

satisfies these requirements. Hence

$$p_n(t_1,t_2) = \left\{E[\, N'(t_1,t_2)]\right\}^n \exp\left\{-E[\, N'(t_1,t_2)\right\}/n!.$$

One may thus evaluate the probability of no failure in the time interval (t_1,t_2) as

$$p_o(t_1,t_2) = \exp\left\{-\int_{t_1^+}^{t_2^+} \lambda(t)\, dt\right\}.$$

Or, over the m^{th} stair, i.e. for $t_{m-1} \leq t < t_m$

$$p_o(t_{m-1},t_m) \equiv p_o(m) = \exp\left\{-\int_{t_{m-1}}^{t_m} \lambda(\tau)\, d\tau\right\} \leq 1. \tag{4.31}$$

Note that $p_o(m)$ is a constant since, for $t \in (t_{m-1},t_m)$, $\lambda(t) \equiv \lambda_m =$ constant. The probability of having no failure up to time t becomes

$$p_o(0,t) = \exp\left\{-\sum_{m=1}^{r}\int_{t_{m-1}}^{t_m} \lambda_m\, d\tau - \int_{t_r}^{t} \lambda_{r+1}\, d\tau\right\} \quad t_r < t \leq t_{r+1},\ r \geq 0$$

$$= \left[\prod_{m=1}^{r} p_o(m)\right] \exp\left\{-\lambda_{r+1}(t - t_r)\right\} \tag{4.32}$$

where, for brevity, one defines

$$\prod_{m=1}^{r} p_o(m) \equiv 1 \qquad \text{for} \qquad r < m .$$

The probability of at least one failure in $(0,t)$ is

$$F_T(t) = 1 - p_o(0,t) . \tag{4.33}$$

Equation (4.33) may be taken as the distribution function of the time to failure T provided

$$\lim_{t \to \infty} [\, 1 - p_o(0,t)] = 1$$

since we already know from equation (4.32) that it is non-decreasing. The additional condition will be satisfied for the present case if one limits the bias function $f(t)$ to be no bigger than the threshold crossing level i.e.

$$|f(t)| \leq U . \tag{4.34}$$

The total number of discontinuities in $f(t)$, S, may be obtained from

$$|f(t)| \leq U \qquad \text{for} \qquad t \geq t_S . \tag{4.35}$$

If ν_s is the rate of zero crossings of $\dot{x}(t)$, and ν_s is bounded, then for large t

$$p_o(0,t) = \left[\prod_{m=1}^{S} p_o(m) \right] \exp \left\{ - \nu_s (t - t_S) \right\}$$

$$\leq \exp \left\{ - \nu_s (t - t_S) \right\}$$

$$\therefore \quad \lim_{t \to \infty} p_o(0,t) \leq \lim_{t \to \infty} \exp \left\{ - \nu_s (t - t_S) \right\} = 0 . \tag{4.36}$$

Thus (4.33) is indeed a distribution function for the failure time and the probability density function and mean of T become

$$p_T(t) = \frac{d}{dt} p_o(0,t)$$

$$= \lambda_{r+1} p_o(0,t) \qquad t_r < t \leq t_{r+1} \tag{4.37}$$

$$E[T] = \int_0^\infty \lambda_{r+1} t p_o(0,t)\, dt$$

$$= \int_0^\infty \lambda_{r+1} t \left[\prod_{m=1}^{r} p_o(m) \right] \exp\left\{ - \lambda_{r+1}(t-t_r) \right\} dt$$

$$= \sum_{s=1}^{S} \int_{t_{s-1}}^{t_s} \lambda_s t \left[\prod_{m=1}^{s-1} p_o(m) \right] \exp\left\{ - \lambda_s (t-t_{s-1}) \right\} dt$$

$$+ \int_{t_S}^{\infty} \nu_s t \left[\prod_{m=1}^{S} p_o(m) \right] \exp\left\{ - \nu_s (t-t_S) \right\} dt$$

i.e.

$$E[T] = \sum_{s=1}^{S} \left[\prod_{m=1}^{s-1} p_o(m) \right] \left\{ (t_{s-1} + 1/\lambda_s) - p_o(s)(t_s + 1/\lambda_s) \right\}$$

$$+ (t_S + 1/\nu_s) \prod_{m=1}^{S} p_o(m) \tag{4.38}$$

$$= \sum_{s=1}^{S} \frac{1}{\lambda_s} \left\{ 1 - p_o(s) \right\} \prod_{m=1}^{s-1} p_o(m) + \frac{1}{\nu_s} \prod_{m=1}^{S} p_o(m). \tag{4.39}$$

The result for an unbiased oscillator may be recovered from equation (4.39) as the case where there is only one jump and it occurs at infinity. Then

$$E[T] = \frac{1}{\lambda_1}\left\{1 - p_o(1)\right\} + \frac{1}{\nu_s} p_o(1)$$

$$= \frac{1}{\lambda_1} \qquad (4.40)$$

since

$$p_o(1) = \exp\left\{-\int_0^\infty \lambda_1 \, d\tau\right\} = 0 .$$

An approximate expression for the expected failure time can be obtained from equation (4.38). One notes that the probability of failure at low bias levels is negligibly small while the time between jumps becomes very small at high bias levels. Consequently the integrations over these steps have negligible contribution to the failure time, which may now be written as

$$E[T] \approx \int_{t_s}^{\infty} \nu_{st} \prod_{m=1}^{S} p_o(m) e^{-\nu_s (t-t_S)} \, dt$$

$$= (t_S + 1/\nu_s) \prod_{m=1}^{S} p_o(m)$$

$$\approx t_S + 1/\nu_s \, . \qquad (4.39a)$$

Each term of equation (4.39) is the expected time to failure at the given threshold level given that there is at least one failure at that level and no failure up to the beginning of the level.

D. Comparison with Experimental Results

The procedure for estimating the expected failure time of the one-degree of freedom system may be briefly summarized. Initially one determines the stationary response of the equivalent linear oscillator to the input excitation from equation (4.3). The times of occurrence, t_k, and magnitudes, d_k, of jumps in the response are next determined sequentially using equation (4.13),(4.17a,b) and (4.20). These account for the effect of gravity and the yielding properties of the model. One now has the threshold level for each interval (t_{m-1},t_m) as $(U - \sum_{k=1}^{m-1} d_k)$, where U is the specified collapse level, and thus can calculate the expected rate of threshold crossings for the interval, λ_m, from equation (4.26). The probability of no collapse during each interval is then given by $p_o(m)$ and computed from equation (4.31). Finally, these values are all used in equation (4.39) to compute the expected failure time.

The above scheme was programmed for digital computer evaluation, the contour integrations of equation (4.3) being calculated directly from standard tables[27]. The equivalent linear system used had an increase in viscous damping of 0.02 and, from equation (2.9), is of form

$$\ddot{z} + 2n\omega_o\dot{z} + \omega_o^2 z = -\frac{\theta\omega_o^2}{g} \qquad (4.41)$$

where $n = 0.04$. Equation (4.38) was actually used in the calculations since it permits the most direct approximation for those regions where $\lambda_m \to 0$ and $p_o(m) \to 1$. It was found that the approximate

TABLE 4.1

Comparison of Calculated and Experimental
Mean Collapse Time of a Single-Degree of Freedom
Elastoplastic System with Gravity

θ	P	Equation (4.39)		$\langle t_f \rangle$	t_c
		n=0.03	n=0.04		
23.0	1.5	-	-	35.43	35.54
23.0	2.0	-	-	39.55	41.06
23.0	2.5	-	-	47.47	45.92
34.5	1.5	9.73	15.12	16.34	16.88
34.5	2.0	15.37	29.74	18.35	19.50
34.5	2.5	22.81	-	20.91	21.81
46.0	1.5	7.93	7.93	10.46	9.96
46.0	2.0	8.18	9.98	11.08	11.50
46.0	2.5	8.43	13.82	12.04	12.86
69.0	1.5	4.34	5.42	5.69	4.73
69.0	2.0	4.59	6.39	6.15	5.46
69.0	2.5	5.74	6.64	6.70	6.11

$\langle t_f \rangle$ - experimental mean

t_c - regression analysis estimate

expression (4.39a) overestimated the failure times slightly. Table 4.1 shows the calculated failure times for damping ratios of 0.04 and 0.03, comparing them with the experimental mean failure times $\langle t_f \rangle$ and values estimated from a regression analysis of the experimental data t_c. The calculated values did not converge for these cases where no values are indicated.

The failure of the above scheme for low excitation levels is expected from the stated limitations of the derivation. However, it gives a very good estimate of failure time at the higher excitation levels. The dependence of these estimates on the equivalent viscous damping of the linear system point out a need for more extensive investigation of the equivalent systems. In particular, one needs to know the dependence of the equivalent system on the duration and magnitude of the excitation. From the results here and in Chapter II one may tentatively conclude that an equivalent viscous damping of 0.02 is appropriate when the duration of excitation is between 5 and 20 seconds.

CHAPTER V

COLLAPSE OF TWO-DEGREE OF FREEDOM HYSTERETIC SYSTEMS WITH GRAVITY

A. Derivation of the Equations of Motion

A diagram of the model for the two-degree of freedom system is shown in Figure 5.1. The assumptions of rigid columns and horizontal translations of the girders are maintained from the single-degree of freedom model; as are the assumptions that spring and dashpot forces couple the columns to the floors in resistance to bending deformation. These assumptions emphasize only the effect of bending deformation in yielding, but even so the model does approximate the yielding behavior of real structures as, for example, in the permanent set observed at the Olive View Hospital in Los Angeles after the San Fernando Valley earthquake of February 9, 1971. A photograph of this hospital is shown in the introduction.

The Lagrangian equation--equation 3.1--will be used to derive the equations of motion. ϕ_1 and ϕ_2 are the generalized coordinates and the generalized forces Q include the same non-conservative forces as before. Thus if $\vec{e}_1$ and $\vec{e}_2$ represent the unit velocity vectors of m_1 and m_2 then

$$L = \frac{1}{2} m_2 \left|\left| \ell_1 \dot{\phi}_1 \vec{e}_1 + \ell_2 \dot{\phi}_2 \vec{e}_2 \right|\right|^2 - m_2 g(\ell_1 \cos \phi_1 + \ell_2 \cos \phi_2)$$

$$+ \frac{1}{2} m_1 \left|\left| \ell_1 \dot{\phi}_1 \right|\right|^2 - m_1 g_1 \ell_1 \cos \phi_1 \qquad (5.1)$$

where $||\vec{r}||$ is the geometric length of $\vec{r}$. Expanding equation (5.1)

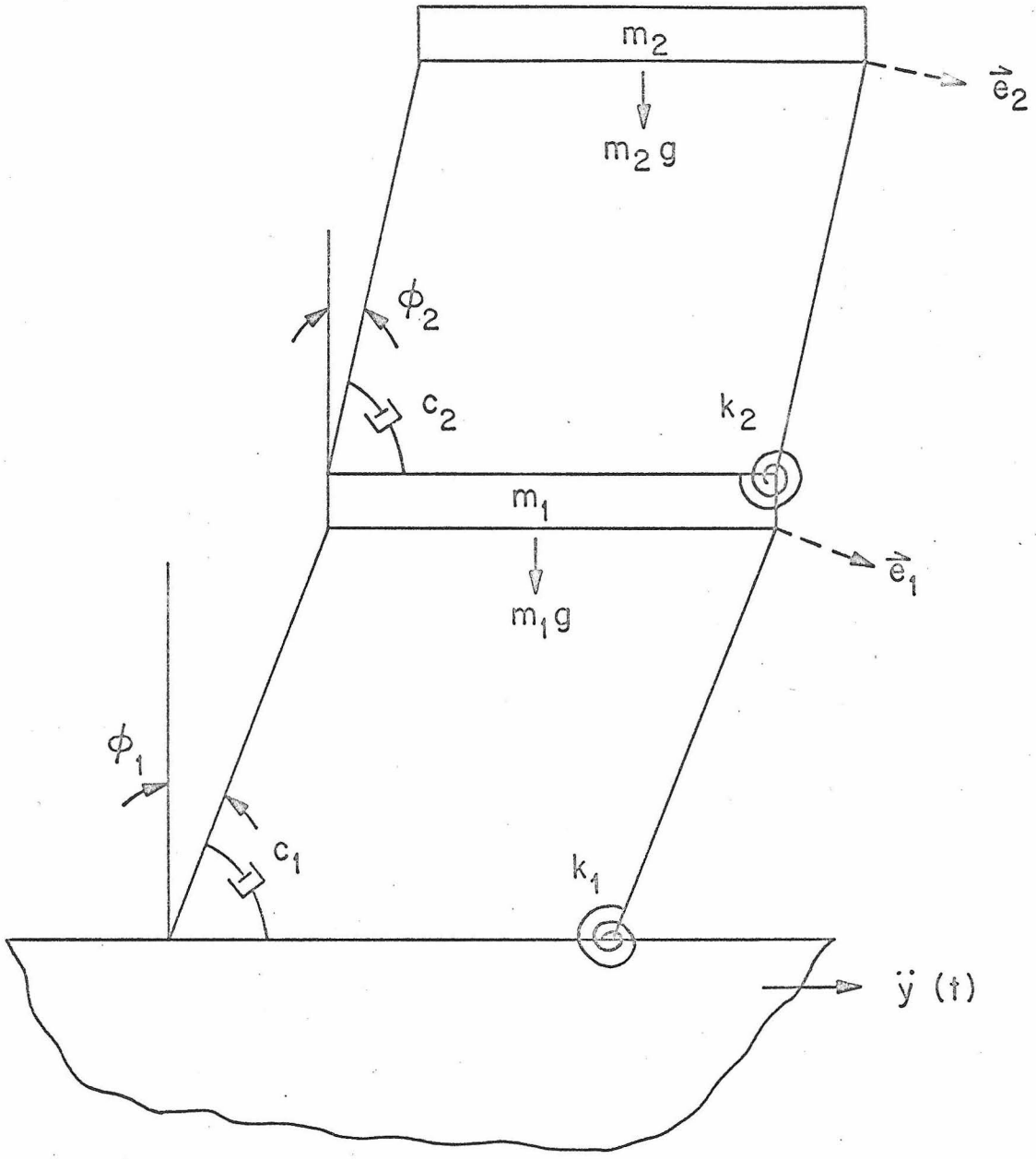

Fig. 5.1 Two-degree of Freedom Structure

gives

$$L = \frac{1}{2} m_2 \left\{ \ell_1^2 \dot{\phi}_1^2 + \ell_2^2 \dot{\phi}_2^2 + 2\ell_1 \ell_2 \dot{\phi}_1 \dot{\phi}_2 \cos(\phi_2 - \phi_1) \right\} + \frac{1}{2} m_1 \ell_1^2 \dot{\phi}_1^2$$

$$- m_1 g \ell_1 \cos \phi_1 - m_2 g (\ell_1 \cos \phi_1 + \ell_2 \cos \phi_2) \qquad (5.2)$$

$$Q_1 = -K_1 F_1(\phi_1, \dot{\phi}_1) - c_1 \dot{\phi}_1 - (m_1 + m_2) \ddot{y} \ell_1 \cos \phi_1 \qquad (5.3)$$

$$Q_2 = -K_2 F_2(\phi_2, \dot{\phi}_2) - c_2 \dot{\phi}_2 - m_2 \ddot{y} \ell_2 \cos \phi_2 \qquad (5.4)$$

where $K_j F_j(\phi_j, \dot{\phi}_j)$, c_j are the effective spring and dashpot forces at the j^{th} floor and the ground acceleration is $\ddot{y}(t)$. Upon substitution of equations (3.2)-(3.4) in the Lagrangian equations one obtains the following equations of motion

$$\frac{d}{dt} \left\{ m_1 \ell_1^2 \dot{\phi}_1 + m_2 \ell_1^2 \dot{\phi}_1 + m_2 \ell_1 \ell_2 \dot{\phi}_2 \cos(\phi_2 - \phi_1) \right\} - m_1 g \ell_1 \sin \phi_1$$

$$- m_2 \ell_1 \ell_2 \dot{\phi}_1 \dot{\phi}_2 \sin(\phi_2 - \phi_1) - m_2 g \ell_1 \sin \phi_1 = Q_1$$

$$\frac{d}{dt} \left\{ m_2 \ell_2^2 \dot{\phi}_2 + m_2 \ell_1 \ell_2 \dot{\phi}_1 \cos(\phi_2 - \phi_1) \right\} + m_2 \ell_1 \ell_2 \dot{\phi}_1 \dot{\phi}_2 \sin(\phi_2 - \phi_1)$$

$$- m_2 g \ell_2 \sin \phi_2 = Q_2$$

hence

$$m_1 \ell_1^2 \ddot{\phi}_1 + m_2 \ell_1^2 \ddot{\phi}_1 + m_2 \ell_1 \ell_2 \ddot{\phi}_2 \cos(\phi_2 - \phi_1) - (m_1 + m_2) g \ell_1 \sin \phi_1$$

$$+ H_1(\dot{\phi}_1^2, \dot{\phi}_2^2, \dot{\phi}_1 \dot{\phi}_2) = Q_1 \qquad (5.5a)$$

$$m_2 \ell_2^2 \ddot{\phi}_2 + m_2 \ell_1 \ell_2 \ddot{\phi}_1 \cos(\phi_2 - \phi_1) - m_2 g \ell_2 \sin \phi_2 + H_2(\dot{\phi}_1^2, \dot{\phi}_2^2, \dot{\phi}_1 \dot{\phi}_2) = Q_2 \qquad (5.5b)$$

where H_1 and H_2 include terms nonlinear in ϕ_1, ϕ_2. It is now assumed that, in the stable range, both ϕ_1 and ϕ_2 are small so that nonlinear terms are negligible--including those in the trigonometric functions. By analogy with the small amplitude oscillations of the one-degree of freedom system, one may define the uncoupled natural frequencies and damping factors as

$$\omega_j^2 \equiv K_j/m_j\ell_j^2 - g/\ell_j \; ; \quad n_j \equiv c_j/2\omega_j m_j \ell_j^2 \qquad j = 1,2 \tag{5.6}$$

Now consider only the cases where $\ell_1 = \ell_2$ and define the mass and stiffness ratios by

$$\beta \equiv m_2/m_1 \; ; \quad \alpha \equiv K_2/K_1 \; . \tag{5.7}$$

Then

$$(1+\beta)\ddot{\phi}_1 + \beta\ddot{\phi}_2 + 2\omega_1 n_1 \dot{\phi}_1 - (1+\beta)\frac{g}{\ell}\phi_1 + (\omega_1^2 + \frac{g}{\ell})F_1(\phi_1, \dot{\phi}_1)$$

$$= -(1+\beta)\ddot{y}/\ell \tag{5.8a}$$

$$\ddot{\phi}_1 + \ddot{\phi}_2 + 2\omega_2 n_2 \dot{\phi}_2 - \frac{g}{\ell}\phi_2 + (\omega_2^2 + \frac{g}{\ell})F_2(\phi_2, \dot{\phi}_2) = -\ddot{y}/\ell \; . \tag{5.8b}$$

These basic equations of motion may be put in a form more suitable for analog programming by rearranging them and defining new variables

$$z_j \equiv \delta\phi_j/\phi_{sj} \qquad j = 1,2 \tag{5.9}$$

such that both floors collapse at δ when the original angle of collapse of the j^{th} floor is ϕ_{sj}. It seems reasonable to assume that the

criterion of static collapse used for the single-degree of freedom system applies here also, i.e. the ratio of collapse angle to angle of yield is

$$\phi_{sj}/\phi_{yj} = 1 + \ell_j \omega_j^2/g \tag{5.10}$$

so that the j^{th} floor yields at

$$b_j = \delta g/(g + \ell\omega_j^2)$$

and, for these scaled variables,

$$b_1/b_2 = \alpha/\beta .$$

Finally, if the excitation's intensity is measured relative to the lower floor, the equations of motion become

$$\ddot{z}_1 + 2\omega_1 n_1 \dot{z}_1 - 2\alpha\omega_2 n_2 \dot{z}_2 - (1+\beta)\frac{g}{\ell} z_1 + \alpha\frac{g}{\ell} z_2 + \frac{\delta}{e_1} \cdot \frac{g}{\ell} f_1\left(\frac{e_1}{b_1} z_1, \frac{e_1}{b_1}\dot{z}_1\right)$$
$$- \alpha\frac{\delta}{e_2} f_2\left(\frac{e_2}{b_2} z_2, \frac{e_2}{b_2}\dot{z}_2\right) = -\frac{\delta\theta}{\ell\left(1 + \frac{g}{\ell\omega_1^2}\right)} x(t) \tag{5.11a}$$

$$\ddot{z}_2 - 2\omega_1 n_1 \frac{\beta}{\alpha}\dot{z}_1 + 2(1+\beta)\omega_2 n_2 \dot{z}_2 + \frac{g}{\ell}(1+\beta)\frac{\beta}{\alpha} z_1 - (1+\beta)\frac{g}{\ell} z_2$$
$$- \frac{\delta}{2_1} \cdot \frac{g}{\ell} \cdot \frac{\beta}{\alpha} f_1\left(\frac{e_1}{b_1} z_1, \frac{e_1}{b_1}\dot{z}_1\right) + (1+\beta)\frac{\delta}{e_2}\frac{g}{\ell} f_2\left(\frac{e_2}{b_2} z_2, \frac{e_2}{b_2}\dot{z}_2\right) = 0 \tag{5.11b}$$

where e_1 and e_2 are the yield levels of the elastoplastic function generators f_1, f_2.

Aside from the assumptions given in the definition of the conceptual model, it was further assumed in deriving equations (3.11) that both floors are the same height, and that, as in the single degree

of freedom system, the magnitude of the angular deformation is small even up to the unstable value and the collapse level is determined by static collapse. The model is then completely specified by the parameters $(n_1, n_2, P_1, \theta, \beta, \alpha/\beta)$. The ratio α/β relates the square of the natural frequencies when gravity is neglected.

B. Analog Simulation of the Two-Degree of Freedom System

The choice of parameters for the two-degree of freedom system is more critical than that for the single-degree of freedom system not only in maintaining a tractable number of variables but also in assuring a meaningful, systematic analysis of the results. The selection was based partly on the known response of linear two-degree of freedom systems to white noise base excitation[22,31], but primarily on the desire to exhibit the effect of the added story on the failure time of the structures. These known results confirm the expectation that the response of lightly damped systems is qualitatively the same for damping factors less than 0.05 and show that the critical region in the values of the mean square responses is the neighborhood of $\alpha/\beta = 1$. One expects, therefore, that a transition from the failure of one story to that of the other will occur in this region. Consequently, a constant damping factor of 0.02 was chosen and α/β was varied between 0.4 and 4.00; corresponding to a frequency ratio range between 0.6 and 2.0.

In order to reflect a wide range of structural problems, mass ratios between 0.01 and 1.0 were investigated. Included in this range is the collapse of an equipment mounted on a simple

structure and that of a roofed two-story structure.

The choice of excitation strength was constrained by the fact that structures failing in less than four seconds may not reflect the average properties of the excitation and by the desire to limit failure times to about 30 seconds. These constraints were discussed earlier. Preliminary testing indicated that a value of $\theta = 23.0$ was appropriate.

Failure times were obtained for the period $P_1 = 2.0$ seconds in the main investigation since the results of the single-degree of freedom system indicate that only slight variations of mean failure time with period should be expected. However, this assumption was independently tested for $\beta = 0.50$ and the critical region $\alpha/\beta = 0.85$ where there was equal likelihood of either story collapsing. This region corresponds to the maximum interaction between the stories and therefore should give the maximum deviation, if any, from the earlier results.

The actual simulation of equations (3.11) on the analog computer was a direct extension of that for the single-degree of freedom system. However much greater care had to be taken in balancing the amplifiers to reduce drift, and in any amplitude scaling employed. Furthermore, the wide variation in the values of the coefficients necessitated a judicious use of summing amplifiers. In the end the drift in all amplifiers was reduced to the same level as in the single-degree of freedom system.

Table 5.1 shows the mean failure times obtained using 300 samples for each point in the range of mass and frequency ratios

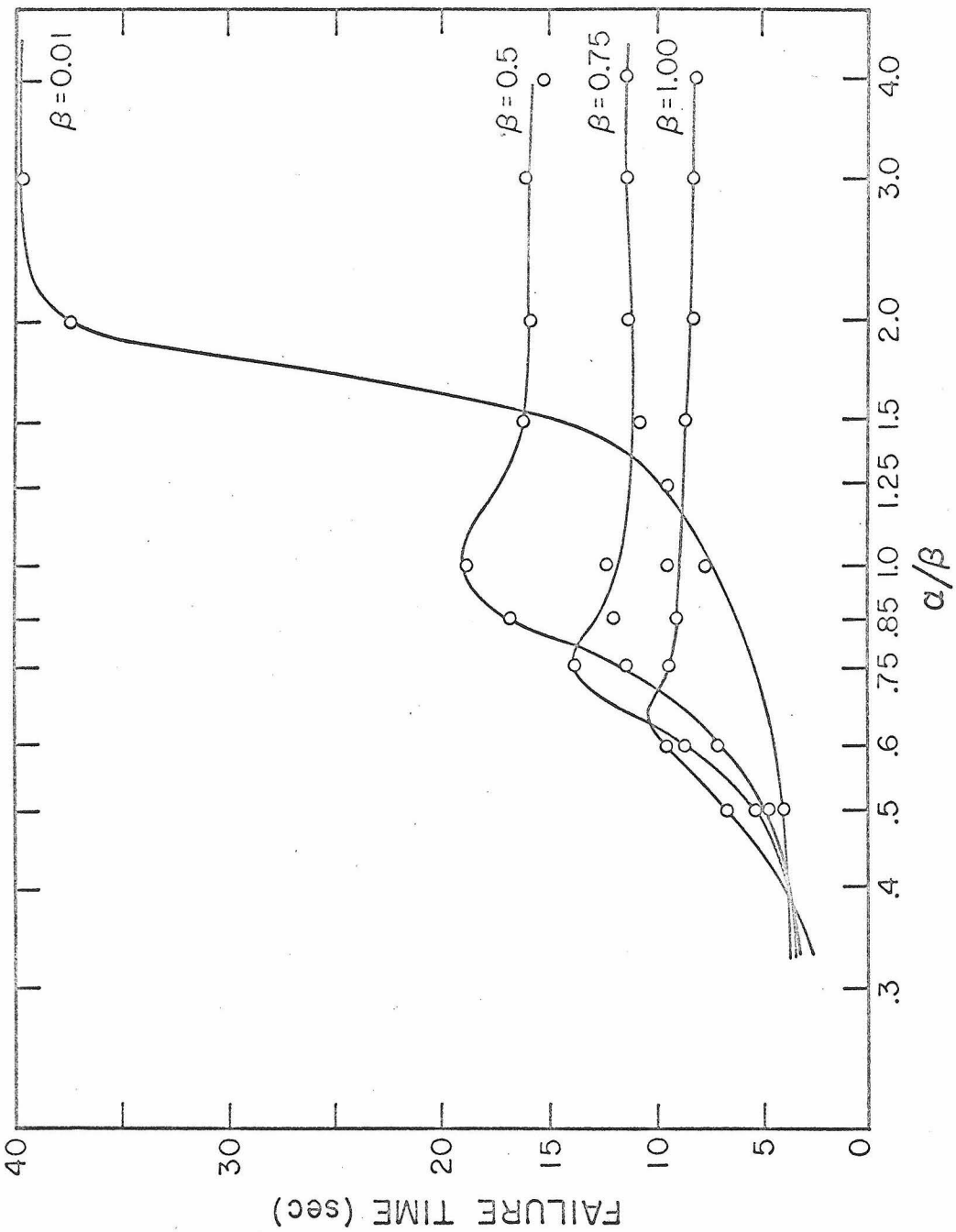

Fig. 5.2 Variation of failure time with mass and frequency ratios

TABLE 5.1

Failure time for two-degree of freedom systems

$\theta = 23.0$, $P_1 = 2.0$

α/β \ β	0.01	0.50	0.75	1.00
0.40	3.93	3.81	4.03	3.99
0.50	3.87	4.81	5.13	6.64
0.60	--	7.15	8.76	9.50
0.75	5.56	11.30	13.76	9.32
0.85	--	16.79	12.04	9.00
1.00	7.66	18.97	12.47	9.39
1.25	9.45	--	--	--
1.50	14.55	16.26	10.86	9.56
2.00	37.38	15.93	11.30	8.14
3.00	30.63	16.15	11.34	8.32
4.00	--	15.22	11.22	8.04
∞	40.21	16.28	10.84	7.32

considered. These same values are plotted in figure 5.2 while the distributions of failure time are shown in figures 5.3 - 5.5 for a few of the points. These latter figures are obtained in the same way as those for the one story structure; i.e. the points represent mid-points of steps in the weakly smoothed histograms of failure times while the continuous curves are Gamma distributions fitted to these points. The values of the ratios of standard deviation to mean are not

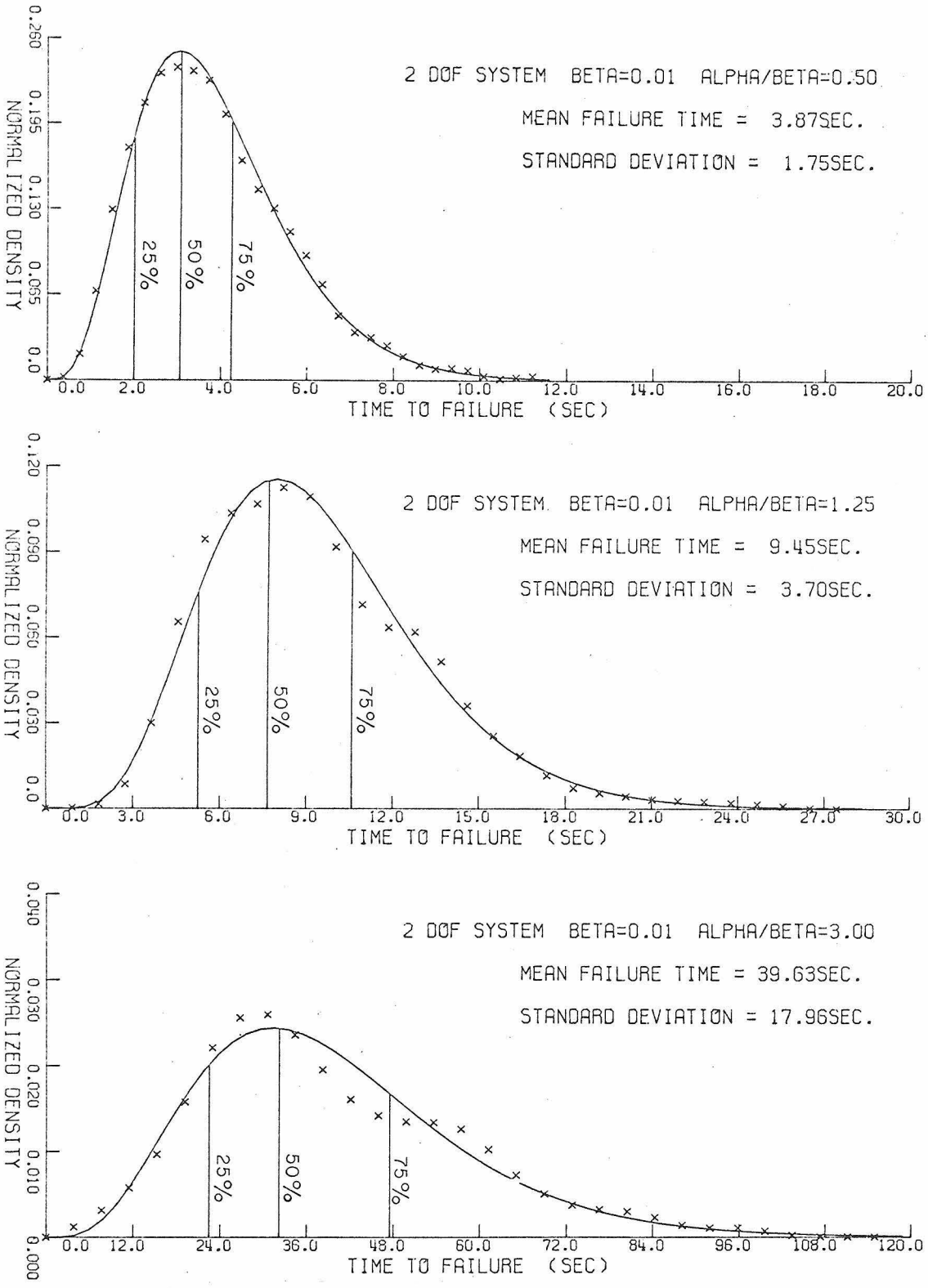

Fig. 5.3 Failure Times of Two-degree of Freedom System

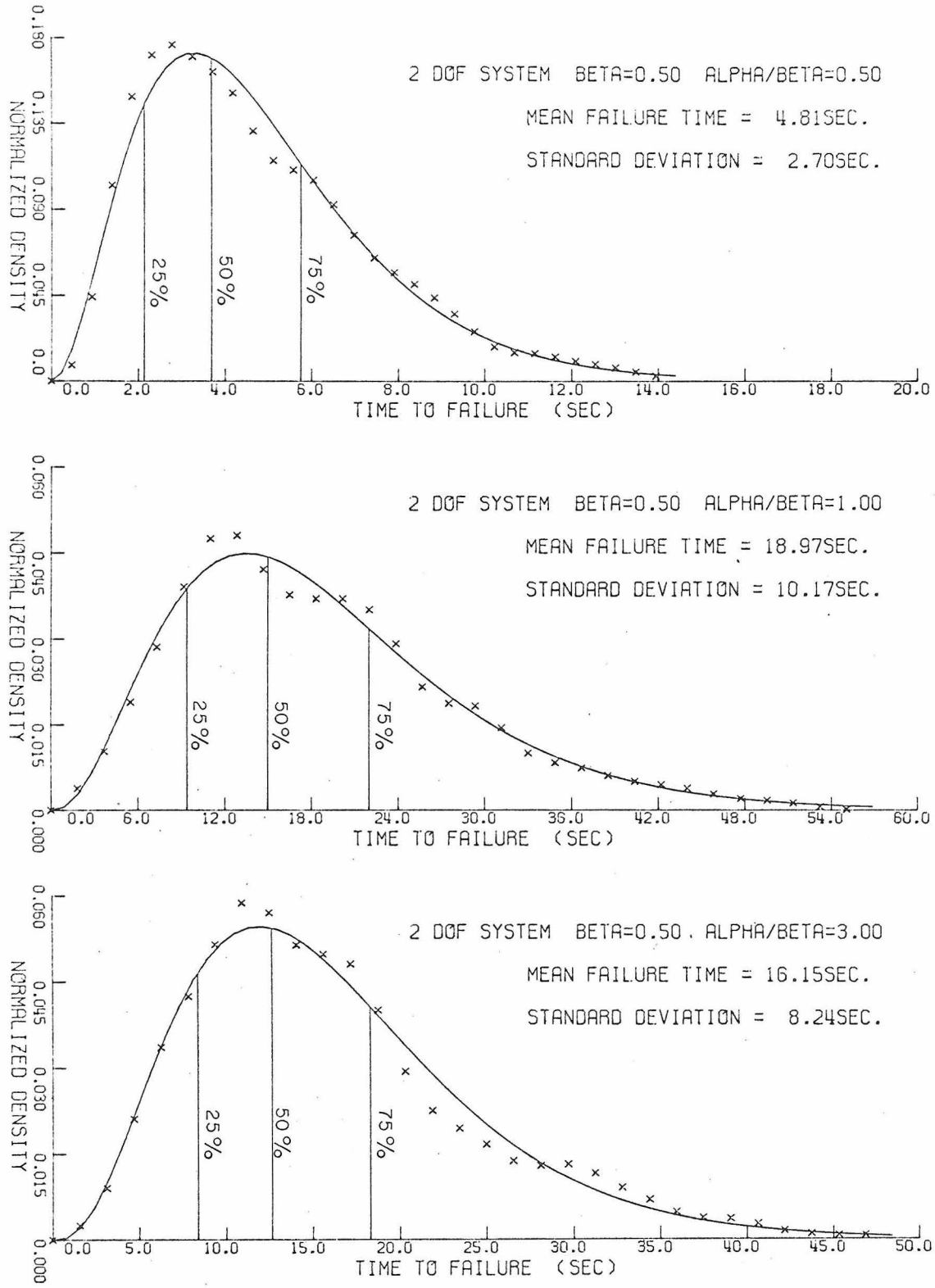

Fig. 5.4 Failure Times of Two-degree of Freedom System

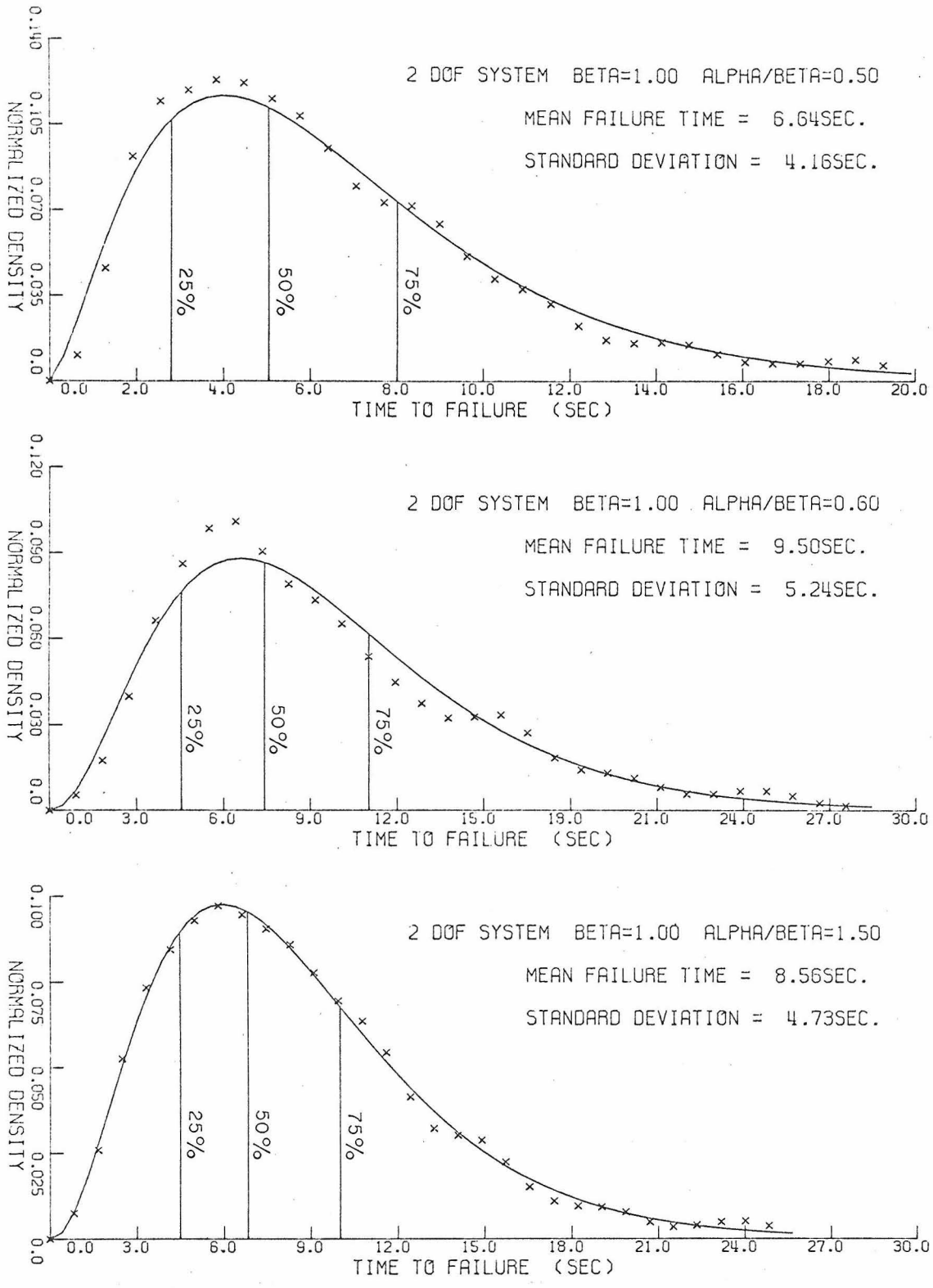

Fig. 5.5 Failure Times of Two-degree of Freedom System

given since these varied as in the case of the one-story structure, i.e. between 0.4 and 0.6. However, the degree of dispersion in the data is illustrated by including the quartiles of the density functions.

The variations of failure time with period and level of excitation at $\beta = 0.05$ and $\alpha/\beta = 0.85$ is shown in table 5.2. To aid in comparing these with earlier results, a regression analysis of the form in equation (3.13) was performed on the data. Its predictions are included in table 5.2 while table 5.3 gives the parameters obtained, their standard errors and their correlation coefficients.

Finally, one expects that at high values of α/β the relative displacements of the masses will be negligible resulting, effectively, in a one-degree of freedom system. This system's natural frequency and relative excitation level may be calculated directly from the definitions in equations (3.3) and (3.7). Thus

$$\omega_e^2 = (\omega_1^2 + \tfrac{g}{\ell})/(1 + \beta) - \tfrac{g}{\ell} \qquad (5.12)$$

$$\theta_e = \theta\omega_1^2/\omega_e^2 \ . \qquad (5.13)$$

These effective values and estimates of the collapse times of the system using the results of the regression analysis in table 3.3 are shown in table 5.4. The estimated collapse times are also included in table 5.1 as asymptotic values of the collapse times of the two-degree of freedom system. The estimates assume that the effect of the change in damping may be neglected relative to the uncertainty in the estimated values.

TABLE 5.2

Variation of failure time with period and excitation level

$\beta = 0.5$; $\alpha/\beta = 0.85$

θ	P_1	$\langle t_f \rangle$	σ_{t_f}	$\sigma/\langle t_f \rangle$	m	v	t_c
23.0	1.5	15.72	6.82	0.434	5.31	0.34	15.12
23.0	2.0	16.25	8.31	0.511	3.83	0.24	16.57
23.0	2.5	18.64	10.69	0.573	3.04	0.16	17.79
34.5	1.5	8.31	3.78	0.455	4.82	0.58	8.29
34.5	2.0	8.57	4.21	0.492	4.13	0.48	9.01
34.5	2.5	9.28	4.95	0.534	3.52	0.38	9.76
46.0	1.5	5.16	2.32	0.450	4.94	0.96	5.42
46.0	2.0	5.72	3.12	0.546	3.36	0.59	5.94
46.0	2.5	5.93	3.10	0.524	3.65	0.62	6.37
69.0	1.5	3.27	1.65	0.505	3.92	1.20	2.97
69.0	2.0	3.33	1.72	0.527	3.75	1.13	3.23
69.0	2.5	3.63	2.11	0.582	2.96	0.82	3.50

TABLE 5.3

Correlation and regression analysis of failure time

	Parameters	Std. error	Parameter correlation a_1	a_2	a_3
a_1	1.38×10^3	1.47×10^2	1.00		
a_2	0.32	0.04	-0.28	1.0	
a_3	-1.48	0.03	-0.96	0.005	1.0

TABLE 5.4

Estimated failure time of two-degree of freedom structure for a stiff upper story

$\theta = 23.$, $P_1 = 2.00$

β	θ_e	P_e	t_c
0.01	23.31	2.01	40.21
0.50	41.22	2.68	16.28
0.75	53.29	3.04	10.84
1.00	68.27	3.45	7.32

C. Observations and Conclusions

It was observed that the failure pattern of the two-degree of freedom structure was quite similar to that of the single-degree of freedom structure for the range of mass and frequency ratios examined. In particular, tables 5.2 and 5.3 indicate that the relative independence of failure time on the structure's period is maintained. An earlier comment that this reflects the dependence of θ on period is borne out in table 5.4 where it is seen that θ increases by almost a factor of 3 for a 72% increase in period; causing a reduction in failure time of over a factor of 5.

A similarity was also observed in the way permanent set tends to occur in jumps and in the observation that, between such jumps, the motion of the structure is essentially a narrow band response. This suggests that an approximate analysis of the failure of the sctructure can be made as in chapter IV if a scheme is found for estimating its rate of energy absorption during yielding.

Furthermore, it was observed in the study of the single-degree of freedom structure that the primary properties affecting collapse time are the magnitude and nature of the excitation and the mechanism for energy dissipation. With respect to the failure of either floor of the structure, the last two properties are essentially unchanged while the effective excitation level at each floor may be estimated from the rms level of its stationary response; thus accounting for the dynamic interaction of the floors. One is thus led to consider estimating the failure time of the two-degree of freedom system

from such stationary responses and the failure times of single-degree of freedom systems.

The linearized equations of motion are obtained from equations (3.8a,b) as

$$(1+\beta)\ddot{\phi}_1 + \beta\ddot{\phi}_2 + 2\omega_1 n_1 \dot{\phi}_1 + \omega_1^2 \phi_1 = -(1+\beta)\ddot{y}/\ell \qquad (5.14a)$$

$$\ddot{\phi}_1 + \ddot{\phi}_2 + 2\omega_2 n_2 \dot{\phi}_2 + \omega_2^2 \phi_2 = -\ddot{y}/\ell. \qquad (5.14b)$$

These reduce to the more standard form

$$\ddot{\phi}_1 + 2\omega_1 n_1 \dot{\phi}_1 - 2\beta\omega_2 n_2 \dot{\phi}_2 + \omega_1^2 \phi_1 - \beta\omega_2^2 \phi_2 = -\ddot{y}/\ell \qquad (5.15a)$$

$$\ddot{\phi}_2 + (1+\beta)2\omega_2 n_2 \dot{\phi}_2 - 2\omega_1 n_1 \dot{\phi}_1 + (1+\beta)\omega_2^2 \phi_2 - \omega_1^2 \phi_1 = 0 \qquad (5.15b)$$

where one now defines

$$\omega^2 \equiv K_j/m_j \quad \text{and} \quad \alpha/\beta = (\omega_2/\omega_1)^2 \equiv \mu^2 . \qquad (5.16)$$

Crandall and Mark[22] have obtained closed form solutions for the rms values of ϕ_1 and ϕ_2 under white noise excitation by direct considerations of the transfer functions. Since we assume low damping, their results may be used here by appropriate choice of the white spectral density. One thus obtains

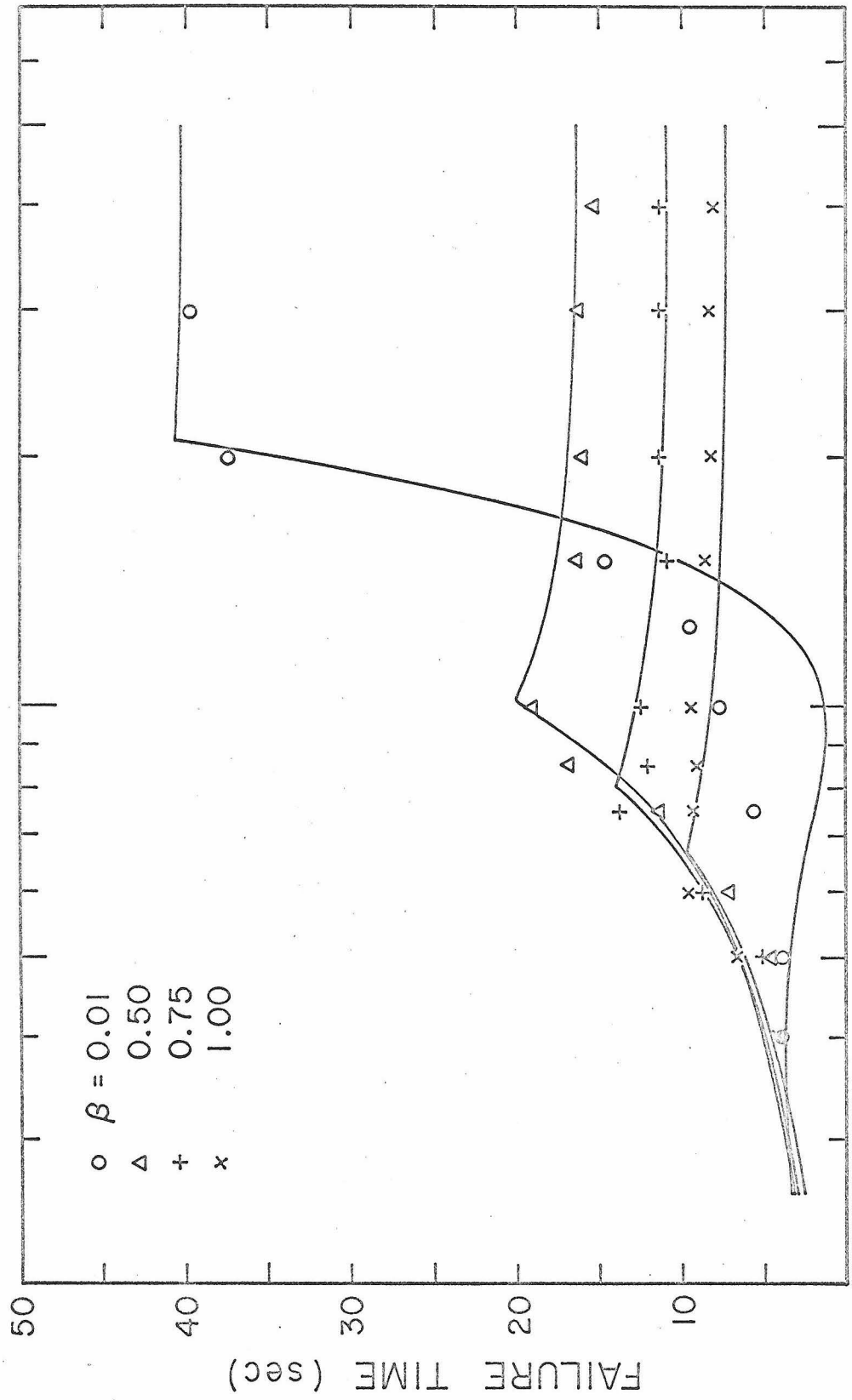

Fig. 5.6 Estimates of variation of failure time with mass and frequency ratios

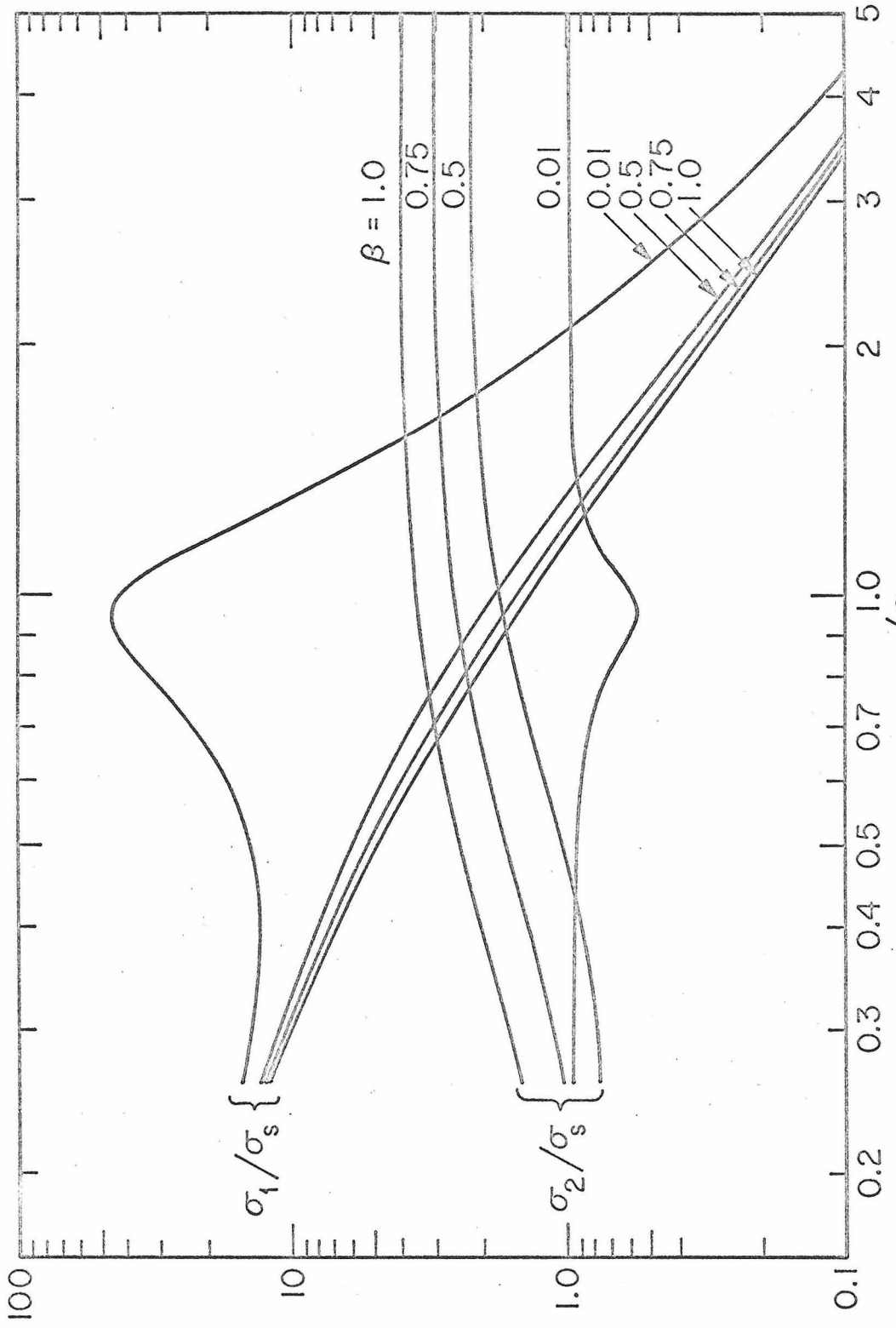

Fig. 5.7 Normalized mean square response of the Linear Two Degree of Freedom System

$$\frac{D\sigma_1^2}{\pi\omega_1^3 G(\omega_1)} = 2n_1\mu^2[\beta^2+\beta(1+\beta)^2\mu^2] + 2n_2\mu\{[1-(1+\beta)^2\mu^2]^2+\beta(1+\beta)^2\mu^2\}$$

$$+8n_1n_2^2\mu^2(1+\beta)^2[1+(1+\beta)\mu^2]+8n_2^3\mu^2(1+\beta)^2[1+\beta+(n_1/n_2)^2] \tag{5.17a}$$

$$\frac{D\sigma_2^2}{\pi\omega_1^3 G(\omega_2)} = 2n_1(\beta+\frac{1}{\mu^2})+2n_2\mu[(1+\beta)^2+\beta/\mu^2]$$

$$+8n_1n_2\{n_1\mu(1+\beta+\frac{1}{\mu^2})+n_2[1+\beta+(n_1/n_2)^2]\} \tag{5.17b}$$

where

$$D = 4\omega_1^6\mu\{\beta\mu(n_1\mu+n_2)+n_1n_2[1-(1+\beta)\mu^2]^2$$

$$+4n_1n_2\mu[\mu(n_1^2+(1+\beta)n_2^2)+n_1n_2(1+(1+\beta)\mu^2)]\}.$$

To calculate the failure time one notes that equations (5.12), (5.13) and the regression equation (3.13) already give estimates of the failure time when the excitation leavel θ is known and μ is large i.e. ≥ 2. Failure times at other frequency ratios are similarly obtained by scaling θ such that

$$\theta' = \frac{\sigma_j}{\sigma_\infty}\cdot\theta \qquad j = 1,2 \tag{5.18}$$

where σ_∞ is the rms level of the lower floor at large μ. The collapse time of the structure then corresponds to the lower of these for the two floors. Estimates of such collapse times are compared with the experimental values in figure 5.6 while, for clarification, the rms values of the stationary responses are plotted in figure 5.7. These have been put in a nondimensional form by dividing them by

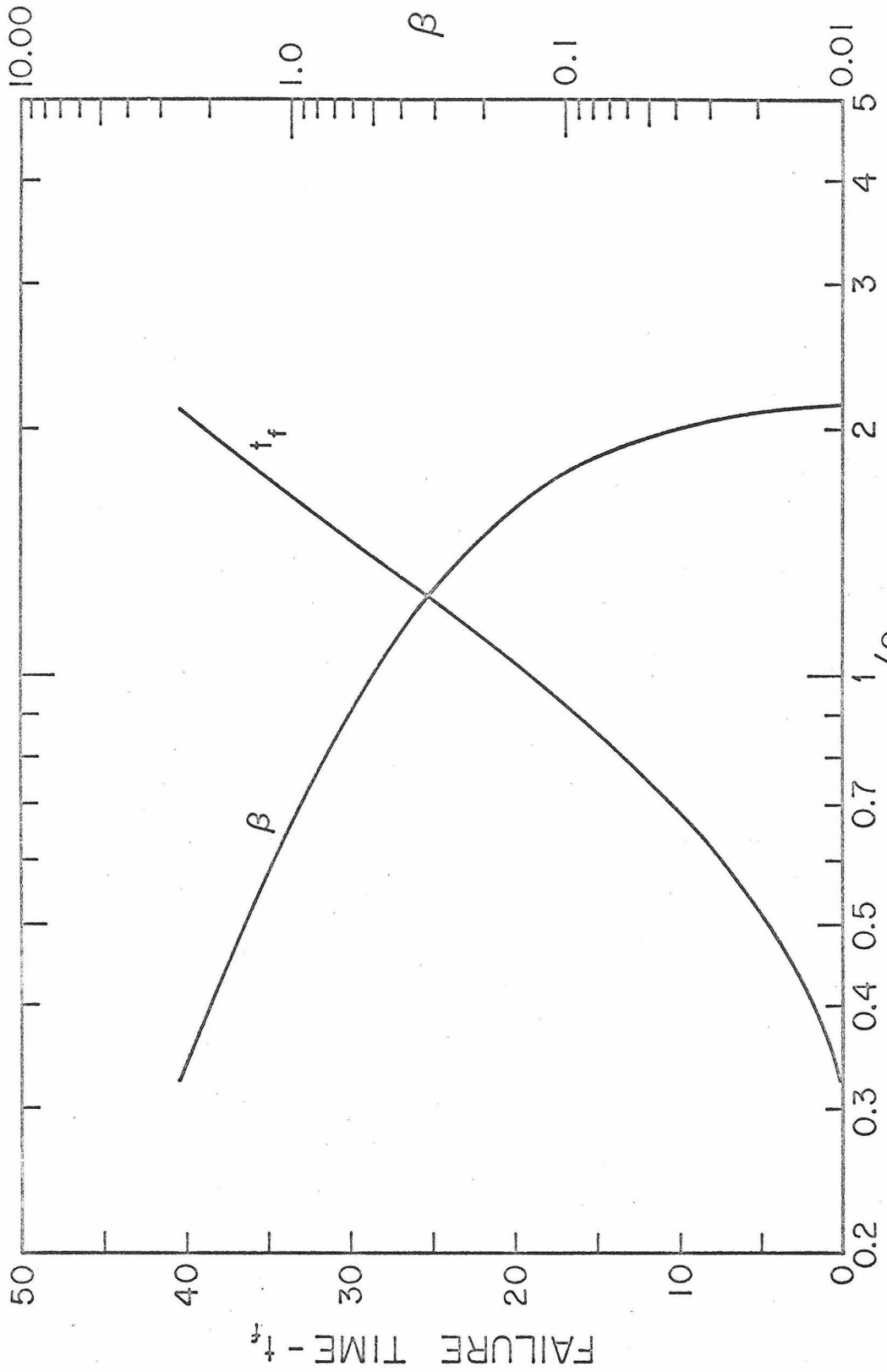

Fig. 5.8 Failure time for optimum combination of mass and frequency ratios

rms displacement of a single degree of freedom structure given by[22]

$$\sigma_s = \pi G(\omega_2)/2n_2\omega_2^2 \ . \qquad (5.19)$$

From the point of view of structural design, the results in both figures 5.2 and 5.6 show the existence of most favorable combinations of mass and frequency ratios that give maximum collapse times. It is noteworthy that the conclusion one draws from figure 5.7 that such combinations correspond to those regions where the floors are equally likely to collapse was observed experimentally. However the large difference between the experimental and estimated failure time for $\beta = 0.01$ and $\alpha/\beta \approx 1$ is difficult to explain. A tentative explanation comes from the observation that the stationary response is not developed appreciably for short failure times and therefore is a relatively inaccurate estimate of the effective excitation level.

Nevertheless one can still conclude that the linearized structure's response magnitude can be used to predict the failure of the real structure. In particular, advantage has been taken of such correspondence to calculate the most favorable combinations of β and α/β and their associated failure times for the two-degree of freedom system. These are shown in figure 5.8 and can be seen to predict the failure times within acceptable limits.

REFERENCES

1. Freudenthal, A. M., Garrelts, J. and Shinozuka, M., "The Analysis of Structural Safety," Journal of the Structural Division, ASCE, 92, No. ST1, Proc. paper 4682, Feb. 1966.

2. Pugsley, A. G., "Concepts of Safety in Structural Engineering," Journal, Institution of Civil Engineers, London, England, 36, No. 5, March, 1951.

3. Cornell, C. A., "Bounds on the Reliability of Structural Systems," Journal of the Structural Division, ASCE, 93, No. ST1, Proc. Paper 5096, Feb. 1967, pp. 171-200.

4. Rowe, R. E., "Current European Views on Structural Safety," Meeting preprint from ASCE Annual Meeting on Structural Engineering, Sept. 30 - Oct. 4, 1968.

5. Lin, Y. K., "Random Processes," Applied Mechanics Reviews,

6. Lin, Y. K., Probabilistic Theory of Structural Dynamics, McGraw Hill Book Company, 1967.

7. Bolotin, V. V., "Statistical Theory of the Aseismic Design of Structures," Proc. Second World Conf. on Earthquake Eng., Tokyo, pp. 1365-1374.

8. Ang, A. H. and Amin, M., "Reliability of Structures and Structural Systems," Journal of the Engineering Mechanics Division, ASCE, 94, No. EM2, April 1968, pp. 671-691.

9. Amin, M. and Ang, A. H., "Nonstationary Stochastic Model of Earthquake Motions," Journal of the Engineering Mechanics Division, ASCE, 94, No. EM2, April 1968, pp. 559-583.

10. Iyengar, R. N. and Iyengar, K. T., "A Nonstationary Random Process Model for Earthquake Accelerograms," Bulletin of the Seismological Society of America, 59, No. 3, June 1969, pp. 1163-1188.

11. Shinozuka, M. and Sato, Y., "Simulation of Non-Stationary Random Processes," Journal of the Engineering Mechanics Division, ASCE, 93, No. EM1, Feb. 1967, pp. 11-40.

12. Goto, H. and Toki, K., "Structural Response to Nonstationary Random Excitation," Proceedings of the 4th World Conference on Earthquakes Eng., A-1, 1969, pp. 130-144.

13. Vickery, B. J., "Wind Action on Simple Yielding Structures," Journal of the Engineering Mechanics Division, ASCE, 96, No. EM2, April 1970, pp. 107-120.

14. Housner, G. W. and Jennings, P. C., "Generation of Artificial Earthquakes," Journal of the Engineering Mechanics Division, ASCE, 90, No. EM1, Feb. 1964.

15. Housner, G. W., "Properties of Strong Motion Earthquakes," Bulletin of the Seismological Society of America, 45, No. 3, July 1955, pp. 197-218.

16. Ward, H. S., "Analog Simulations of Earthquake Motions," Journal of the Engineering Mechanics Division, ASCE, 91, No. EM5, Oct. 1965, pp. 173-190.

17. Kanai, K., "On the Spectrum of Strong Earthquake Motions," Bulletin, Earthquake Research Institute, Univ. of Tokyo, Tokyo, Japan, 40, 1962, pp. 71-90.

18. Brady, A. G., "Studies of Response to Earthquake Ground Motion," Ph.D. Thesis, California Institute of Technology, Pasadena, California, 1966.

19. Coleman, J. J., "Reliability of Aircraft Structures in Resisting Change Failure," Operations Research, 7, 1959, pp. 639-645.

20. Bogdanoff, J. L. and Kozin, F., "Comment on the 'Reliability of Structures in Resisting Chance Failure'," Operations Research, 9, 1961, pp. 123-126.

21. Lyon, R. H., "On the Vibration Statistics of a Randomly Excited Hard Spring Oscillator. II," The Journal of the Acoustical Society of America, 33, No. 10, Oct. 1961, pp. 1395-1403.

22. Crandall, S. H. and Mark, W. D., Random Vibration in Mechanical Systems, Academy Press, 1963.

23. Shinozuka, M., "Probability of Structural Failure Under Random Loading," Journal of the Engineering Mechanics Division, ASCE, 90, No. EM5, Oct. 1964.

24. Sato, H., "On the Response Spectrum of the Building-Machine Structure System to Strong Earthquake," Bulletin, Japan Society of Mechanical Engineers, 9, 36, 1966, pp. 684-693.

25. Yamada, Y. and Takemiya, H., "Statistical Estimation of the Maximum Response of Structures Subjected to Earthquake Motion," Proceedings of the Japan Society of Civil Engineers, 182, Oct. 1970.

26. Iyengar, R. N. and Iyengar, K. T., "Probabilistic Response Analysis to Earthquakes," Journal of the Engineering Mechanics Division, ASCE, 96, No. EM3, June 1970, pp. 207-225.

27. James, H. M., Nichols, N. B. and Phillips, R. S., Theory of Servomechanisms, MIT Radiation Lab. Series, Vol. 25, McGraw Hill, New York, 1947.

28. Amin, M., Ts'Ao, H. S. and Ang, A. H., "Significance of Non-Stationarity of Earthquake Motions," Proc. of the 4th World Conf. on Earthquake Engineering, A1, 1969, pp. 97-113.

29. Rosenblueth, E. and Bustamante, J. I., "Distribution of Structural Response to Earthquakes," Journal of the Engineering Mechanics Division, ASCE, 88, No. EM3, June 1962, pp. 75-106.

30. Caughey, T. K. and Gray, A. H., "Discussion on 'Distribution of Structural Response to Earthquakes'," Journal of the Engineering Mechanics Division, ASCE, 89, No. EM2, April 1963, 159-168.

31. Curtis, A. J. and Boykin, T. R., "Response of Two-degree of Freedom System to White Noise Base Excitation," The Journal of the Acoustical Society of America, 33, No. 5, May 1961, pp. 655-663.

32. Khinchin, A. Ya., "On Poisson Sequences of Chance Events," Theory of Probability and its Applications, (English Translation of Soviet Journal), 1, No. 3, 1956, pp. 291-297.

33. Parzen, E., Stochastic Processes, Holden-Day Inc., San Francisco, 1962.

34. Hudson, D. E., "Equivalent Viscous Friction for Hysteritic Systems with Earthquake-Like Excitations," Proc. of the 3rd World Conf. on Earthquake Engineering, II, New Zealand, 1965, pp. 185-206.

35. Lutes, L. D., "Stationary Random Response of Bilinear Hysteritic System," Ph.D. Thesis, California Institute of Technology, 1967.

36. Penzien, J. and Liu, S., "Nondeterministic Analysis of Nonlinear Structures Subjected to Earthquake Excitation," Proc. 4th World Conf. on Earthquake Engineering, Santiago de Chile, 1969.

37. Levine, L., Methods for Solving Engineering Problems Using Analog Computers, McGraw-Hill Book Company, 1964.

38. Kanai, K., "Semi-Empirical Formula for the Seismic Characteristics of the Ground," Bulletin of the Earthquake Research Institute, Univ. of Tokyo, Japan, 35, June 1967, pp. 308-325.

39. Tajimi, H., "A Statistical Method for Determining the Maximum Response of a Building Structure During an Earthquake," Proc. of the 2nd World Conf. on Earthquake Engineering, Japan, II, 1960.

40. Rice, S. O., "Mathematical Analysis of Random Noise," in Selected Papers on Noise and Stochastic Processes, edited by N. Wax, Dover, New York, 1954.

41. Middleton, D., An Introduction to Statistical Communication Theory, McGraw-Hill, New York, 1966, pp. 426.

42. Merchant, H. C. and Hudson, D. E., "Mode Superposition in Multi-degree of Freedom Systems Using Earthquake Response Spectrum Data," Bulletin of the Seismological Society of America, 52, No. 2, pp. 405-416, April, 1962.

43. Bielak, J., "Base Moments for a Class of Linear Systems," Journal of the Engineering Mechanics Division, ASCE, 95, No. EM5, Oct. 1969.

44. Housner, G. W., "Behavior of Structures During Earthquakes," Journal of the Engineering Mechanics, ASCE, 85, No. EM4, Oct. 1959, pp. 109-129.

45. Huston, W. B. and Skopinski, T., Probability and Frequency Characteristics of Some Flight Buffet Loads, NACA TN 3733, August, 1956.

46. Husid, R., "Gravity Effects on the Earthquake Response on Yielding Structures," Ph.D. Thesis, California Institute of Technology, Pasadena, California, June 1967.

47. Ruge, A. C., "The Determination of Earthquake Stresses in Elastic Structures by Means of Models," Bulletin of the Seismological Society of America," 24, No. 3, July 1934.

48. Jacobsen, L. S., "Dynamic Behavior of Simplified Structures up to the Point of Collapse," Proceedings of the Symposium on Earthquake and Blast Effects on Structures, Los Angeles, California, 1952.

49. Nielsen, N. N., Dynamic Response of Multistory Buildings, California Institute of Technology, June 1964.

50. Iwan, W. D., "The Dynamic Response of Bilinear Hysteretic Systems," Ph. D. Thesis, California Institute of Technology, Pasadena, California, 1961.

51. Caughey, T. K., "Sinusoidal Excitation of a System with Bilinear Hysteresis," Journal of Applied Mechanics, 27, No. 4, Dec. 1960, pp. 640-643.

52. Caughey, T. K., "Random Excitation of a System with Bilinear Hysteresis," Journal of Applied Mechanics, 27, No. 4, Dec., pp. 649-652.

53. Bendat, J. S., Principles and Applications of Random Noise Theory, New York, John Wiley and Sons, 1958.

54. Greenwood and Durand, "Aids for Fitting the Gamma Distribution by Maximum Likelyhood," Technometrics, 2, 1960, pp. 55-65.

55. Raltons, A. and Wilf, H. S., Mathematical Methods for Digital Computers, John Wiley and Sons, 1965.

56. Marquardt, D. W., "An Algorithm for Least-Squares Estimation of Non-linear Parameters," Journal Soc. for Industrial and Applied Math., 11, No. 2, June, 1963.

57. Roach, S. A., The Theory of Random Clumping, Methuen and Co., London, 1968.

58. Transistor Manual, General Electric Corporation.

APPENDIX A

ANALOG SIMULATION PROCEDURE AND RELATED EQUIPMENT

A1. Random Noise Generator

All the systems examined in this study had resonant frequencies lower than 4 Hz. Consequently, the excitation was simulated by filtering a white noise process generated by a low-frequency random noise generator--Hewlett Packard model 3722A--with a bandwidth from d.c. to a variable nominal cutoff frequency, f_e, specified by the half-power point. A cutoff frequency of 15 Hz was chosen. The spectral density is reasonably flat up to f_e, being specified within ± 0.2 dB at 0.5 f_e; while low-pass digital filtering assures a sharp cutoff, > 25 dB at 2 f_e. The noise output can be selected as a Gaussian white noise with a stable zero mean and fixed power at 10 volts. Hence the power spectral density and nominal bandwidth, f_e, are related by

$$S(\omega) = \frac{10}{f_e} \frac{(\text{volts})^2}{\text{Hz}} \quad . \tag{A.1}$$

This property is very convenient in electronic analog experiments since time scaling of the input excitation may be readily achieved by appropriate scaling of the bandwidth e.g. if computer time is $\tau = \alpha t$, one needs only select $f_e(\tau) = \frac{1}{\alpha} f_e(t)$.

In addition to the purely random noise, the generator can also give periodic, 'pseudo-random' patterns having the same

spectral properties as the true random noise but generated in a predetermined and repeatable sequence of given length N. A sync pulse and gate output (12.5 - 0 volts) are available relative to the beginning of the pattern selected. These pseudo-random functions were used periodically to test the repeatability of the analog set-up and, as in chapter 3, to compare results of the analog simulation with numerical evaluation on the digital computer. Digital records were obtained by plotting the excitations on a brush recorder and digitizing these on a Data Reducer System--Benson-Lehner 099D.

A2. Electronic Analog Simulation

The basic element used in the analog simulation was the K5-U Universal Linear Operator--Philbrick Researches, Boston. This combines a summing and an operational amplifier to simulate an input-output relation of form

$$e_o = e_c + 10^m L \sum_{j=1}^{4} \pm a_j e_j \qquad (A.2)$$

where the linear operator L may be selected as either an integrator or a summer. The voltages e_j, $j = 0,\ldots,4$ have a nominal range of ± 50 volts, m can be set to 0,1,2 or 3 and the coefficients $a_1,\ldots,a_4$ can be adjusted in steps of 0.01 volts within the limits ± 11.10 volts. The index voltage e_c can be adjusted in steps of 0.1 volts within ± 50 volts. Input and output overloads are indicated by standard bulbs. The amplifier incorporates precision

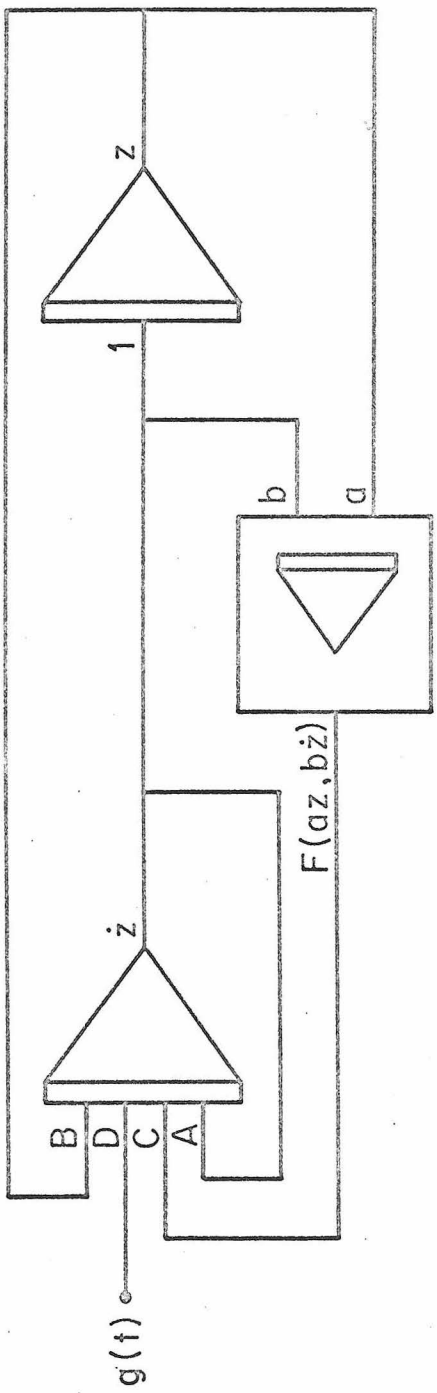

$$\ddot{z} + A\dot{z} + Bz + CF(az, b\dot{z}) = Dg(t)$$

Fig. A.1 Analog Simulation of a Second Order Differential Equation

resistors and capacitors so that the error in selected coefficients is specified less than 1.5% while the drift in the output voltage can be adjusted to about 2 mv per second when $m = 0$. The drift rate increases significantly with higher m. However, it can generally be made negligible when a set of amplifiers is used in a closed loop arrangement.

Run and reset relays for the amplifiers can be operated either individually at each amplifier or collectively, and simultaneously, from a Relay Control Component. In addition, the latter can be set manually or controlled externally by application of reset (20 - 25 v) and run (< 3v) voltages. This permits synchronous, automatic control of all amplifiers and related equipment.

The linear operations in equation (A.2) may be readily modified, if necessary, since the summing point of each operational amplifier is available externally. Thus, as detailed below, the amplifier may be used as a versatile elastoplastic function generator.

A recurrent requirement in this study is the simulation of the second order differential equation

$$\ddot{z} + A\dot{z} + Bz + CF(az, b\dot{z}) = Dg(t) \,. \qquad (A.3)$$

The analog setup is shown in figure A.1. Note that it is often necessary to work with scaled values of the variables in order to keep the coefficients within the allowed range and not saturate any amplifier. In this respect, one observes that theoretically there will always be peaks above the saturation level in the Gaussian random excitation.

Crandall and Mark[22] have shown that clipping of such peaks has negligible effect on the rms value of the output if the input is scaled such that the expected rms of the output is less than three-tenths of the saturation voltage. In this case the limit is thus about 15 volts.

The accuracy of the coefficient settings was verified by simulating the free vibrations of a linear one-degree of freedom system with known initial displacement. Measurement of the times for 15 cycles of oscillation showed negligible difference between expected and observed periods of vibration over the range 0.3 to 3.0 seconds. A negligible difference was also found on calculating the damping factor for 2% damping by comparing peaks in the oscillation. However, a negative damping factor of between 0.1 and 0.15% was observed for the nominally undamped oscillator. It was concluded that the coefficient settings may be taken as satisfactorily accurate for damped systems but that the more sensitive undamped systems have to be individually adjusted by including appropriate positive damping.

Finally, the computer can be run at a scaled time $\tau = \alpha t$ by simply multiplying the input to all integrators by a factor $1/\alpha$. While this can be conveniently done in decades by adjusting m it is worthwhile to note that the drift rate has to be rechecked whenever m is varied.

A3. Subsidiary Switching Equipment

As noted above, the operational amplifiers, and hence the whole analog model, can be simultaneously switched by application of external voltages to the Relay Control Component. Hence such switch-

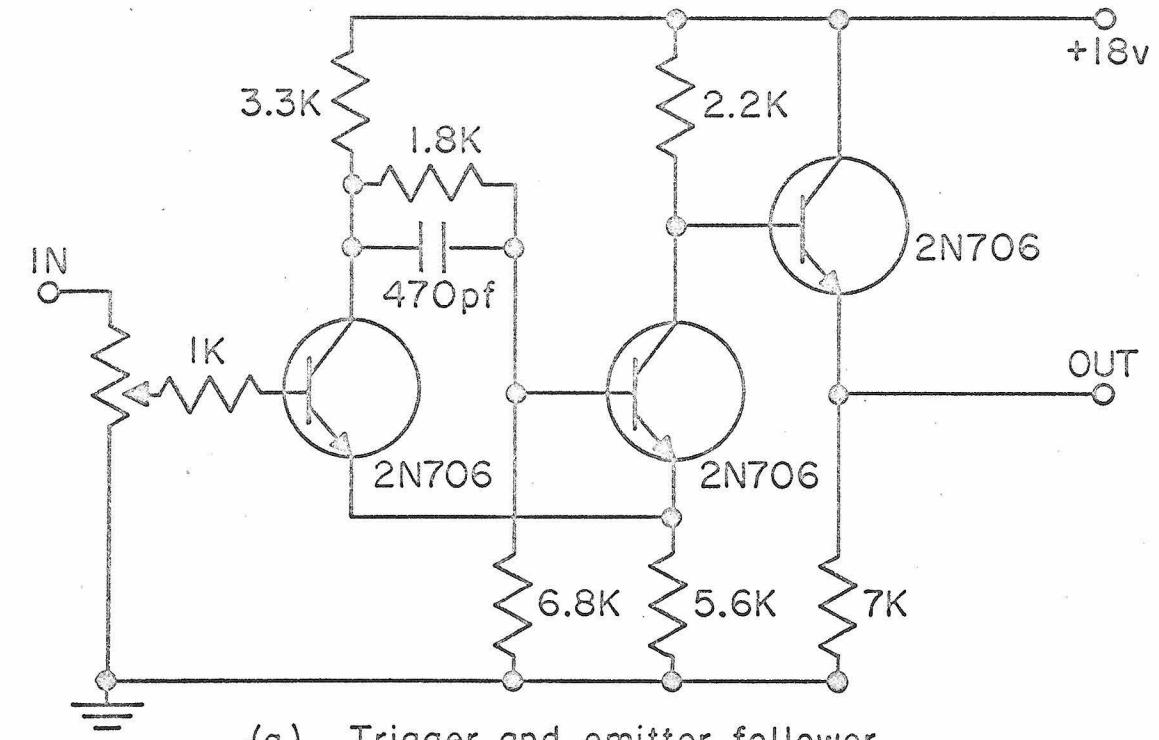

(a) Trigger and emitter follower

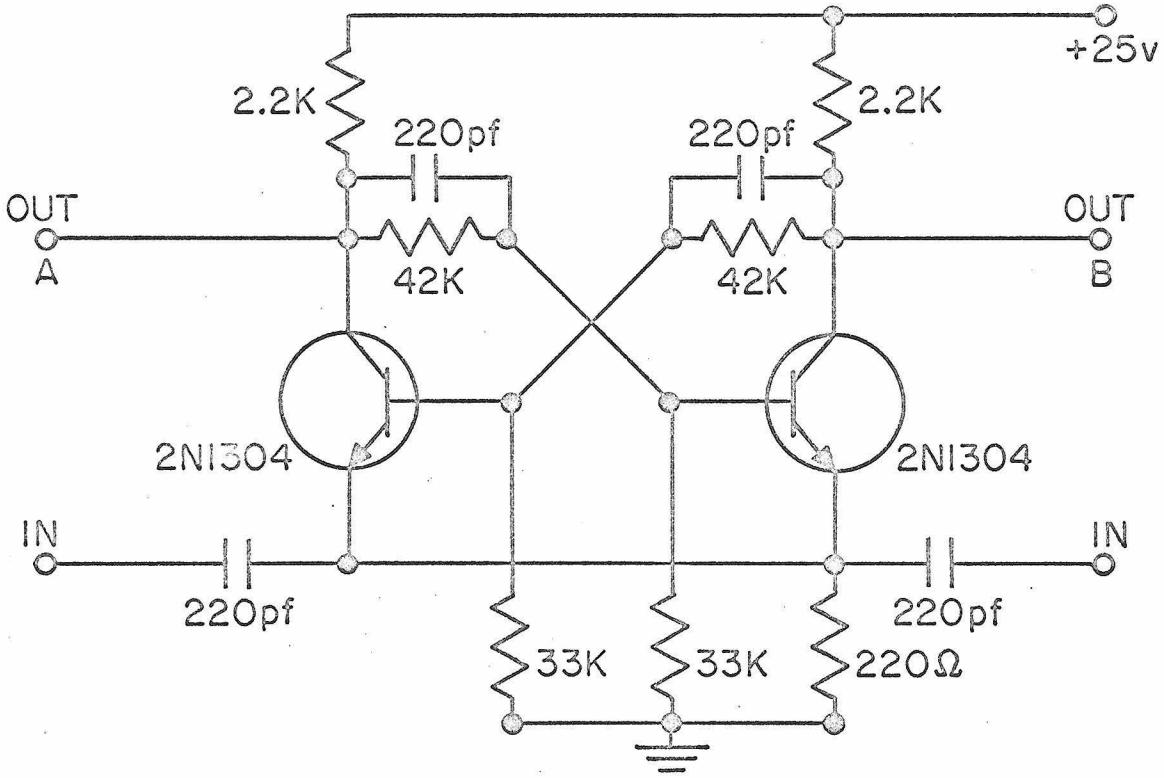

(b) Flip-flop

Fig. A.2

ing may be done by either a continuous square wave generator or a flip-flop circuit since the current requirements are low. The former was used when repeated computer runs of fixed duration were desired as in the simulation of the stable oscillators examined in chapter II. The latter was used primarily to achieve alternate switching of the analog computer by several components. Its circuity--figure A.2b--is a slight modification of the standard design of saturated flip-flops[58]. Transistor 2N1304 were used to give positive output voltages (+23 v, +2.5 v) and capacitor coupling permitted the use of up to 3 inputs. These inputs were further isolated from the flip-flop, where possible, by an emitter follower stage. The flip-flop changes state an application of a positive voltage step or impulse greater than 3 volts.

Elastoplastic System with Gravity

In the study of the unstable yielding systems, it was necessary to measure the time interval between the start of the computer run and the collapse of the structure; defined as when the displacement reaches a given voltage. This voltage was sensed by the Schmitt trigger circuit shown in figure A.2a with an isolating emitter follower. A box diagram of the switching and timing arrangement is shown in figure A.3a. When the response reaches the collapse voltage, the trigger pulses the flip-flop causing the latter to change state and turn off the analog model. The second output of the flip-flop initiates a delayed step voltage from a square-wave generator. This then completes the cycle by reversing the state of the flip-flop and thus turning on the analog model. The collapse time was measured by a time interval

Block Diagrams for Switching and Timing the Analog Computer

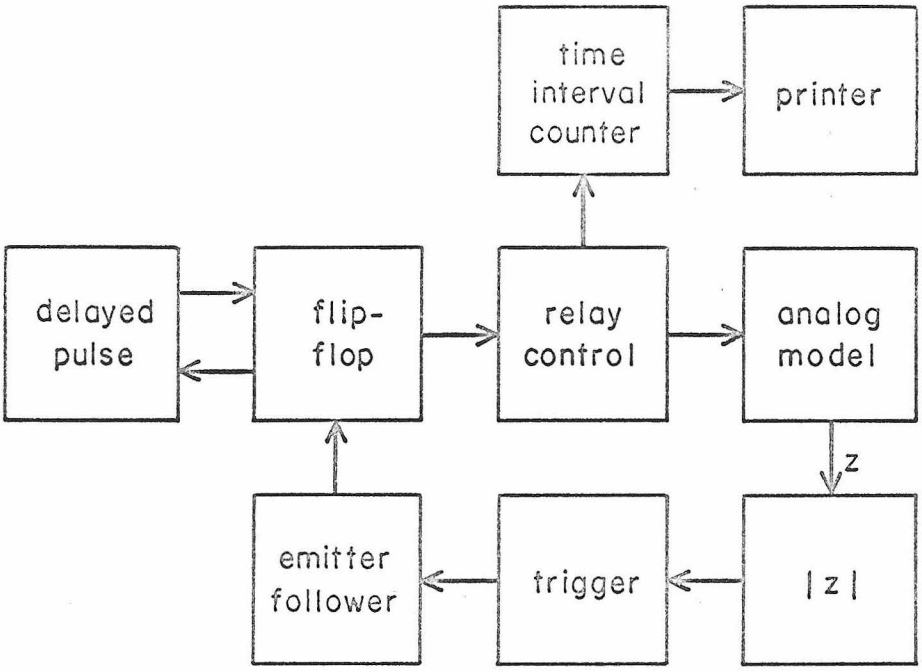

(a) Elastoplastic System With Gravity

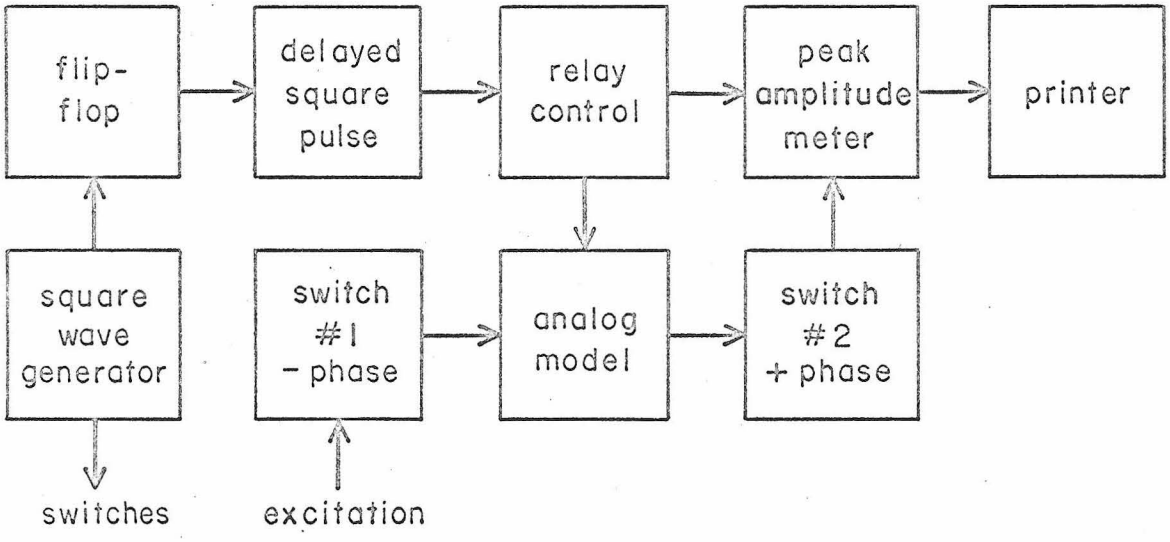

(b) Fourier Amplitude Spectrum

Fig. A.3

counter--Hewlett Packard 5245M and 5262A--and recorded directly on a digital printer--Hewlett Packard model 562a. The speed of the printer limited the delay time to at least 0.2 second which is very much longer than the reset time of the operational amplifiers.

Note that switching times of the equipment were not a source of concern since they were of the order of microseconds while computer times were of the order of seconds.

The simulation of the two-degree of freedom yielding system was a direct extension of the single-degree of freedom system, except that now two displacements are sensed from the analog model. Hence an extra Schmitt trigger was used to make a third input to the flip-flop.

Stable Oscillators' Response Spectra

In addition to the analog model, figure A.1, the only other equipment for measuring the maximum pseudo-velocity of stable oscillators were a square wave generator to switch the computer, and a peak amplitude meter. The main components of the latter are shown in figure A.4a,b. These consist of an absolute value generator and a maximum amplitude meter. The operation of the absolute value generator follows directly from the properties of summing operational amplifiers. Basically, the maximum amplitude meter uses the diode to charge the capacitor to the maximum value of the input. To minimize leakage the diode has a very high backward impedance (> 10 m) and the capacitor's voltage is measured via a high input impedance (> 10" Ω) voltage follower arrangement using a field effect operational

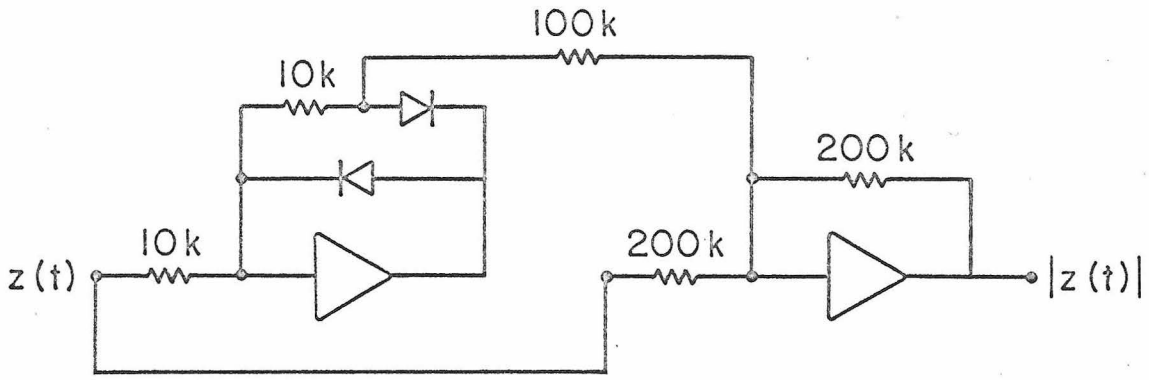

(a) Absolute Value Generator

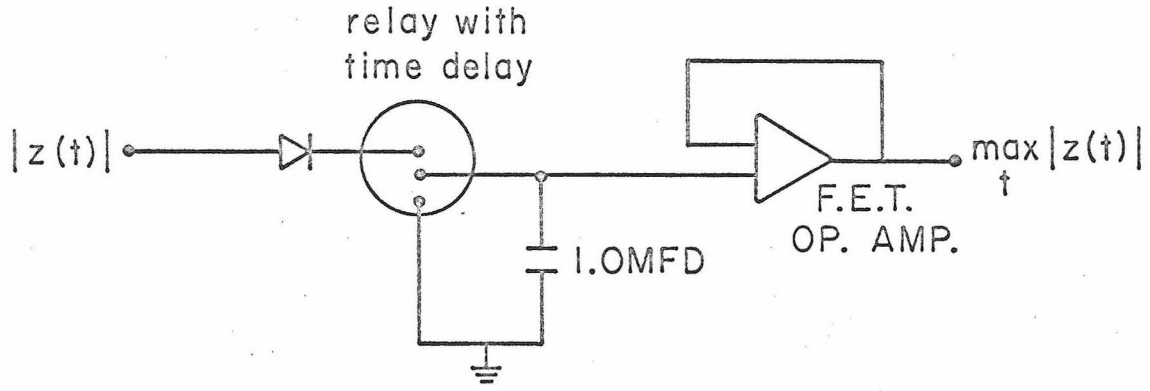

(b) Maximum Amplitude Meter

Fig. A.4 Measurement of Response Spectra

amplifier (Philbrick/Nexus model 100901). Thus the capacitor's charge can be held within less than 1% for over 15 seconds.

The relay normally makes contact with the diode and discharges the capacitor on being energized. Since the output was measured by a digital voltmeter (Hewlett-Packard model 405CR) requiring at least 0.2 second to make a reading, the discharge of the capacitor was delayed relative to the end of the excitation by using a square wave generator triggered externally by the Relay Control Component. This generated a single, delayed square pulse which activated the relay. The voltmeter reading was also initiated by the Relay Control Component on turning off the analog model. Its reading was recorded directly on a digital printer (Hewlett-Packard model 561B). Hence repetitive readings of the maximum absolute value of any analog output can be made.

While tests showed that the 1.mfd capacitor was sufficiently large for the peak amplitude meter to record the sharpest peaks in the input functions used, the forward voltage drops of the diodes led to an offset between the actual and recorded maximum amplitudes. Hence the whole meter system was calibrated experimentally by plotting several input functions and comparing their peaks with the recorded values. The offset voltage varied between -0.7 and -0.9 volts independent of the oscillator's natural period (range 0.3 to 3 seconds.

Fourier Amplitude Spectrum

The sole difference between the experimental set-up for measuring the Fourier amplitude spectrum and that for pseudo-

velocity spectra is in the switching arrangements. The arrangement for the former is shown in the box diagram of figure A.3b. The excitation is available to the analog model during alternate intervals of length, say T_1, determined by the square wave generator. The analog model is on at all times except for a short interval, $T_2 < 0.3\,T_1$, beginning after a delay $T_3 > 5P$ from the end of excitation; where P is the period of the oscillator. Thus the analog model--zero initial conditions--is excited for an interval T_1, after which it vibrates freely for an interval T_3. The free vibration's amplitude is measured by the peak amplitude meter whose recording is initiated by the computer turning off.

A4. Elastoplastic Function Generator

A basic way of simulating an elastoplastic function of x, say, is by switching off the integration of $\dot{x}$ whenever x is greater than its yield level, x_y. While complex switching circuits can be built to assure sharp cutoffs[35], the direct method using Zener breakdown current-voltage characteristics (figures A.5a,b,c) was found satisfactory in this study. The advantages of this method are that it uses only one operational amplifier and, if that is taken as one of the K5-U units, permits accurate, dial selection of the coefficients of the generator. The disadvantages are that the yield voltage is not easily varied and that, as shown in figure A.5c, its current-voltage characteristics has a rounded knee and a small, non-zero yield slope.

The effect of the imperfect operation of the double Zener diode may be evaluated. Let its impedance be Z_d and given by

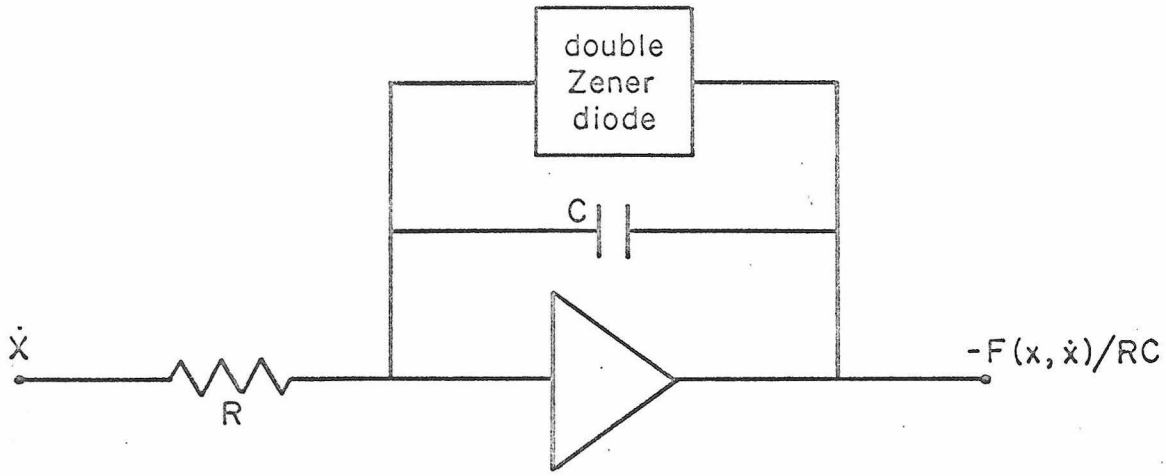

(a) Elastoplastic Function Generator

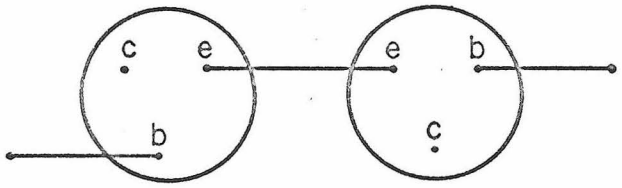

(b) Double Zener Diode
From Two Transistors

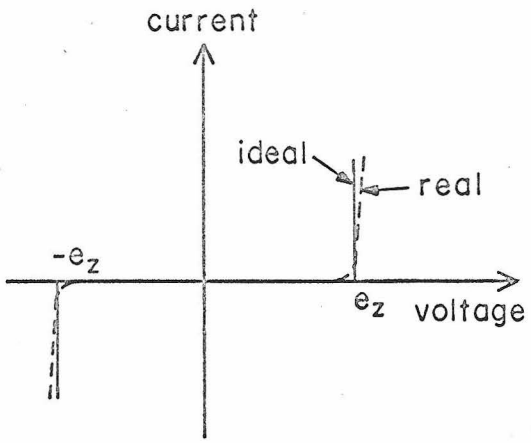

(c) Current-voltage
Characteristic

Fig. A.5

$$Z_d = \begin{cases} \epsilon_y & |F(x,\dot{x})/RC| \geq x_y \\ \epsilon >> 1 & |F(x,x)/RC| < x_y \end{cases} \tag{A.4}$$

where ϵ_y is assumed very small and ϵ large. Then, during yielding, the effective feedback impedance is

$$Z_{eff} = \frac{\epsilon_y Z_c}{\epsilon_y + Z_c} \doteq \epsilon_y \quad \text{for} \quad \epsilon_y << Z_c = 1/j\omega C . \tag{A.5}$$

Hence, assuming that ϵ_y is capacitive ($\equiv C_\epsilon << 1$), the output voltage is

$$e_{out} = x_y + \frac{1}{RC_\epsilon}\dot{x}. \tag{A.6}$$

Similarly, the effective feedback before yielding occurs is

$$Z_{eff} = \frac{\epsilon Z_c}{\epsilon + Z_c} \doteq Z_c \quad \text{for} \quad \epsilon >> Z_c. \tag{A.7}$$

In general, the requirement in equation (A.7) was met by most diodes since their leakage current was negligible up to the knee in the characteristic (< 0.1 μa). Equations (A.5) and (A.6) require that R be large and C small and, more directly, that the diode's yield impedance be as small as possible. The error in the yield voltage is proportional to the input current. In this respect, one notes that R is generally of the order of megohms in standard amplifier design,

in order to minimize the input current.

Extensive testing showed that commercial Zener diodes had a more rounded knee and larger yield slope than did the transistor arrangement in figure A.3b for a proper choice of transistors. Pairs of 2N5130 transistors with similar base-emitter reverse bias characteristics were carefully selected and tested in a summing circuit with a ramp voltage input. It was found that a typical yield voltage varied from 6.13 to 6.21 volts as the input rose to 50 volts. In such an instance the effective yield level was chosen as 6.15 volts; corresponding to a mean input voltage of 25 volts. Only transistors with the same input to yield voltage characteristics were paired to form the double Zener diode. It was concluded that errors from both the rounded knee and yield slope of the transistors should be less than 1% of the nominal yield voltage.